SPECKLED WORM EEL (*MYROPHIS PUNCTATUS*) IN THE ESTUARINE WATERS OF TEXAS: A "DOVE TALE" OF THE ELUSIVE AMERICAN EEL (*ANGUILLA ROSTRATA*)

by

Justin Ray Hansen, B.S.

THESIS

Presented to the Faculty of

The University of Houston-Clear Lake

In Partial Fulfillment

Of the Requirements

For the Degree

MASTER OF SCIENCE

in Environmental Science

THE UNIVERSITY OF HOUSTON-CLEAR LAKE

MAY, 2020

SPECKLED WORM EEL (*MYROPHIS PUNCTATUS*) IN THE ESTUARINE WATERS OF TEXAS: A "DOVE TALE" OF THE ELUSIVE AMERICAN EEL (*ANGUILLA ROSTRATA*)

by

Justin Ray Hansen

APPROVED BY:

_____
George Guillen, Ph.D., Chair

_____
Marc Mokrech, Ph.D., Committee Member

_____
Stephen Curtis, M.S., Committee Member

RECEIVED/APPROVED BY THE COLLEGE OF SCIENCE AND ENGINEERING:

_____
David Garrison, Ph.D., Associate Dean

_____
Miguel A. Gonzalez, Ph.D., Dean

Dedication

I dedicate this work to both James Hansens in my world. The elder, my twin, is a man whom garners respect and admiration from those who have the privilege to share even the most subtle, everyday interactions with him. I have continually looked to him as the standard for what it means to grow and learn as a teenager, young adult and into fatherhood. The younger, my little boy, who received his name sake from the elder, serves as an everyday inspiration to be more than just an individual concluding life with the circumstances which were provided since birth. My son is the sweetest little boy who can make anyone smile with his silly nature and kind, loving heart.

Acknowledgements

I would like to thank my thesis chair, Dr. George Guillen and all of my committee members. I possess a tremendous helping of gratitude for the Environmental Institute of Houston (EIH) as they allowed me to work towards my master's degree as part of their commitment to scientific excellence. EIH graciously provided troves of assistance with the gear deployment, processing and clean up, all of which would not be possible without the dedicated heart beats of all individuals involved. I would also like to extend acknowledgments to Texas Parks and Wildlife Department for funding this project, with a big thanks to Stephen Curtis for being an excellent collaborator through the entire process.

ABSTRACT

SPECKLED WORM EEL (*MYROPHIS PUNCTATUS*) IN THE ESTUARINE WATERS OF TEXAS: A "DOVE TALE" OF THE ELUSIVE AMERICAN EEL (*ANGUILLA ROSTRATA*)

Justin Ray Hansen
University of Houston-Clear Lake, 2020

Thesis Chair: George Guillen, Ph.D.

Atlantic Anguillids share unique life histories where they undergo metamorphosis as they move from deep water to nearshore habitats, though their life history strategies differ slightly; some of the primary mechanisms driving their distribution and recruitment are the same. The juvenile American Eel (*Anguilla rostrata*), a catadromous species, was targeted for this study. Historically, all American Eel life stages have been subjected to commercial fishing pressure and dramatic reductions have been observed in indices of their abundance. The Gulf of Mexico is data deficient with respect to early life history of this unique species, and more specifically the Texas coast. The central and upper Texas coastal marsh and estuarine habitats were targeted for this study to detect ingressing glass eels as they settle in the coastal habitats and eventually pursue upstream migration. In an unexpected turn of events, juvenile American Eel were not captured; however, Speckled

Worm Eel (*Myrophis punctatus*) were captured every month of the study period from July 2018 to July 2019 using modified fyke nets as the standard sampling technique. Furthermore, metamorphic, glass and elver life stages were detected with the early life stages appearing in estuarine waters in December 2018 and peaking in February and March of 2019, suggesting recruitment of Speckled Worm Eel occurs in the winter and spring months along the Texas Coast. Though consistently captured, there was high spatial variability in catch per unit effort across coastal subbasins ($CPUE_{SB}$) defined by total Speckled Worm Eel captured divided by cumulative hours fished within each subbasin. The highest $CPUE_{SB}$ sampled were Matagorda Bay (4.050), Brazos River (2.879) Galveston Bay (0.203), and Sabine Lake (0.223). The occurrence of Speckled Worm Eel was modeled using Binomial Logistic Regression with various predictors. Regression results indicated significant negative relationships between occurrence with Secchi depth (m), a proxy for water clarity, and water temperature (℃), and a positive relationship with salinity (psu). As Speckled Worm Eel metamorphosed to elvers, morphometric comparisons revealed dramatic increases in average head length from 5% to 10% of their total length, decreased average body depth as a ratio of total length from 4.3% to 2.4%, and no change in the average preanal length by total length ratio. Weight length relationships were characterized by a non-linear power model relationship $W=aL^b$ and shows that metamorphic life stage ($b=2.666$) displayed reverse negative allometric growth (body shrinkage), while glass eel ($b=2.917$) and elver ($b=3.013$) both displayed isometric growth. As a species, positive allometric growth is observed ($b=3.127$). The results presented in this study help to better characterize the life history of a very cryptic species along the Texas coast, which may be underrepresented in catches by state fisheries independent monitoring programs. The results of this study contribute to the knowledge base of the species as a whole and supports the notion that fyke nets are an

excellent passive method for detecting Anguillids at all life stages. Furthermore, the effectiveness of the fyke nets in collecting Speckled Worm Eel suggests that the observed zero CPUE of American Eels is likely due to the true absence of this species and not due to gear selectivity or active avoidance.

TABLE OF CONTENTS

LIST OF TABLES

LIST OF FIGURES

CHAPTER 1:

AMERICAN EEL

Introduction

The American Eel (*Anguilla rostrata*) is a facultative catadromous fish inhabiting North America, the Caribbean, Gulf of Mexico (GOM) (Benchetrit and McCleave, 2016) and the northern reaches of South America (Lamson et al., 2006). They undergo extensive migrations during their adult life stage (Silver eel) and leptocephalus larval stage (Béguer-Pon et al., 2015; Miller et al., 2015). The adults travel from continental waters to the Sargasso Sea, where they are assumed to undergo panmictic and semelparous reproduction. More recently, extensive genetic efforts of heterogeneity across space and time have supported the assumption of the panmictic reproduction (Côté et al., 2013). The random nature of mating is presumed to be a stable component of their population and thus provides some plasticity to long term trends in the indices of abundance (Shepard, 2015b).

Once the eggs hatch, the Gulf Stream becomes the primary transport mechanism dispersing American Eel larvae along the Western Atlantic Ocean (Kleckner and McCleave, 1982). Movement into the GOM and how the Gulf Current Loop influences their dispersion has not been well studied. Miller et al. (2015) suggests the southernmost spawned larvae are subjected to south-northwest and/or south-westward currents that facilitate Caribbean and Northern GOM transport. Leptocephali may drift for 8 to 12 months prior to metamorphosis (Kleckner and McCleave, 1985) and as they approach nearshore habitat, metamorphosis to glass eel occurs to prepare for estuarine settlement (Antunes and Tesch, 1997; Wang and Tzeng, 2000; van Ginneken and Maes, 2005). Metamorphic duration from letptocephalus to glass eel is estimated to be between 18 and 52 days and recruitment as glass eel is between 171 and 252 days (Arai et al., 2000),

although what triggers the metamorphosis in still unclear (Miller, 2009a). Cresci et al. (2017) recently discovered evidence for the ability of European glass eels (*Anguilla Anguilla*) to utilize the magnetic field to orient towards the Gulf Stream after being displaced from European waters which maximizes the probability of successful migration back to Europe. This finding suggests that leptocephali are also likely to exhibit the same homing behavior and the authors postulate it is most likely a mechanism shared by congeners of the European Eel, which American Eel are the closest extant sister taxa. This newly discovered information compliments the hypothesis that the link between olfaction and fresh water cues plays a vital role in the migration and settlement of recently metamorphosed glass eels (Sorensen, 1986; Sola and Tongiorgi, 1996; Sullivan et al., 2006).

It was historically presumed that fresh water ingression of catadromous eels was obligatory; however, otolith microchemistry has demonstrated a substantial degree of plasticity in their life history strategy where inhabitation occurs in fresh, brackish and saltwater environments or distinct transient movements between (Jessop et al., 2002; Morrison and Secor, 2003; Daverat et al., 2006; Lamson et al., 2006). The findings of non-obligatory existence in freshwater are underscored by evidence of spatially varying allele selection driven by extensive variation in habitat and environmental conditions throughout their extensive range (Gagnaire et al., 2012). Glass eels will halt ingression near the bottom of the channel during ebb tide and will use the incoming tidal currents to enter estuarine habitats (McCleave, 1987; Wippelhauser and McCleave, 1987). Tidal cycles have been well established in scientific literature as a primary factor influencing upstream migration of juvenile American Eel and other Anguillids (Martin, 1995). As glass eels move within the estuarine environment towards rivers and streams, their behavior and movement is highly linked to the timing and intensity of ebb and flood

tides. This linkage and process is defined as Selective Tidal Stream Transport (STST) (McCleave and Kleckner, 1982; Wippelhauser and McCleave, 1987). Selective Tidal Stream Transport strategy is exhibited by all catadromous fishes (Trancart et al., 2014). American Eel also exhibit this unique rhythmic activity that corresponds to changing tidal cycles but forgo this behavior once they reach the upstream non-tidal reaches of fresh water systems (Wippelhauser and McCleave, 2009). Upon reaching the non-tidal interface, glass eels apparently delay their upstream migration, which is speculated to be a result of physiological and behavioral changes (Sorensen and Bianchini, 1986). After the first year of post recruitment development into estuaries, glass eels usually develop into elvers and begin their upstream migration, while it is estimated that up to 25% of the upstream freshwater ingression is composed of yellow eel juveniles (Jessop et al., 2008). Glass eels of the Shortfin Eel (*Anguilla australis*) and Longfin Eel (*Anguilla dieffenbachii*) are more concentrated along river edges during ebb tides, likely to avoid high downstream flow (Jellyman, 1979; Jellyman and Lambert, 2003a). Glass eels of American Eel actively swim along stream and river shorelines past tidal currents (Barbin and Krueger, 1994), while elvers have been shown experimentally to use the sediment as a reprieve from current velocity (Barbin and Krueger, 1994).

Conservation Status

American Eel populations have undergone extensive review over the past several decades to assess status under the Endangered Species Act (ESA). Strong declining trends in commercial landings of American Eel emerged in the 1980s and 1990s across various spatial scales. These data were limited and most likely underrepresented, providing researchers with an incomplete understanding of the population declines (Haro et al., 2000). The United States Fish and Wildlife Service (USFWS) was tasked with evaluating the potential listing of American Eel under the ESA. In 2007, the USFWS

determined that a threatened or endangered protection of the American Eel was not justified with the current evidence (USFWS, 2007). After a proceeding petition to consider the listing in 2010, USFWS determined again the American Eel did not meet listing criteria (Shepard, 2015b). The Atlantic State Marine Fisheries Commission (ASMFC) 2017 American Eel Stock Update demonstrated that the status of American Eel reported during the 2012 assessment had changed little and the American Eel stock is was still considered depleted (ASMFC, 2017).

The Global NatureServe Rank for American Eel was last reviewed in 2011 and is listed as a G4 or "Apparently Secure" (NatureServe 2.0). In the GOM, American Eel are listed as a Species of Greatest Conservation Need in Texas, Louisiana, and Florida (TPWD, 2012). The State of Louisiana has recommended a State NatureServe Rank of S4 or "Apparently Secure" (Shanks, 2014). While Texas has recently updated their State NatureServe Rank for American Eel from an S4 to an S2 or "Imperiled" (Cohen et al., 2018).

Historically, subadult American Eels have been found in large river drainages across Texas from the Rio Grande to the Red River. Recent efforts have considered them extirpated from several systems due to migratory impediment by dams (Hubbs, 2002).

An important area of study for the American Eel is related to juvenile (glass eel and elvers) recruitment along the continental shelf and into the bays and estuaries of the Atlantic, GOM and the Caribbean. The ingress of larval fishes, especially metamorphic larvae, may heavily influence the outcome of their resulting adult population success (Able et al. 2011). American Eel early life history and recruitment is well studied along the Western Atlantic coastline, yet the GOM, and more specifically Texas, have been poorly studied. Given their panmictic reproduction, collection of American Eel data from the GOM and Texas would provide better population estimates and critical information

on spatially varying trends that may compliment the long-term monitoring of American Eel in the Atlantic. The primary objectives of this study are 1) To assess spatial distribution of juvenile American Eel in Texas, 2) To quantify relative abundance of juvenile American Eel in Texas, 3)To describe the temporal recruitment in which juvenile American Eel make their ingression in Texas.

Methods

Study Area

The sampling area ranged from the Lower Corpus Christi Bay Basin (27°39' 25.4"N, 97°24' 7.27"W) to the Sabine Basin (30°01'06.0"N, 93°45'20.5"W) along the Texas/Louisiana Border (Figure 1). The sampling locations were selected primarily within the estuarine environment along the Texas Coast. For the purposes of this study, the sampling events were divided into five areas along the Texas Coast. The sampling spanned west to east across 1) Corpus Christi Bay and Aransas Bay watersheds, 2) Matagorda Bay watershed, 3) Colorado and Brazos River watersheds, 4) Galveston Bay watershed, and 5) Sabine Lake watershed. Historically, the Colorado River discharged into Matagorda Bay; however, the river was diverted by the U.S Army Corp of Engineers and completed in 1991. The Brazos River too was historically diverted and empties directly into the GOM along with other major order rivers in the area, such as the San Bernard River. The Gulf Intracoastal Waterway connects all major bays within the study area.

Sampling

Sampling occurred from the week of June 25th, 2018 through the week of July 15th, 2019 on a biweekly basis across one of the four sampling areas. Fyke nets were the standard sampling method used for the duration the project. Fyke nets are generally accepted as the most effective passive sampling technique for capturing juvenile and

adult life stages of Anguillids on the Atlantic Coast (Oliveira, 1999; Jellyman and Graynoth, 2005; Lake, 2013; Bowser, 2018). When possible, fyke nets were deployed in tidal rivers and streams below obstructions or barriers that impeded upstream movement (Figure 2). Nets were oriented in a downstream direction and placed in the water adjacent to the bank with one wing positioned at the shoreline while the second wing extended at a fixed distance of 13.5 ft towards the channel (Figure 3). Gear placement was selected to capitalize on an observed behavior by which glass eels are forced along the shoreline in rivers and streams during ebb tides (Jellyman and Lambert 2003). A series of three to four nets were deployed with one net at each site over the course of two days which resulted in seven to eight net sets total per sampling event. Due to the cryptic and nocturnal nature of American Eel and the need to fish an entire tidal cycle, nets were allowed to soak overnight.

Ambient water quality and habitat data were collected at each site during the initial set and retrieval of the sampling gear. A YSI ProDSS data Sonde was used to measure water quality variables including temperature (°C), specific conductance (µS/cm), conductivity (µS/cm), salinity (psu), pH, dissolved oxygen concentration (mg/L) and saturation (%). Water clarity was estimated using a 1-meter deep Secchi tube with the depth recorded at the disappearance of the disc. In-stream habitat was quantified using percent area covered from wing to wing and 10 meters out (Table 1). Habitat data were recorded for adjacent instream and shoreline areas. Shoreline habitat for each site was characterized by dominant macro-habitat type and dominant sediment was classified (Table 1). Primary aquatic vegetation was identified to lowest possible taxon, usually genus or species. Stream width (m), net depth (m) and thalweg depth (m) were estimated using a range finder and a stadia rod, respectively. In the event stream width could not be estimated in the field, Google Earth was used. Tide stages and Mean Low-Low Water

(MLLW) levels (ft) were gathered from the closest National Oceanic and Atmospheric Administrations (NOAA) tide stations. Lunar phase and percent illumination were recorded as well. Eight-digit hydrological unit codes (HUCs) which correspond to major watershed subbasins, developed by the United States Geological Survey (USGS), were reported for each net deployment site. Two HUC-8 IDs, 12100401 and 120904002, carry the same subbasin name: East Matagorda Bay. For the purposes of this study, the HUC-8 ID 12100401 was classified as "East Matagorda Bay-W" for its western most position relative to 120904002, which was categorized as "East Matagorda Bay-E."

Nekton captured in the cod end of the net were identified to species and all finfish were enumerated. Nekton trapped at the excluder, but not captured in the cod end of the net, were identified and placed in relative abundance categories (1=rare, 2=common, 3=abundant) (Figure 3). All invertebrates captured were placed into the same three relative abundance categories. If proper identification was not feasible in the field or when biomass or abundance were exceptionally high (>500), specimens were administered a lethal dose of MS-222, preserved in a buffered 10% formalin solution and later transferred to 70% ethanol and identified in the lab. Any Anguilliformes captured in the fyke nets were retained in site water and stored on ice until a positive identification was made (which often required returning to the laboratory to use microscopes to confirm identification of small individuals).

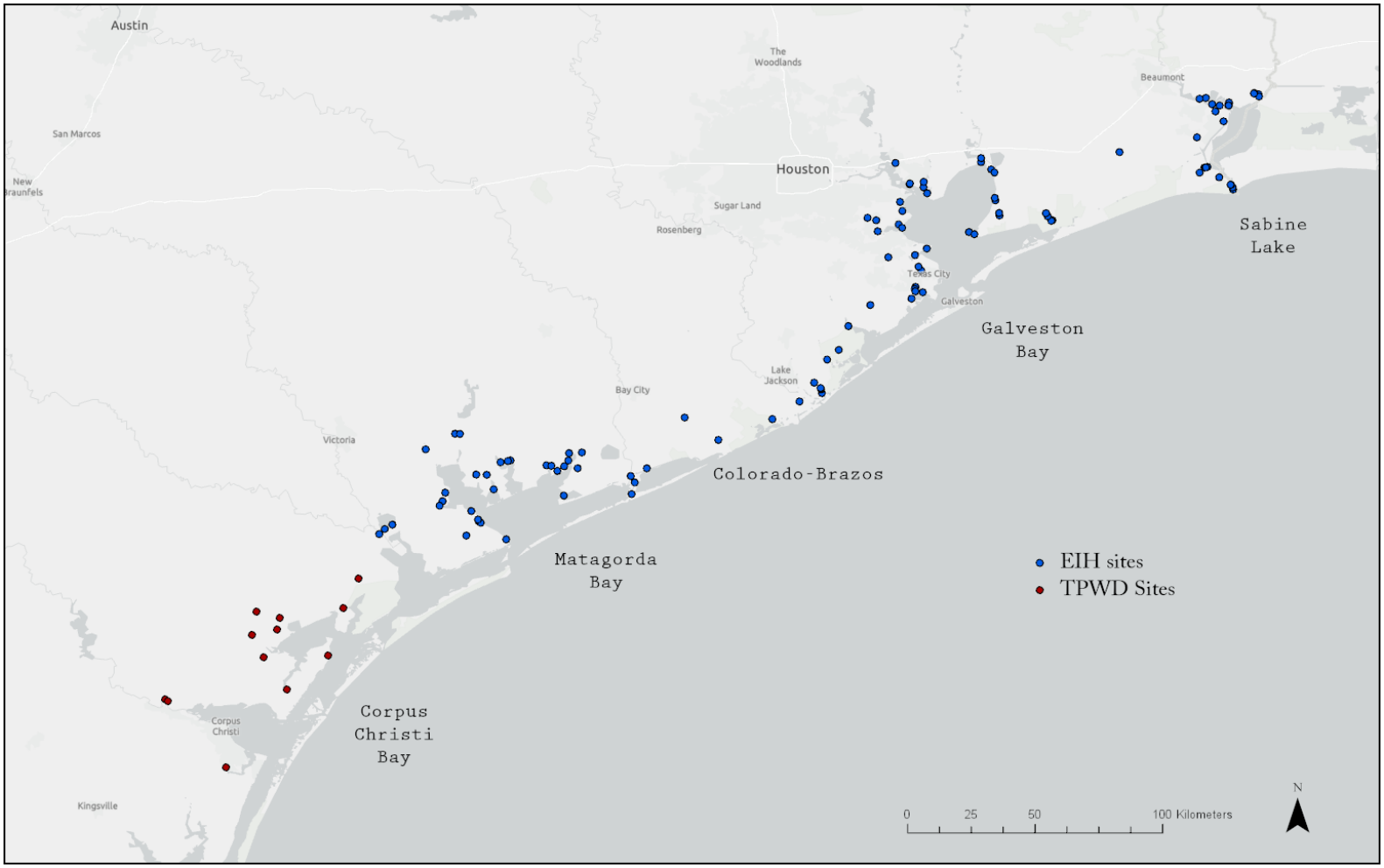

Figure 1 Map of all sample sites along the Central and Northern Texas Coast from Corpus Christi Bay, TX to Sabine Lake, TX. Red circles indicate Texas Parks and Wildlife Department sites and blue circles represent sites from Environmental Institute of Houston.

Figure 2 Display of ideal placement of a fyke net in an estuarine habitat with an obstruction upstream of the net placement.

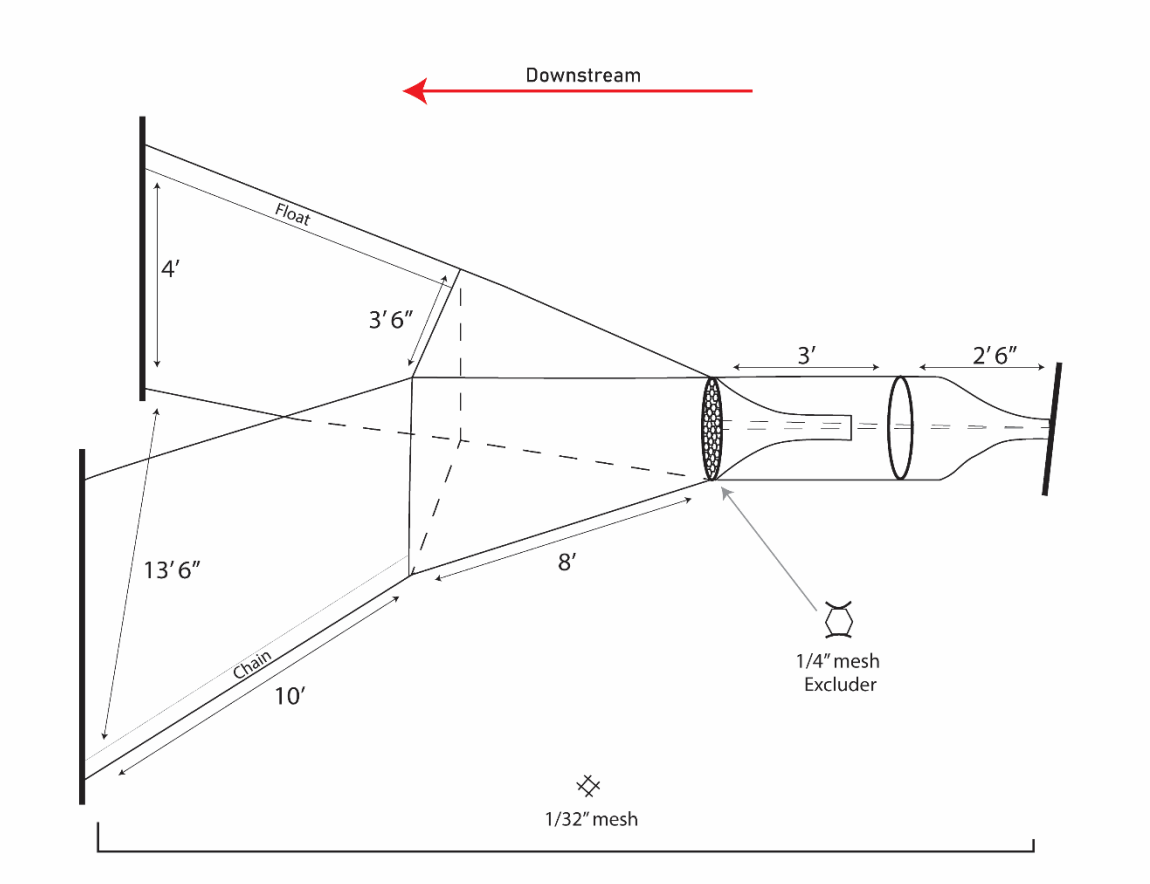

Figure 3 Schematic of a modified fyke net used for sampling with specifications in feet for all netted components and suggested orientation.

Table 1 Descriptions and examples of instream habitat, shoreline habitat and sediment classifications used during this study.

Instream Habitat		**Shoreline habitat**		**Sediment**
Type	**Examples**	**Type**	**Examples**	**Type**
Macrophyte	Saltmarsh cordgrass, needle rush, Hydrilla	Emergent Aquatic Vegetation	Saltmarsh cordgrass, needle rush	Silt
Wood debris	Sticks and logs	Woody Vegetation	Trees or shrubs	Clay
Overhanging vegetation	Tree branches and leaves, inflorescence	Bare ground	Dirt or sand	Sand
Oyster reef	Oyster reefs or bars/beds	Oyster	Oyster beds/reef	Shell hash
Boulders/ Ledges	Rocks, steep drop off	Rip/rap	Rocks and boulders or slabs of concrete	
Artificial structure	Tires, pipes, road debris	Artificial substrate	Bridges, concrete trials	
Undercut Bank	Eroded bank			
Filamentous algae	Attached to rocks, plants or floating			

Results

A total of 202 net deployments were conducted at 110 sites from June 2018 to July 2019. Texas Parks and Wildlife Department (TPWD) staff conducted additional sampling at 11 sites for a total of 24 net deployments to expand the study range in the Corpus Christi Bay area (Figure 1). A total of 108,485 fishes comprised of total of 61

species representing 29 families were collected during this study (Table 2). American Eel were not captured.

Most of these specimens were juveniles, due to the ¼" excluder, and the gear was biased towards fish that are laterally or dorsoventrally compressed. The adult fishes present in the catch were primarily Fundulids (topminnows and killifish), which use estuarine wetland habitat as permanent residents (Table 2). The five most abundant fish species comprised 83.1% of the total catch. This included Gulf Menhaden (*Brevoortia patronus*) at 36.6%, Bay Anchovy (*Anchoa mitchilli*) at 21.1%, Ladyfish (*Elops saurus*) at 16.7%, Atlantic Croaker (*Micropogonias undulatus*) at 6.1% and Rainwater Killifish (*Lucania parva*) at 2.6%. Invertebrates present in the catch represented six families and were composed primarily of shrimp species: in the families Palaemonidae and Penaeidae (Table 3). The two species with the highest average relative abundance category were Dagger Blade Grass Shrimp (*Palaemonetes pugio*) and White Shrimp (*Litopenaeus setiferus*) with 2.1 and 2.2, respectively.

Water quality variables, including water temperature and dissolved oxygen followed expected seasonal patterns in their respective ranges (Table 4).

Table 2 Summary of fish species captured in the cod end of the fyke nets from June 2018 to July 2019, with estimates of total catch included.

Family	Scientific Name	Common Name	Total Catch
Elopidae	*Elops saurus*	Ladyfish	18,113
Ophichthidae	*Myrophis punctatus*	Speckled Worm Eel	2,323
Engraulidae	*Anchoa mitchilli*	Bay Anchovy	22,933
Clupeidae	*Brevoortia patronus*	Gulf Menhaden	39,747
	Dorosoma cepedianum	Gizzard Shad	1
	Dorosoma petenense	Threadfin Shad	1,877
Cyprinidae	*Cyprinella lutrensis*	Red Shiner	1
	Cyprinella venusta	Blacktail Shiner	14
	Opsopoeodus emiliae	Pugnose Minnow	1
Catostomidae	*Ictiobus niger*	Black Buffalo	1
Characidae	*Astyanax mexicanus*	Mexican Tetra	1
Ictaluridae	*Ictalurus furcatus*	Blue Catfish	1
Esocidae	*Esox americanus*	Red fin Pickerel	4
Mugilidae	*Mugil cephalus*	Striped Mullet	1,829
Atherinopsidae	*Menidia beryllina*	Inland Silverside	1,255
Fundulidae	*Adinia xenica*	Diamond Killifish	393
	Fundulus chrysotus	Golden Topminnow	9
	Fundulus grandis	Gulf Killifish	592
	Fundulus jenkinsi	Saltmarsh Topminnow	312
	Fundulus similis	Longnose Killifish	9
	Lucania parva	Rainwater Killifish	2,814
Cyprinodontidae	*Cyprinodon variegatus*	Sheepshead Minnow	454
Poeciliidae	*Gambusia affinis*	Western Mosquitofish	2,442
	Heterandria formosa	Least Killifish	78
	Poecilia formosa	Amazon molly	56
	Poecilia latipinna	Sailfin Molly	1,047
Syngnathidae	*Syngnathus louisianae*	Chain Pipefish	16
	Syngnathus scovelli	Gulf Pipefish	44
Centrarchidae	*Lepomis gulosus*	Warmouth	1
	Lepomis macrochirus	Bluegill	30

Table 2 Summary of fish species captured in the cod end of the fyke nets from June 2018 to July 2019, with estimates of total catch included.

Family	Scientific Name	Common Name	Total Catch
	Lepomis megalotis	Longear Sunfish	1
	Micropterus punctulatus	Spotted Bass	9
	Pomoxis annularis	White Crappie	1
Lutjanidae	*Lutjanus griseus*	Grey Snapper	1
Gerreidae	*Eucinostomus argenteus*	Spotfin Mojarra	13
	Eucinostomus melanopterus	Flagfin Mojarra	180
Sciaenidae	*Bairdiella chrysoura*	Silver Perch	12
	Cynoscion arenarius	Sand Sea Trout	23
	Cynoscion nebulosus	Spotted Seatrout	889
	Leiostomus xanthurus	Spot	1,719
	Micropogonias undulatus	Atlantic Croaker	6,624
	Sciaenops ocellatus	Red Drum	72
	Stellifer lanceolatus	Star Drum	22
Sparidae	*Lagodon rhomboides*	Pinfish	833
Carangidae	*Oligoplites saurus*	Leatherjack	6
Cichlidae	*Herichthys cyanoguttatus*	Rio Grande Cichlid	2
Gobiesocidae	*Gobiesox strumosus*	Skilletfish	1
Gobiidae	*Ctenogobius boleosoma*	Darter Goby	289
	Gobioides broussonetii	Violet Goby	20
	Gobiosoma bosc	Naked Goby	346
	Gobiosoma robustum	Code Goby	111
	Microgobius gulosus	Clown Goby	1
	Microgobius thalassinus	Green Goby	1
Eleotridae	*Dormitator maculatus*	Fat sleeper	49
	Eleotris pisonis	Spiny-cheek Sleeper	1
	Erotelis smaragdus	Emerald Sleeper	3
Paralichthyidae	*Paralichthys lethostigma*	Southern Flounder	4
Achiridae	*Trinectes maculatus*	Hogchoker	41
Cynoglossidae	*Symphurus plagiusa*	Blackcheek Tonguefish	229
Grand Total			108,485

Table 3 Summary of invertebrates collected in the cod end of the net from June, 2018 to July, 2019, including average relative abundance.

Family	Scientific Name	Common Name	Average Relative Abundance
Ctenophora	*Ctenophora*	Comb Jellyfish	2
Astacoidea	*Astacoidea spp.*	Crayfish	1
Palaemonidae	*Macrobrachium ohione*	Ohio River Shrimp	2
	Palaemonetes pugio	Daggerblade Grass Shrimp	2.1
	Palaemonetes spp.	Grass Shrimp	1.9
Penaeidae	*Farfantepenaeus aztecus*	Brown Shrimp	2
	Litopenaeus setiferus	White Shrimp	2.2
	Penaeidae spp.	Penaeid Shrimp	1.5
Portunidae	*Callinectes sapidus*	Blue Crab	1.7

Table 4 Summary statistics for water quality variables measured at all sampling sites across all sampling events from June, 2018 to July, 2019.

Variable	Minimum	1st Quartile	Mean	3rd Quartile	Maximum
Temperature (°C)	11.1	16.27	22.24	27.9	31.30
Salinity (psu)	0.07	0.43	5.47	8.37	35.10
Dissolved Oxygen (mg/L)	1.03	5.11	6.53	8.22	11.77
pH	6.62	7.34	7.64	7.94	9.24
Secchi (m)	0.01	0.15	0.27	0.32	1.01

Discussion

Despite extensive biweekly sampling efforts, juvenile American Eel were not detected within the sampling area. Thus, juvenile American Eel ingression in Texas has

not been well documented to date. Yellow stage American Eel, the subadult life stage that primarily uses freshwater systems to reach reproductive maturity, are commonly documented across river systems of Texas, implying that successful recruitment of juveniles has occurred in recent decades and is still likely occurring. A few historical records and specimens that may demonstrate juvenile detection are housed in the Biodiversity Collections at the University of Texas at Austin, though collection information such as gear type is limited. Potential elver life stages have been documented along the central portion of the Texas Coast based on the lengths and estimation of life stage for three specimens (TNCH3140, 50436 and 59565) (Hendrickson and Cohen, 2015). The dates of capture were from March 1952, October 1953 and August 2008, respectively. Specimen TNCH3140 was found further inland in a completely freshwater environment in the Guadalupe River near Cuero, Texas. Capture in non-tidal, fresh water reaches signifies the individual has successfully recruited. Total length of this specimen was recorded at 112.6mm, which is similar in size to young of the year individuals observed migrating into rivers in Maine (Shepard, 2015a). Specimen 50436 was captured along a concrete barrier near Lake Corpus Christi Dam. Less information regarding this specimen is available, yet aggregation at impassible barriers is commonly observed for the elver life stage (Sullivan et al., 2009b). Specimen 59565 was located near Aransas Wildlife Refuge, an environment in the upper estuary that transitions into freshwater habitat. Because of the facultative nature of their catadromy, it is highly plausible that elvers would continue their life cycle near coastal habitats (Jessop et al., 2002; Daverat et al., 2006; Lamson et al., 2006). Furthermore, three individuals of American Eel leptocephali were collected (TNHC31476), presumably, by the USFWS (Hendrickson and Cohen, 2015).The specimens were collected on November 12th, 1980 near the Lower

Colorado River where it historically drained into Matagorda Bay prior to 1990. These specimens have not been confirmed; thus, this life stage identification should be viewed with caution since past studies have shown metamorphosis from leptocephalus to glass eel stage occurs as individuals approach the offshore continental shelf.

Standardized sampling effort along the Texas Coast by TPWD consists of continual fishery independent monitoring of coastal, estuarine, and nearshore Gulf of Mexico waters using a variety of methods including bag seines, trawls, gillnets, and oyster dredges. American Eel are mentioned as a species that has been collected with such gear, yet the most recent manuscript (Campbell and Fuls, 2005) that summarizes catches of select species sampled long term along Texas coastal waters yields just the detection of the species. Although extensive sampling effort has been conducted along the Texas Coast by TPWD, American Eel likely remain undetected due to their nocturnal nature and selectivity bias of the gear type used in standardized monitoring.

Recent studies have been conducted in the Sabine River in preparation for relicensing of hydropower reservoirs at Toledo Bend Reservoir (HDR, 2011). Consistent densities of juvenile and subadult American Eel with varying size classes have been collected from the Sabine River just below Toledo Bend Dam at River mile 146 from 2009 to 2010 via (BIO-West, 2011b). These studies suggest only a limited number of juvenile eels migrate to this point of the river each year during mostly warmer months extending from April to November. Yet, based on size class structure of this sample, recruitment appears to be occurring regularly in this portion of the river.

Even though sampling effort during the first year of this study failed to detect ingression of American Eel glass or elver ingression into the estuarine and freshwater systems of the central and northern coast of Texas, the effort was able to detect fishes

from other taxa within the super order Elopomorpha which share the leptocephalus larvae life stage with American Eel as a prominent derived characteristic (Greenwwod et al., 1966; Hulet and Robins, 1989; Chen et al., 2013). Fyke nets yielded variable catches of Ladyfish and Speckled Worm Eel larval and early juvenile life stages. Furthermore, Speckled Worm Eel were captured during every month of sampling and detected in 69 of the 226 net deployments. Leptocephalus and metamorphic larvae of elopomorphs are subject to oceanic currents and fronts (Munk et al., 2010) and are transported to nearshore environments where settlement occurs in estuarine nursery habitats. American Eel metamorphosis is assumed to occur as they approach the continental shelf and the general gross transport mechanisms of larvae are similar between American Eel and Speckled Worm Eel (Miller, 2009; Miller and McCleave, 2007; Miller et al., 2015; Miller and Tsukamoto, 2016).

These findings suggest the fyke nets used in this study were effective at capturing the early life history stages of elopomorphs as they ingress and settle, and reinforces the suitability of this gear for detection of American Eel juveniles (Jellyman and Graynoth, 2005; Lake, 2013; Oliveira, 1999). The net design used in this study was modeled after the fyke nets used in the Hudson River American Eel Project (Bowser, 2018). Yearly recruitment and peak densities of glass and elver American Eel are regularly documented in the Hudson River Estuary further supporting the use of this gear type.

The life stages and body sizes of Speckled Worm Eel detected during this study were similar to the targeted glass and elver stages of American Eel. In addition, Speckled Worm Eel, like American Eel, utilize stream sediment and substrate to hide and bury themselves and are not captured with traditional sampling methods (Able et al., 2011; Springer and Woodburn, 1960). Ironically, at the Guana River Dam in Florida, glass

Speckled Worm Eels were accidently enumerated as glass American Eels until a large ingression of glass Speckled Worm Eel occurred, which helped investigators better distinguish the similarly transparent glass eels (Bonvechio, 2016). Repeated co-occurrence (Warlen and Burke, 1990; Able et al., 2011; Bonvechio, 2016) of these two species implies there may be a shared underlying mechanism driving their ingression. In the Florida Keys, onshore transport of leptocephali and glass eels were driven by overnight New Moon flood tides and strong onshore winds (Harnden et al., 1999). Thus, it can be concluded that if American Eel juveniles were present in high abundances during the dates and locations surveyed, their ingression would have likely been detected with sampling design used in this study.

Larval transport of American Eel leptocephali into the GOM has not been well studied. American Eel larvae have not been detected in the Northern GOM from plankton tows conducted in winter, spring and fall since 1983 by the Gulf State Marine Fisheries Commission (GSMFC) Southeast Area Monitoring and Assessment Program (GSMFC, 2016). Miller et al. (2015) suggests a south-northwestward or south-westward drift that encourages movement towards the GOM. Physical oceanic processes and circulation are further influenced by the interaction of large-scale processes occurring across the massive expanse of the GOM and their interactions with localized, coastal mechanisms. Though purely speculative, the lack of juvenile American Eel detection in the estuaries of the Texas coast may be linked to a highly variable transport mechanism throughout the GOM for the leptocephalus larval stage.

General circulation in the GOM is heavily influenced by the Gulf Loop Current where large anticyclonic rings are shed on an irregular basis (Sturges et al., 2010). Whereas primary nearshore movement is driven by wind, with summer winds primarily

driven from the south and winter winds driven form the north. The Gulf Loop Current primarily advances north as water comes up from the Caribbean GOM where the water then proceeds to make a 90° turn before proceeding out between the Caribbean and Florida into the Florida Current (Sturges and Leben, 2000). The anticyclonic eddies are described as areas of low productivity and are generally depleted of nitrate and chlorophyll in the upper 100m of the water column, leading to low productivity and low zooplankton biomass (Biggs, 1992). However, cold-core rings that spin in a cyclonic rotation are produced in close association with the anticyclonic eddied rings from the Loop Current (Lee et al., 1994), which are quite nutrient rich and harbor substantial densities of phytoplankton (Biggs et al., 1997). The authors move on to speculate that unlike the cold core rings produced in by the Gulf Stream in the Atlantic, the GOM cold core rings should sustain populations of zooplankton and nekton as the pockets of productivity are diminished by mixing with the surrounding waters.

Approximately 45% of net inflow driven into the GOM and the Loop Current from the Caribbean originates from the Southern Atlantic Ocean (Schmitz Jr and Richardson, 1991), with the remaining inflow derived from the North Atlantic Region. If the south-westward movement mechanism speculated by Miller et al. (2015) is correct, American Eel larvae drifting into the GOM would be subjected to the oceanic forcing driven by the Gulf Loop Current. Leptocephali collected in the Florida Current utilized the upper 140m of the water column at night and the upper 350m column during the day (Kleckner and McCleave, 1982). Thus, it would be reasonable to expect the leptocephali transport in the GOM and ingress into the estuary and freshwater tributaries would be influenced to a degree by the primary circulation mechanism in the GOM.

There are limitations present in the sampling design of this project that could have influenced the ability to collect juvenile American Eel. A primary objective of this project was to assess the spatial distribution of American Eel along the Central and Northern Texas Coast by deploying gear in as many accessible areas as possible. However, the gear were limited to a depth of less than five feet. Furthermore, the fyke net mesh diameter was quite small and would subject the nets to exceptional cross sectional drag if placed in the centroid of the flow and potentially dislodge them from their fishing position. These limitations on net deployment and orientation reduced the potential locations in where nets could be deployed. In addition, detection probabilities may have been reduced if the nets were not in the direct path of their migratory route. Though, glass eels have been observed along the margins of streams during peak ebb tides (Jellyman and Lambert, 2003b) and are known to actively swim along the shoreline once they move upstream of the head of the tide (Barbin and Krueger, 1994). This suggests they are likely to use the shoreline as the most likely migratory route and river and stream margins in tidal and non-tidally influenced locations appear to be the best locations for fyke net deployment.

The biweekly sampling effort conducted during this study may have provided a very narrow window of time for juvenile American Eel to be detected over a large spatial extent. Sullivan et al. (2009a) has shown high variability in the number of glass eel and elvers collected across several New Jersey estuaries. Collectors captured between one to greater than 1,500 individuals between sampling locations and sampling events. In general; however, ingression windows for American Eel on the Atlantic Coast can be quite extensive temporally with some estimates ranging from November to April depending on location (Sullivan et al., 2006). It is more likely that juvenile American Eel

are not reaching Texas shores in high enough densities to be easily detected by the sampling gear and methods used in this study.

Future Work

During this study, sampling effort spanning large spatial and temporal scales were unable to detect American Eel. More spatial specific sampling efforts should be conducted over shorter intervals, especially in water bodies where subadults are being captured presently, such as the Sabine River (Bio-West, 2011a). Employing alternative passive sampling methods in conjunction with the fyke nets may enhance detection probabilities. Eel ramps and eel collectors are common passive methods used in areas where dams, spillways or weirs are easily accessible and create an impassable barrier over which eels would then have to negotiate (Sullivan et al., 2009b).

A larger, more comprehensive ichthyoplankton monitoring program is needed to evaluate the timing and location of larval eel movement into and within the GOM. Currently, only speculation is given on their migratory route into the GOM. Understanding the general route, timing and processes influencing their movement would help local resource managers' better estimate ingression of recently metamorphosed glass eels to support the conservation and management of American Eel along the Texas Coast and the Gulf Coastline in general.

CHAPTER 2:

SPECKLED WORM EEL

Introduction

The range of Speckled Worm Eel (*Myrophis punctatus*) extends from New Jersey, USA in the Western Atlantic contouring the entire Southern Atlantic Coast, to the Caribbean, across the GOM, and off the East coast of South America (Warlen and Burke, 1990; Able et al., 2011). This species commonly inhabits various estuarine and shallow water habitats including sea grass beds, mangroves, wild celery, and coastal marshes (Harnden et al., 1999; Barletta et al., 2000; Johnson and Heck Jr, 2006; Rozas and Minello, 2006). Although represented in the literature as composing a substantial proportion of catches in many instances, common occurrence of Speckled Worm Eel within their range is underpinned by a lack of information regarding their general ecology, reproduction, and life history strategies in certain portions of their range, notably the Northern GOM. Juvenile Speckled Worm Eel are seldom captured with traditional sampling gear with few exceptions, and it is speculated that their affinity to conceal themselves in sediment during their juvenile and adult stages may be the reason (Springer and Woodburn, 1960; Able et al., 2011). Studies conducted along the Western Atlantic Coast of North America have provided valuable information regarding this species and may provide insight into the ecology of this species in the GOM.

The reproductive ecology of Speckled Worm Eel is predicted to be similar to other Anguillids, where reproduction primarily occurs offshore (Able et al., 2011; Miller et al., 2015). Spawning is often reported in Florida, the South Atlantic Bight near Cape Hatteras (Fahay, 1978), and near the northern banks of the Bahamas (Miller, 1995; Miller and McCleave, 2007). Recently, data on several leptocephali occurring as far north as

New York State, have provided additional evidence of potential range expansion for this species (Schmidt and Wright, 2018). Recruitment of Speckled Worm Eel into estuaries and bays as larvae and juveniles has been well documented along the North American Atlantic Coast and within the eastern region of the GOM. Like American Eel, ingression of leptocephali and glass Speckled Worm Eel can vary widely. In Florida ingression is observed from November through March (Harnden et al., 1999; Bonvechio, 2016). In North Carolina, Warlen and Burke (1990) noted ingression is observed during December and tapered off in late spring with no observations after April; however, Fahay and Obenchain (1978) describe larval and juvenile stages present in North Carolina from November to April with no occurrences from May forward.

Like other Anguillids, Speckled Worm Eel exhibit diel ingression associated with low light periods which includes utilization of STST (Harnden et al., 1999). Unlike species of Anguillidae which metamorphose to glass eel nearshore, these fish enter estuaries at multiple life stages including metamorphic leptocephali, glass eels and elvers. Because this critical period of development is in some instances very brief, data gaps can exist in general life history of many fishes which undergo rapid extreme metamorphosis. Descriptions of particular morphological characteristics for early life stages of Speckled Worm Eel along the Atlantic Coast have been well summarized in Able et al. (2011), yet it is unclear if the same characteristics are consistent for Speckled Worm Eel in the Northern GOM.

The purpose of this chapter is to 1) characterize the relative temporal and spatial ingression of Speckled Worm Eel larval and juvenile life history stages in the Central and Northern Texas Coast, 2) describe potential associations between Speckled Worm Eel occurrence and ambient water quality using binomial logistic regression, 3) Develop

statistical models that describe length vs weight relationships, and 4) determine key metamorphic differences in life history stages as ingression occurred using Able et al. (2011) as a foundational point of comparison.

Methods

The environmental and biological data collected and discussed for this chapter were obtained using the methods outlined in chapter one, including fyke net deployment, habitat and water quality assessment measurements.

Spatial and Temporal Patterns

Temporal and spatial patterns in the relative abundance of Speckled Worm Eel were represented as catch per unit effort (CPUE) by the month and the subbasin in which the sties were sampled. Monthly CPUE is defined as the $CPUE_M$ = total eel abundance in each month / total hours fished in each month. Sites were grouped by the USGS HUC 8 subbasins to describe the spatial extent of data collection, therefore the CPUE through sampling space was defined as $CPUE_{SB}$ = total eel abundance in each subbasin / total hours fished in the given subbasin.

Habitat and Water Quality

Environmental and meteorological variables were used to assess potential association between individual variables and the presence and absence of Speckled Worm Eel. Fisher's exact test ($\alpha = 0.05$) was used to detect differences in the proportion of sites where eels were collected by moon phase and sediment type. Binary logistic regression modeling was used to evaluate the outcome of presence or absence of Speckled Worm Eel across all sites where the outcomes were described as follows: presence = 1, absence =0.

$$\pi = \frac{1}{1 + e^{-(\beta_0 + \beta_1 X_1 + \cdots \beta_i X_i)}} \quad (1)$$

Where π is represented as the overall probability of observing a positive outcome, i.e. a 1 vs 0 given a 1-unit increase in predictor variable $\beta_i X_i$. Applying the logit function and the binomial logistic regression to this study, π is the probability of detecting Speckled Worm Eel at a given site, and 1-π is the probability of not observing Speckled Worm Eel at a given site. In addition, the regression coefficient can be viewed as the odds ratio:

$$logit(\pi) = \ln\left(\frac{\pi}{1-\pi}\right) = \beta_0 + \beta_1 X_1 + \cdots + \beta_i X_i \quad (2)$$

$if\ logit(\pi) = 1\ ; \pi = 1 - \pi = 0.5$, odds are equal

$if\ logit(\pi) > 1\ ; \pi > 1 - \pi$, odds favor detection

$if\ logit(\pi) < 1\ ; \pi < 1 - \pi$, odds favor no detection

Environmental and habitat parameters were used as predictors which include values recorded during the net retrieval: Secchi depth (m), net depth (m), temperature (ºC), salinity (psu), pH, moon illumination (%), and tide stage. An iterative stepwise process was used to determine significant predictors in the model using Akaike Information Criteria (AIC) (Ramsey and Schafer, 2012). The goal was to determine the smallest number of predictors with the strongest effects. All data analysis was conducted using R and R studio (versions 3.6.3 and 1.2.5001).

Morphometrics and Length-Weight Relationships

The total length of each eel was measured and recorded to nearest 0.1mm and the corresponding total weight to the nearest 0.1g. Eels were subsequently persevered in 70% ethanol and weights were recorded at one minute after specimen removal from preservation solution. All other measurements and descriptions provided in Able et al. (2011) were used to distinguish between early life history stages of Speckled Worm Eel represented in this study: metamorphic (MET) defined as leptocephali currently metamorphosing or reducing in size, glass eels (GE) defined as transparent, yet a more cylindrical eel shape while continuing to reduce in size, and elvers (ELV) defined as the stage where pigmentation is covering the body and somatic growth begins. Morphometric measurements (Figure 4), also recorded to 0.1mm, included head length (*HL*) measured from the tip of the snout to the posterior edge of the operculum, preanal length (*PAL*) measured from tip of the snout to the origin of the anus, body depth (*BD*) measured at deepest portion of the body and body width (BW) measured from the point at which body depth was taken, as an additional measurement not described in Able et al. (2011).

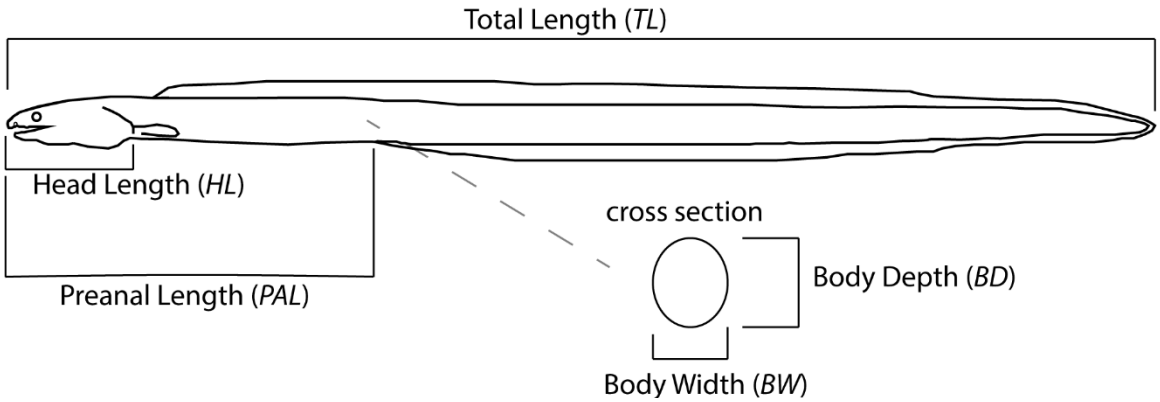

Figure 4 Illustration of Speckled Worm Eel and the morphometric measurements recorded including total length (TL), head length (HD), preanal length (PAL) body depth (BD), and body width (BW).

A length-weight relationship for the early life history stages of Speckled Worm Eel were modeled using Simple Linear Regression. However, when raw length was regressed against raw weight the relationship showed non-linearity and increasing variance with length. This pattern suggests a two-parameter power function with a multiplicative error term that may better describe the relationship:

$$W_i = aL_i^b e^{\varepsilon_i} \quad (3)$$

Where a and b are parameters and ε_i is defined as the multiplicative error term for the i^{th} fish (Ogle, 2016). Transforming the length-weight relationship using the natural logarithm (ln) of each variable allows the use of a simple linear model that the user can utilize to predict *ln(W)* with *ln(L)*:

$$ln(W_i) = ln(a) + b * \ln(L) + \varepsilon_i \quad (4)$$

Furthermore, the transformation facilitates the solving for the parameters of a linear equation with $y = ln(W)$, $x = \ln(L)$, $slope = b$ and $intercept = ln(\text{a})$.

To assess allometric growth of each life stage, and as a species, the estimated slope of linear length-weight relationship was tested. Isometric growth (b=3) suggests the weight of the fish changes with the cube of its length. Negative allometric growth (b < 3) is when the body of the individual becomes slenderer as the length increases. Positive allometric growth (b < 3) suggests the body increases in girth as a function of length. The difference between the estimated slope values for each life stage b_i and the expected value from isometric growth b= 3 were individually tested with one-sample t-test.

Morphometrics data were compared between all three life stages. All metrics were standardized by individual total lengths which provided proportional comparison across each life history stage. In addition, the body width was divided by body depth to assess the growth towards a more cylindrical form associated with juvenile development. The

Kruskal-Wallis rank-sum test (non-parametric ANOVA) was used to initially detect at least one difference between each life stage, followed by the Wilcoxon rank sum pairwise test (non-parametric pairwise test) between all life stages. All *alpha* levels were set to 0.05 and p-values below 0.05 were considered statically significant.

Results

Spatial and Temporal Patterns

Speckled Worm Eel were present at 69 of the 226 sites sampled during this study. A total of 2,338 Speckled Worm Eel were captured over the course of the study. Speckled Worm Eel were collected during each month of the study with peak catch observed in February 2019 (Figure 5), during which one net captured 1,514 individuals. All three life stages were represented in the catch with a total of 210 metamoprhic (MET) individuals collected from January to March of 2019, a total of 1,756 glass eel (GE) collected from December 2018 to April 2019, and a total of 357 elvers (ELV) collected during each month at variable densities (Figure 5). During December to April all three life stages were detected in variable numbers. In December, only glass eel and elvers were detected, composing up to 36% and 64% of the Speckled Worm Eel catch, respectively. Metamorphic individuals began appearing in the catch during January 2019, composing 17% of the total catch with glass eel representing 71% and elvers 12% of the total catch. During February, metamorphic and glass eel stages represented up to 13% and 86%, respectfully, while elvers represented only 1% of the total catch during this time period. Metamorphic eels were not detected in March while glass eel represented 58% of the eel catch followed by elver at 42%. April catches contained the second largest composition of glass eel at 77% and 23% of the total catch was composed of elver.

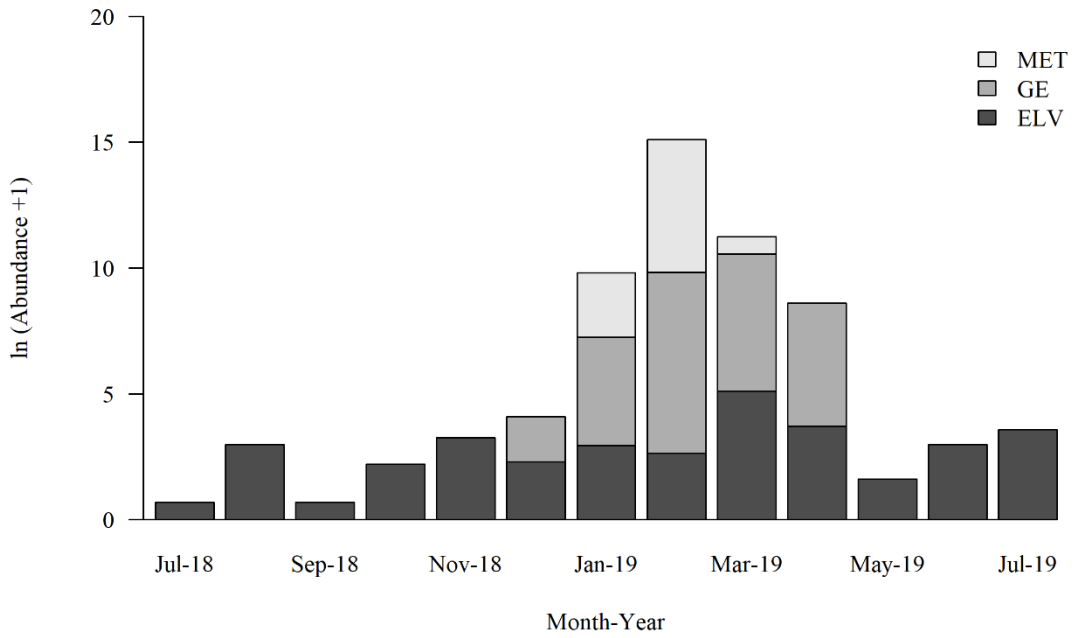

Figure 5 Stacked barplot displaying the natural log (ln) of abundance +1, for each life stage of Speckled Worm Eel collected from July 2018 to July 2019.

The $CPUE_M$ ranged from 0.006 eels/hour to 3.103 eels/hour for the entire sampling period (Figure 6). The $CPUE_M$ started an upward trend from December 2018 and tapered off in April 2019. From December to February $CPUE_M$ increased an order of magnitude each month and reached its maximum of 3.103 eels/hour for the entire sampling period.

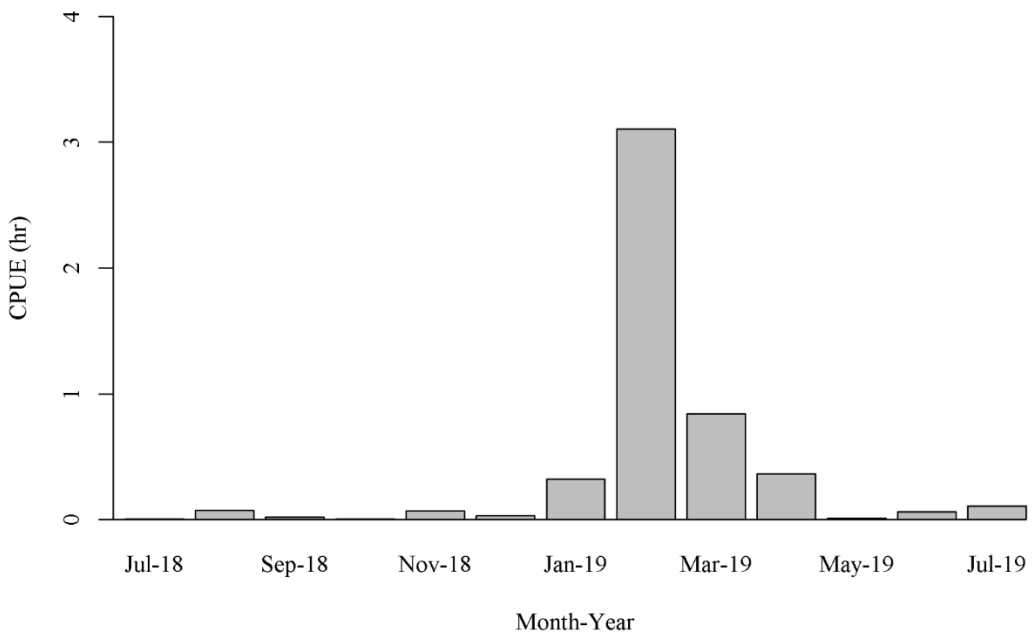

Figure 6 Monthly CPUE for Speckled Worm Eel from July 2018 to July 2019.

Sampling spanned across 24 unique coastal subbasins from Aransas Bay to Sabine Lake (Table 5; Figure 7), and Speckled Worm Eel were detected within 16 subbasins. Catch per unit effort for each subbasin ($CPUE_{SB}$) varied substantially across the sampling area from 0 eels/hour to 4.050 eels/hour. Highest $CPUE_{SB}$ were East Matagorda Bay-W and Lower Brazos with values of 4.050 eels/hour and 2.879 eels/hour, respectively. East Matagorda Bay-W and Lower Brazos were the only subbasins with observed $CPUE_{SB}$ above one. Several subbasins in Sabine Lake, Galveston Bay, and Matagorda Bay were characterized by relatively high $CPUE_{SB}$, though the values were quite variable (Table 5). The Buffalo-San Jacinto subbasin had $CPUE_{SB}$ of 0.203 eels/hour. Sabine Lake subbasin, which borders Sabine Lake and Sabine Pass was the

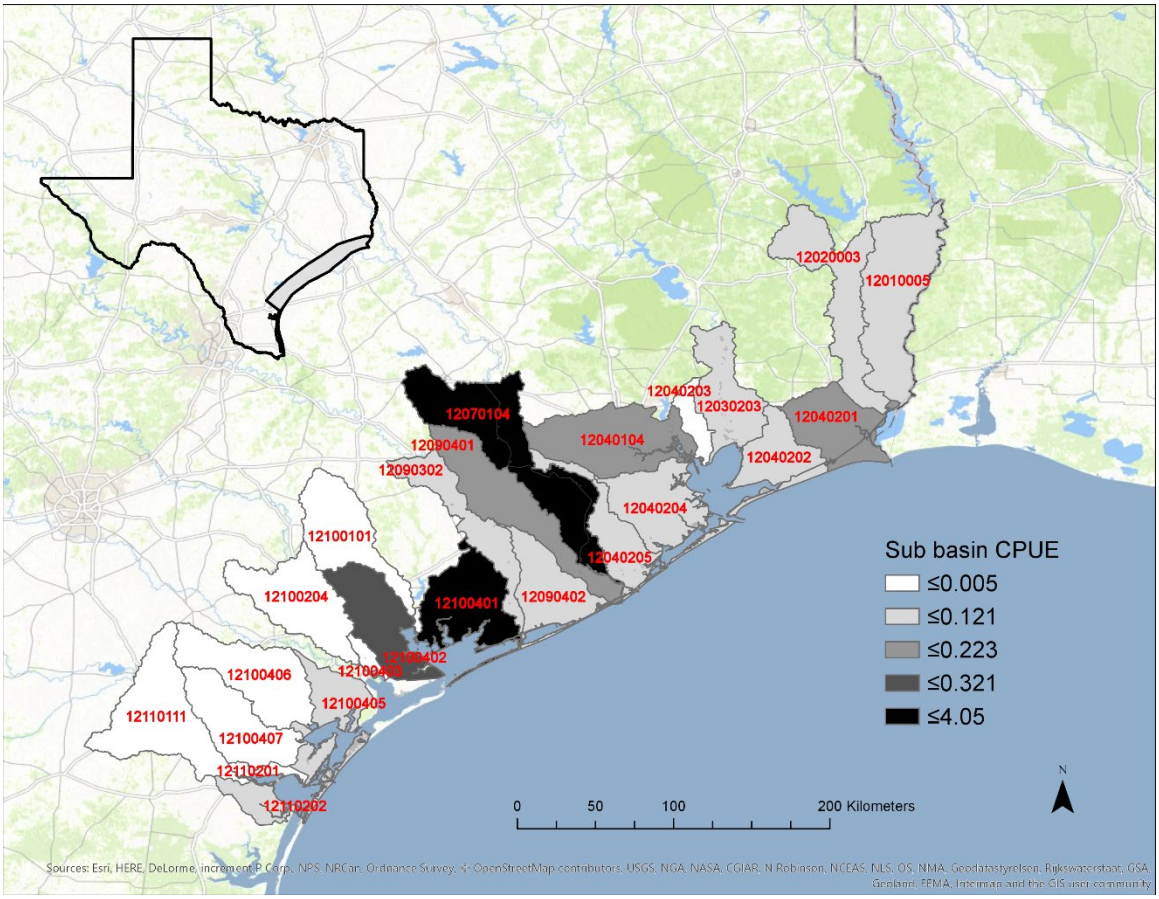

Figure 7 Map displaying CPUE for each sampled subbasin in the sampling area. The red numbers represent the 8-digit Hydrolocial Unit Code (HUC-8 ID) corresponding to Table 5

highest within the Sabine Lake watershed with $CPUE_{SB}$ 0.223 eels/hour. In Matagorda Bay localized abundances of Speckled Worm Eel within the West Matagorda Bay and East Matagorda Bay-W subbasins resulted in high $CPUE_{SB}$ for this bay system. The cumulative abundance for both subbasins was 1,930 individuals and the average was 2.102 eels/hour.

The life stages detected varied between each subbasin was highly variable between each site (Table 5). Elvers were present in all the subbasins sampled from Sabine Lake to Matagorda Bay, yet only present in Aransas Bay and South Corpus

Christi Bay along the more southern reaches of these Texas estuaries. Glass eels were the second most ubiquitous life stage detected being present in 10 of the 24 subbasins and extending from Matagorda Bay to Sabine Lake. The metamorphic life stage was only detected in three subbasins: West Matagorda Bay, East Matagorda Bay-W, and Sabine Lake.

Table 5 A list of the subbasins sampled with corresponding total catch, effort and CPUE, by both the Environmental Institute of Houston (EIH) and Texas Parks and Wildlife Department (TPWD). Stage is life stage in each subbasin M=metamorphic, G=glass eel, and E-=elver.

Sampling Team	Subbasin	HUC 8 ID	Stage	Catch	Effort (hrs)	CPUE (#/hr)
EIH	Lower Sabine	12010005	E	1	88.3	0.011
	Lower Neches	12020003	G,E	20	248.3	0.081
	Lower Trinity	12030203	E	3	107.3	0.028
	Buffalo-San Jacinto	12040104	G,E	22	108.5	0.203
	Sabine Lake	12040201	M,G,E	117	524.1	0.223
	East Galveston Bay	12040202	E	32	265.4	0.121
	North Galveston Bay	12040203	E	1	68.0	0.015
	West Galveston Bay	12040204	G,E	29	797.9	0.036
	Austin-Oyster	12040205	E	20	356.1	0.056
	Lower Brazos	12070104	G,E	128	44.5	2.879
	Lower Colorado	12090302	G,E	23	88.8	0.259
	San Bernard	12090401	G,E	4	158.8	0.025
	East Matagorda Bay - E	12090402	G,E	6	261.4	0.023
	Lavaca	12100101	-	0	61.2	0.000
	Lower Guadalupe	12100204	-	0	38.8	0.000
	East Matagorda Bay - W	12100401	M,G,E	1776	438.6	4.050
	West Matagorda Bay	12100402	M,G,E	154	479.6	0.321
TPWD	East San Antonio Bay	12100403	-	0	19.4	0.000
	Aransas Bay	12100405	E	1	168.9	0.006
	Mission	12100406	-	0	61.4	0.000
	Aransas	12100407	-	0	98.7	0.000
	Lower Nueces	12110111	-	0	38.8	0.000
	North Corpus Christi Bay	12110201	-	0	56.2	0.000
	South Corpus Christi Bay	12110202	E	1	49.2	0.020

Habitat and Water Quality

Speckled Worm Eels were collected over a wide range of ambient water quality conditions. Notably, eels were captured in near freshwater with a salinity of 0.08 psu up to 35.1 psu, like marine conditions (Table 6). Dissolved oxygen concentrations varied from hypoxic conditions at 2.12 mg/L to 10.49 mg/L (Table 6). Water clarity, approximated by Secchi depth (m), ranged from 0.01m to 0.74m.

Table 6 Summary statistics of select water quality variables measured during the study.

Variable	Minimum	1st Quartile	Mean	3rd Quartile	Maximum
Temperature (°C)	11.90	14.70	21.10	27.70	31.30
Salinity (psu)	0.08	0.91	6.70	11.18	35.10
Dissolved Oxygen (mg/L)	2.12	5.47	7.05	8.74	10.49
pH	6.71	7.29	7.66	7.98	8.86
Secchi (m)	0.01	0.13	0.22	0.30	0.74

The three most common estuarine vegetation species encountered across the 226 sampling sites were smooth cordgrass (*Spartina alterniflora*) (n=83 sties), common reed (*Phragmites australis*) (n=32 sites), and marsh elder (*Iva frutescens*) (n=17 sites). Speckled Worm Eel were observed at 33 of the 83 sites associated with smooth cordgrass. Common reed was observed at 5 sites and marsh elder was observed at 7 sites with Speckled Worm Eel.

Sediment and corresponding composition of eels collected in each classification are presented in Table 7. There were no significant differences detected between the proportions of sites where eels were collected between each sediment classification

(Fisher's Exact Test, p-value =0.60). Clay, silt, and sand were the most common sediment types observed within the study area. The number of sites where Speckled Worm Eel were collected per sediment classification ranged from 0 to 25. Of all sites within each sediment category, eels were detected at 35.1% of the sites with sand, 31.9% of the sites with silt, and 25.7% of the sites with clay. However, Speckled Worm Eels numerical abundance was highest at sites containing clay with 84.5% of all Speckled Worm Eels captured in association with clay substrate. In contrast only 5.9% and 9.5% of the total eel catch were at sites containing silt and sand, respectively.

Table 7 Sediment classification across all sites with corresponding number of sites where eels were present within the sediment type and the total number of eels observed within each sediment classification.

Sediment	**Total Sites**	**Sites With Eels**	**Eel Catch**
Clay	97	25	1975
Silt	69	22	139
Sand	57	20	221
Shell hash	2	1	3
Detritus	1	0	0

Eels were detected under all eight moon phases (Table 8). The proportion of sites where eels were detected relative to the total number of sites under a specific moon phase ranged from 18% to 36%. There were no significant differences in the proportion of sites with captured eels between all moon phases (Fisher's Exact Test, p-value =0.80). Abundance was highest during the Waning Crescent moon phase at 1,944 or 83% of all catch. Sampling also coincided most with the Waning Crescent moon phase. The lowest number of eels observed occurred during the New, First Quarter and Full Moon phases, with the combined catch of eels representing less than 1 % of the total eel catch.

Table 8 A list of moon phases under which sampling occurred. The total sites under each moon phase and the sites where eels were detected with total catch under each moon phase.

Moon Phase	Total Sites	Sites With Eels	Eel Catch
New Moon	12	3	7
Waxing Crescent	42	14	279
First Quarter	4	1	7
Waxing Gibbous	44	16	66
Full Moon	14	3	3
Waning Gibbous	28	5	20
Last Quarter	8	2	12
Waning Crescent	74	24	1,944

The results from the binomial logistic regression and the stepwise model selection process showed three variables that were significantly associated with the presence-absence of eel (Table 9). Secchi appear depth (m) and water temperature (°C) at retrieve were both negatively correlated with the presence of Speckled Worm Eel, while salinity (psu) had a significant positive relationship. In other words, as the water became clearer, or warmer, the odds of detecting eel decreased and as salinity increased, the odds of detecting eel increased. The fit of the logistic regression model where π gives the probability of detecting Speckled Worm Eel was $\ln(\pi) = 1.30 - 3.79secchi - .07\ temperature + 0.06\ Salinity$. Taking the antilogarithm of the Secchi coefficient, the odds of observing the presence of Speckled Worm Eel is estimated to decrease by 97.8% with a one meter increase in Secchi appear depth for similar water temperature and salinity (95% CI: 100% decrease to 74.3% decrease). Likewise, a one-degree increase in water temperature is estimated to decrease the odds of detecting Speckled

Worm Eel by 7% with similar water clarity and salinity (95% CI: 12% decrease to 2% decrease). A one-psu increase in salinity is estimated to increase the odds of detecting Speckled Worm Eel by 6.7% with similar water clarity and temperatures (95% CI: 2.3% increase to 11.5% increase).

Table 9 Binomial logistic regression output with predictors that were retained after the AIC stepwise model selection process.

Predictor	Log Odds	Standard Error	z-statistic	p-value
Intercept	1.30	0.05	1.637	0.057
Secchi (m)	-3.79	1.31	-2.798	0.004
Temperature (°C)	-0.07	0.72	-2.174	0.007
Salinity (psu)	0.06	0.02	2.967	0.003

Morphometrics and Length-Weight Relationships

Significant morphometric differences between at least two of the three life stages were detected for head length, body depth and body width (Table 10, Figure 8). There was suggestive evidence of a significant difference between two of the three life stages for PAL/TL ratio, therefore the Wilcoxon rank-sum test was performed for this ratio (Kruskal-Wallis rank sum test, $\chi 2$ =4.958, df=2, p-value = 0.08936). HL/TL ratio for MET averaged 6.2% and was significantly different from GE and ELV ratios of 10.1% and 10.0%, respectively (Wilcoxon rank-sum pairwise test, p-value < 0.0001) (Table 10). The BD/TL and BW/TL ratio was significantly different between all life stages (Table 10, Figure 8). Though there was a significant difference found between glass eels and elvers for the PAL/TL ratio, glass eels estimated PAL/TL was 39.5% and elver was 39.2% with no practical significant difference.

Table 10 The average proportions of each metric (mm) as a ratio of total length (mm) presented as a percentage with the associated Wilcoxon rank-sum pairwise comparison test p-values between each life stage.

Morphometric Ratio (metric divided by total length)	**Life Stage Average**			**p-value**		
	MET	**GE**	**ELV**	**a**	**b**	**c**
Head Length	6.2%	10.1%	10.0%	**< 0.0001**	**< 0.0001**	0.052
Body Depth	4.3%	2.4%	2.7%	**< 0.0001**	**< 0.0001**	**< 0.0001**
Body Width	1.8%	2.1%	2.6%	**< 0.0001**	**< 0.0001**	**< 0.0001**
Preanal Length	39.5%	39.8%	39.2%	0.739	0.111	**0.037**

a= p-value between MET and GE, b= p-value between MET and ELV, c = p-value between GE and ELV. Significance at p-value ≤ 0.05.

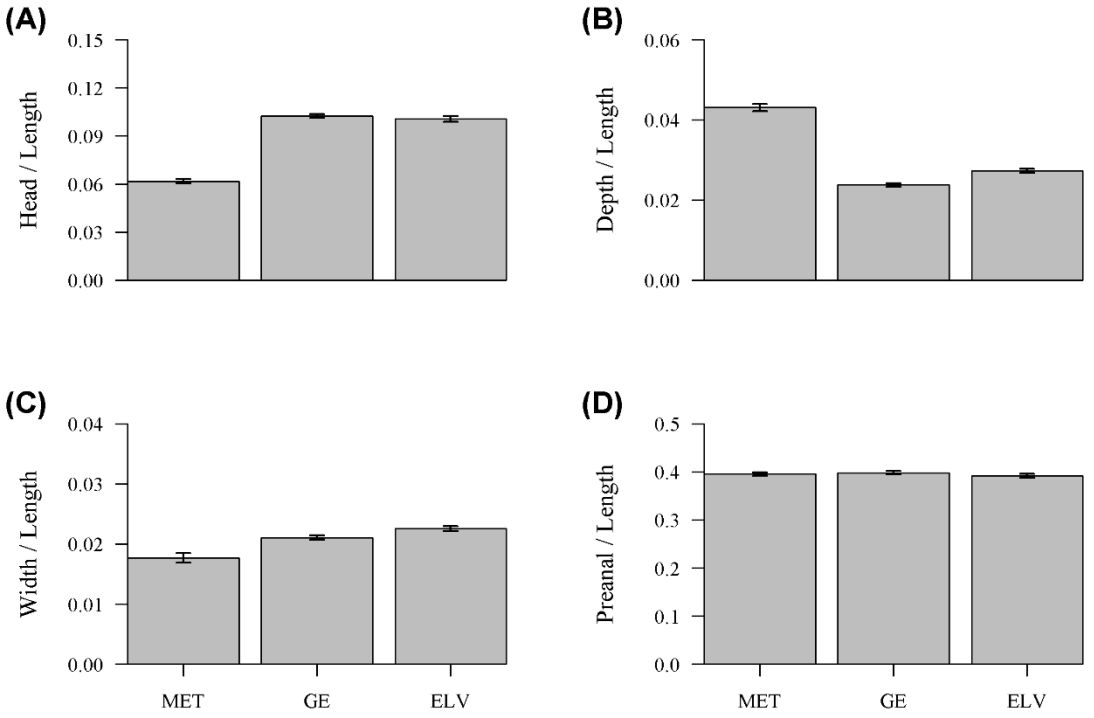

Figure 8 Barplots displaying mean (95% CI) body proportions of metamorphic (MET), glass eel (GE) and elver (ELV) life stages. (A) Displays head length to total length ratio (B) body depth to total length ratio (C) body width to total length ratio (D) preanal length to total length ratio.

A total of 737 eels were measured and weighed from all life stages (Table 6). The largest individual captured had a total length of 276mm while the smallest individual measured was a glass eel at 40.9mm (Table 11). Fish greater than 150mm were less numerous within the samples collected during the study. Glass eel maximum size was 62.6mm with a 21.7mm disparity within this life stage.

Table 11 The total number of each life stage measured and weighed with total length (mm) and the minimum, mean, and maximum values for each life stage.

		Total Length (mm)		
Stage	**n**	**Min.**	**Mean**	**Max**
Metamorphic	194	45.0	67.5	82.8
Glass Eel	280	40.9	50.3	62.6
Elver	263	41.5	81.5	276.0

Length-weight relationships were developed overall for Speckled Worm Eel, for each life stage, and then metamorphic and glass eel combined (Table 12). As a species, the relationship from metamorphic to elver is nonlinear (Figure 9). Using equation four, natural logarithmic transformation of length and weight resolves the non-linearity and in turn creates constant variance around the mean for all lengths (Figure 10); however, it doesn't resolve the metamorphosis paradox; as larvae age and move through time, they begin to shrink (Figure 11). When metamorphic and glass eels continue to age, both the weight and length reduce in a nonlinear manner. Therefore, the reduction in size as aging occurred was modeled separately for metamorphic and glass eel combined and elver alone (Table 12, Figure 9).

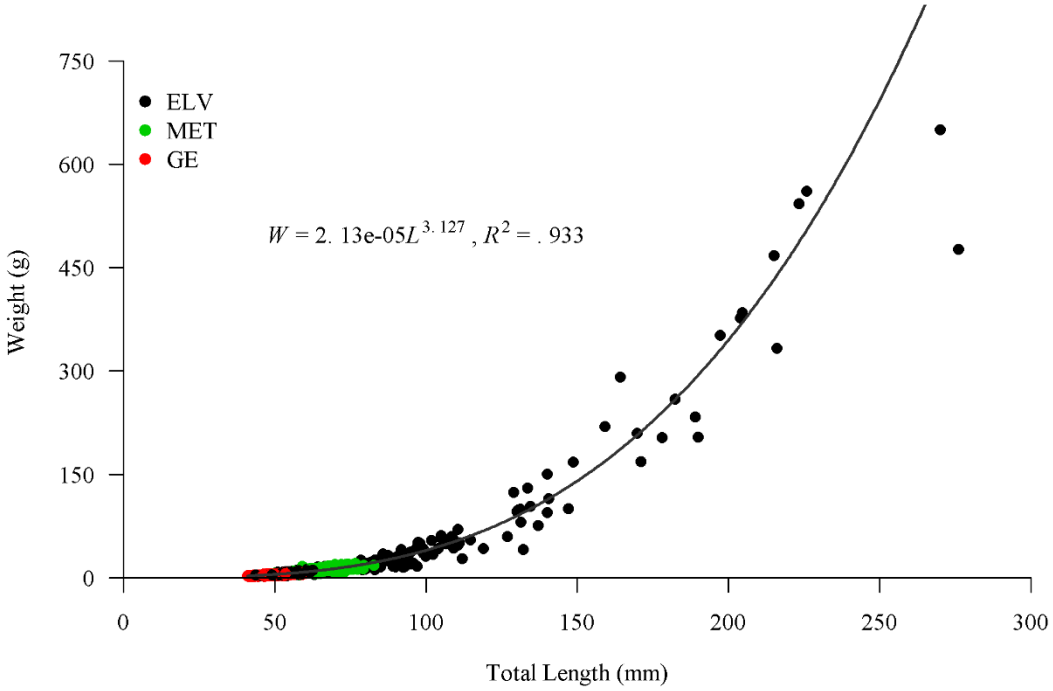

Figure 9 Plot of total length (mm) ~ weight (g) of Speckled Worm Eel with estimated best fit equation and adjusted R^2 value derived from the estimation of parameters using linear regression of natural log transformation length and weight. Black circles (ELV) indicate elver life stage, green circles (MET) indicate metamorphic life stage and red circles (GE) indicate glass eel life stage.

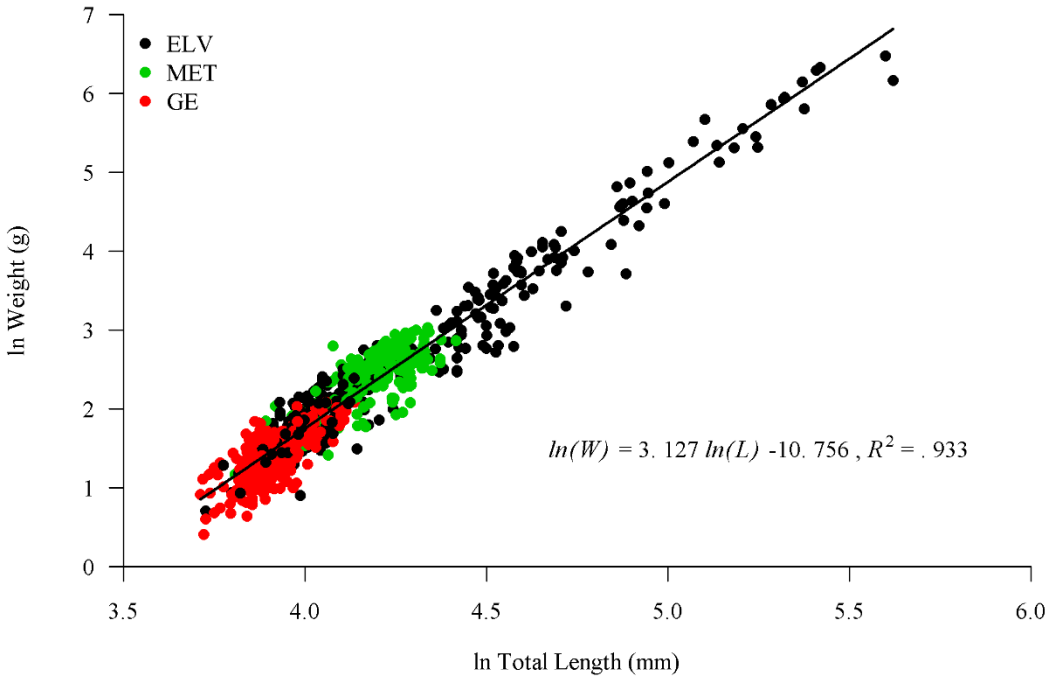

Figure 10 Natural log transformation of total length (mm) ~ weight (g) for Speckled Worm Eel. Black circles (ELV) indicate elver life stage, green circles (MET) indicate metamorphic life stage and red circles (GE) indicate glass eel life stage.

Table 12 Linear Regression model summaries that predict the ln(Weight(g)) from ln(Length (mm)) by individual life stages, with metamorphic and glass combined, and all life stages presented in this study combined.

Stage	Predictor	*b*	L 95% CI	U 95% CI	p-value	R^2	R^2 adj.
Metamorphic	ln Length	2.666	2.360	2.972	**< 0.0001**	0.605	0.603
Glass Eel	ln Length	2.917	2.590	3.244	**< 0.0001**	0.526	0.525
Elver	ln Length	3.013	2.931	3.096	**< 0.0001**	0.952	0.952
Met. + Glass	ln Length	3.400	3.268	3.532	**<0.0001**	0.845	0.845
All	ln Length	3.127	3.060	3.184	**<0.0001**	0.933	0.933

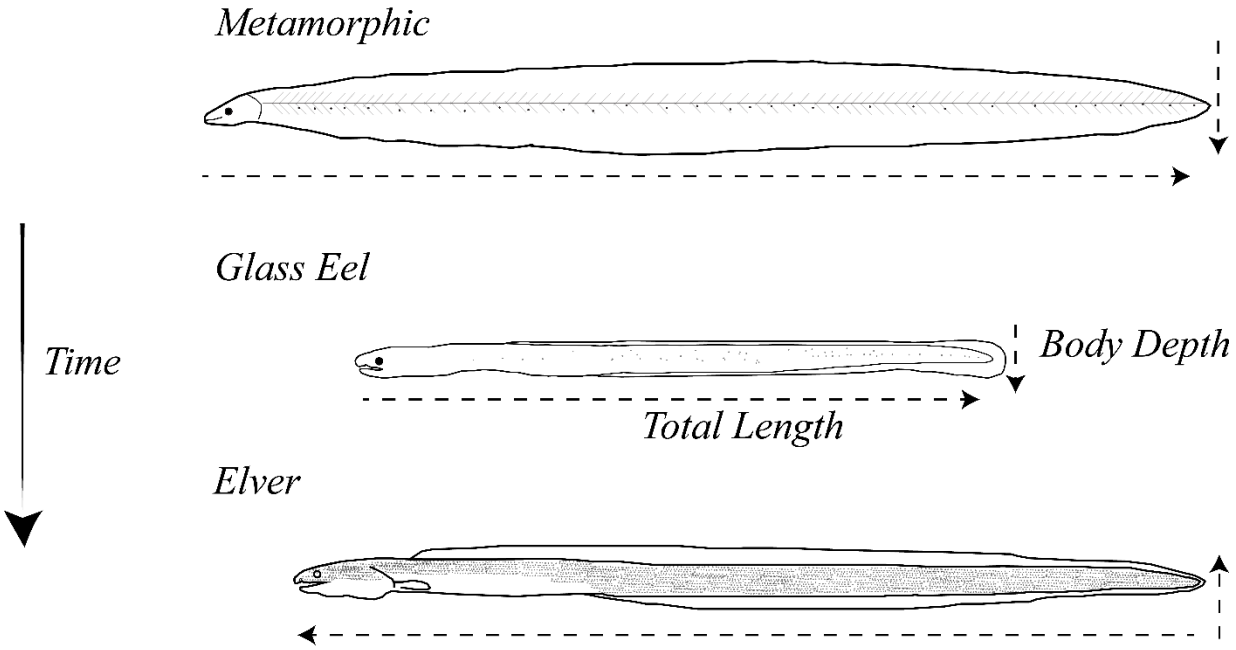

Figure 11 An illustration of metamorphic, glass eel and elver life stages with dashed arrows pointing in the right direction indicating shrinkage of total length, while arrows pointing left indicate growth. Dashed arrows down indicate shrinkage, while up indicates growth.

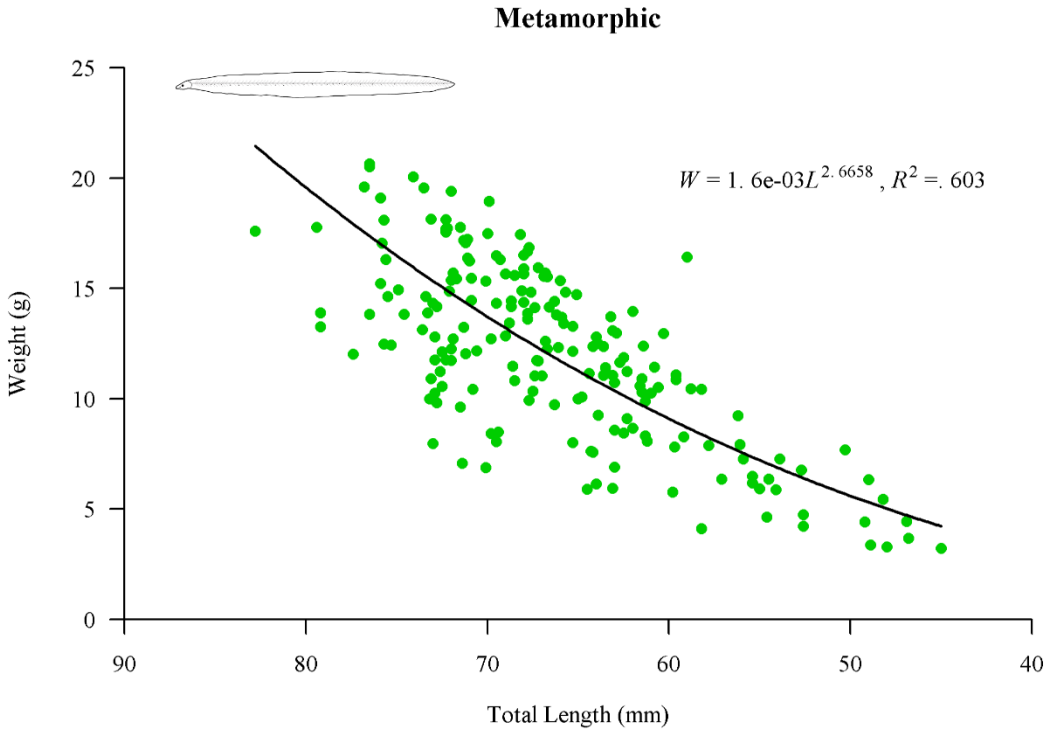

Figure 12 Plot of total length (mm) ~ weight (g) of the metamorphic life stage of Speckled Worm Eel with best fit equation and adjusted R^2 value derived from estimation parameters using linear regression of the natural log transformation of length and weight.

All linear regression models of natural log transformed length and weight by life stage were highly significant (Table 12). The adjusted R^2 values ranged from 0.525 to 0.952. Both metamorphic and glass eel had relatively low adjusted R^2 values (Table 12) indicating very little of the variation in the ln transformed weight was explained by changes in the ln transformed length. The length-weight relationship for the metamorphic life stage displayed an R^2 value of 0.603 (Figure 12). Glass eel displayed a smaller R^2 value of 0.525 (Figure 13). Elvers displayed the best fit relationship with 95.2% of the variation in weight explained by total length (Figure 14). When combined, 84.5% of the variability in weight could be explained by the corresponding total length relationship for metamorphic and glass eels stages (Figure 15).

The slope estimates *b* for all length-weight models were tested against the value of 3.00 to determine if allometric or isometric growth occurs during each life stage and various combinations of life stages. The slope (b=2.666) of the metamorphic stage was significantly different than from 3.00 (p-value = 0.032), indicating negative allometric growth. The estimated slopes for both glass eel and elver (b=2.917, b= 3.013, respectively) were not significantly different than 3.00 (p-values = 0.618, 0.754), which indicates both life stages display isometric growth. Metamorphic and glass eel displayed positive allometric growth when slope (b= 3.400) was compared to 3.00 (p-value < 0.0001), while all life stages combined also showed allometric growth when the slope (b=3.127) was compared to 3.00 (p-value <0.0001).

As the eels changed from elongated and laterally compressed in the metamorphic stage, dorsoventral compression occurred and transition into the glass eel stage began; concurrently there was a dramatic reduction in the *BD* with an increase in *BW* to a more cylindrical shape. The *BD/BW* ratio in the metamorphic life stage ranged from 0.08 to 0.73. The range within glass eel present in this study was from 0.56 to 1.0. The observed *BD/BW* ratio for elver stage ranged from 0.47 to 1.14.

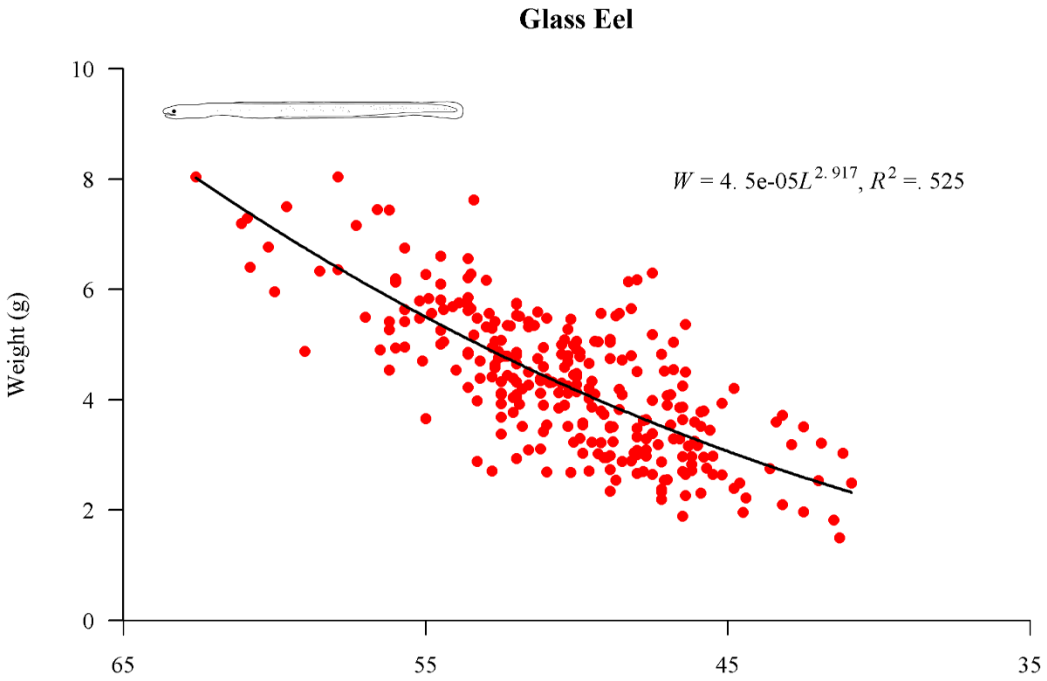

Figure 13 Plot of total length (mm) ~ weight (g) for glass eel stage of Speckled Worm Eel with estimated best fit equation and adjusted R^2 value derived from the estimation of parameters using linear regression of natural log transformed length and weight.

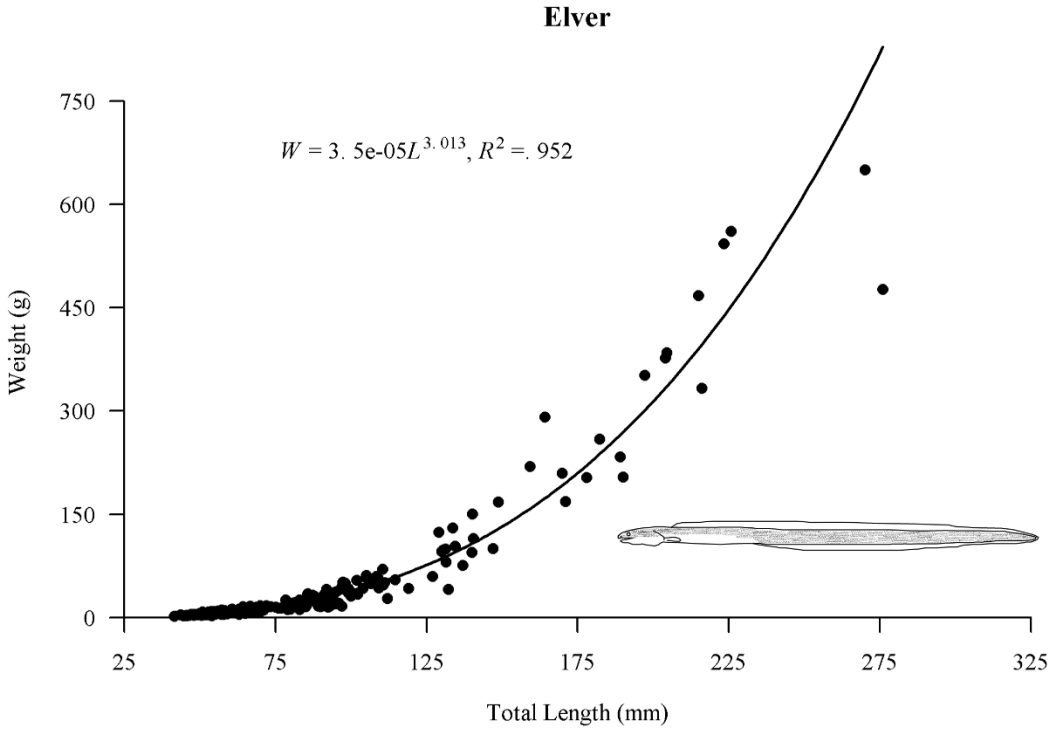

Figure 14 Plot of total length (mm) ~ weight (g) for the elver life stage of Speckled Worm Eel with estimated best fit equation and adjusted R^2 value derived from estimation of parameters using linear regression of natural log transformed length and weight.

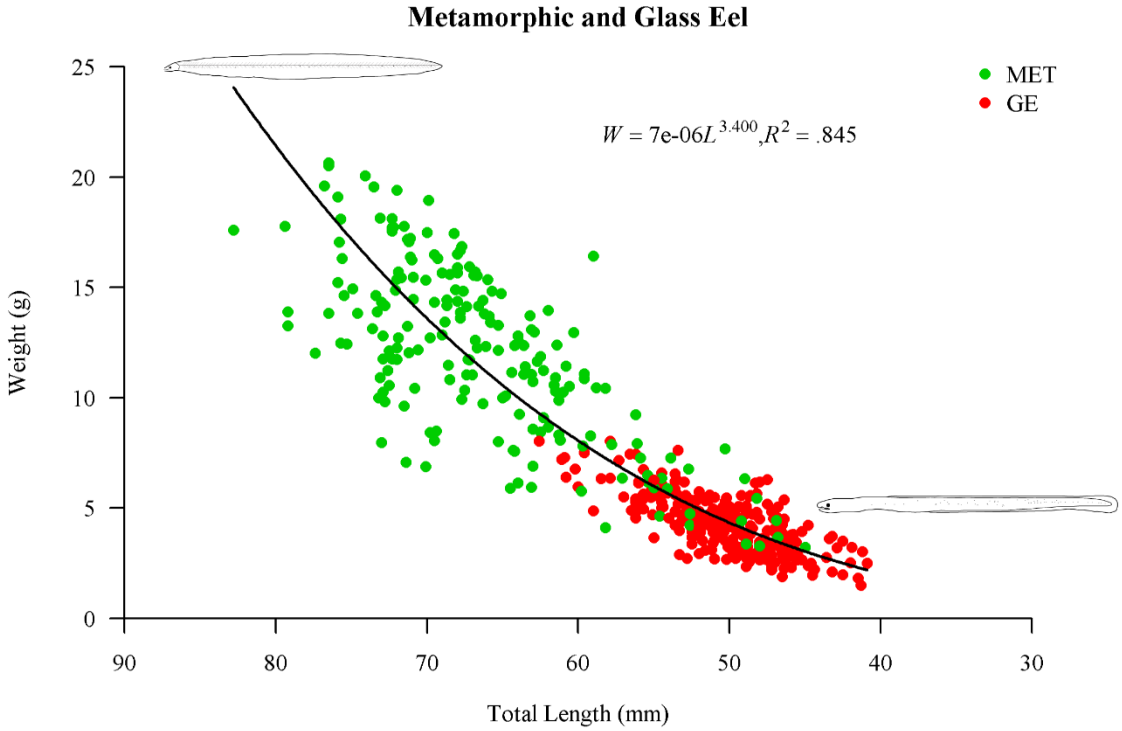

Figure 15 Plot of total length (mm) ~ weight (g) relationship of metamorphic (green dots) and glass eel (red dots) combined with estimated best fit equation and correspoinding R^2 value.

Pigmentation is considered a defining characteristic for identifying species within the Ophichthidae family, to which Speckled Worm Eels belong (Fahay and Obenchain, 1978). Though Able et al. (2011) provides a more inclusive synthesis of life stage morphological characteristics, their description regarding pigmentation for each life stage is not well supported with photographic records. A primary characteristic of pigmentation is the occurrence of melanophores along the midventral and midline of the body. The metamorphic stage described here have single melanophores making a single row along the lateral and ventral length of the body posterior of the head to the caudal region (Figure 16, Figure 17). The ventral pigmentation runs along the body from the head approximately near the gular region along the length of the fish.

As the metamorphic stage transitions to glass eel stage, there is an increase in *HL* from approximately 5% of the total length to approximately 10% of the total length (Table 7). The rostrum rounds out from a less pronounced point (Figure 21). The juvenile head starts developing pigmentation along the dorsal side (Figure 18). A single row of lateral pigmentation observed as the eels are metamorphosing and becomes more pronounced throughout the glass eel stage (Figure 19). As the glass eel transitions into the elver stage, the prominent melanophores become less pronounced and begin to fade into a peppering of spots that cover the dorsal, lateral, and caudal regions of the body (Figure 20 and Figure 22). As elvers grow, the spotting covers their body from head to caudal region (Figure 23). The elver life stage morphology is indistinguishable from adults.

Figure 16 Photograph displaying the head of a metamporhic eel (TL: 70.0mm, BD: 2.1mm).

Figure 17 Photograph displaying lateral pigmentation of a metamorphic showing a single row of single melanophores (TL: 70.0mm, BD: 2.1mm).

Figure 18 Photograph displaying the head of a glass eel recently metamporhosed with the lighlty scattered pigmentation along the dorsal region of the head (TL: 50.0mm, BD: 1.2mm)

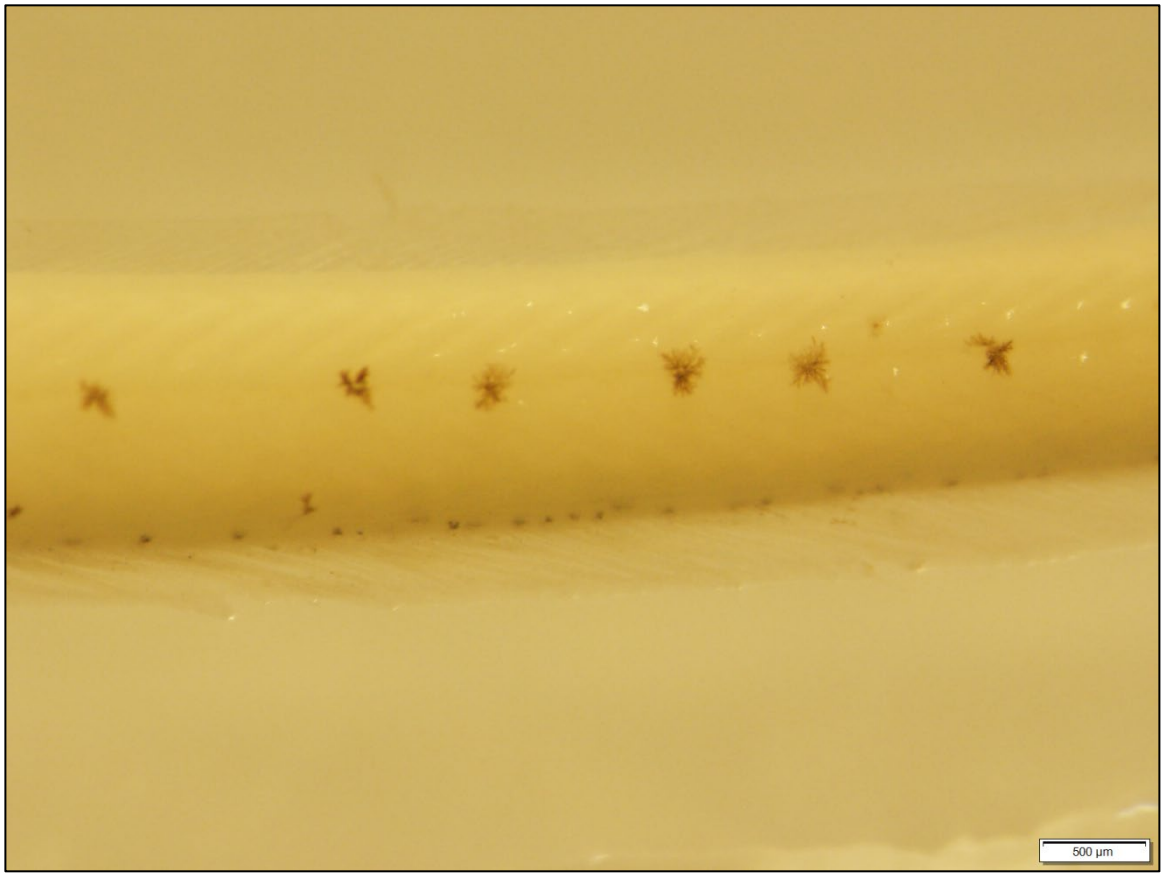

Figure 19 Photograph displaying the lateral side of a recently metamorphosed glass eel displaying melanophores (TL: 51.0mm, BD: 1.6mm).

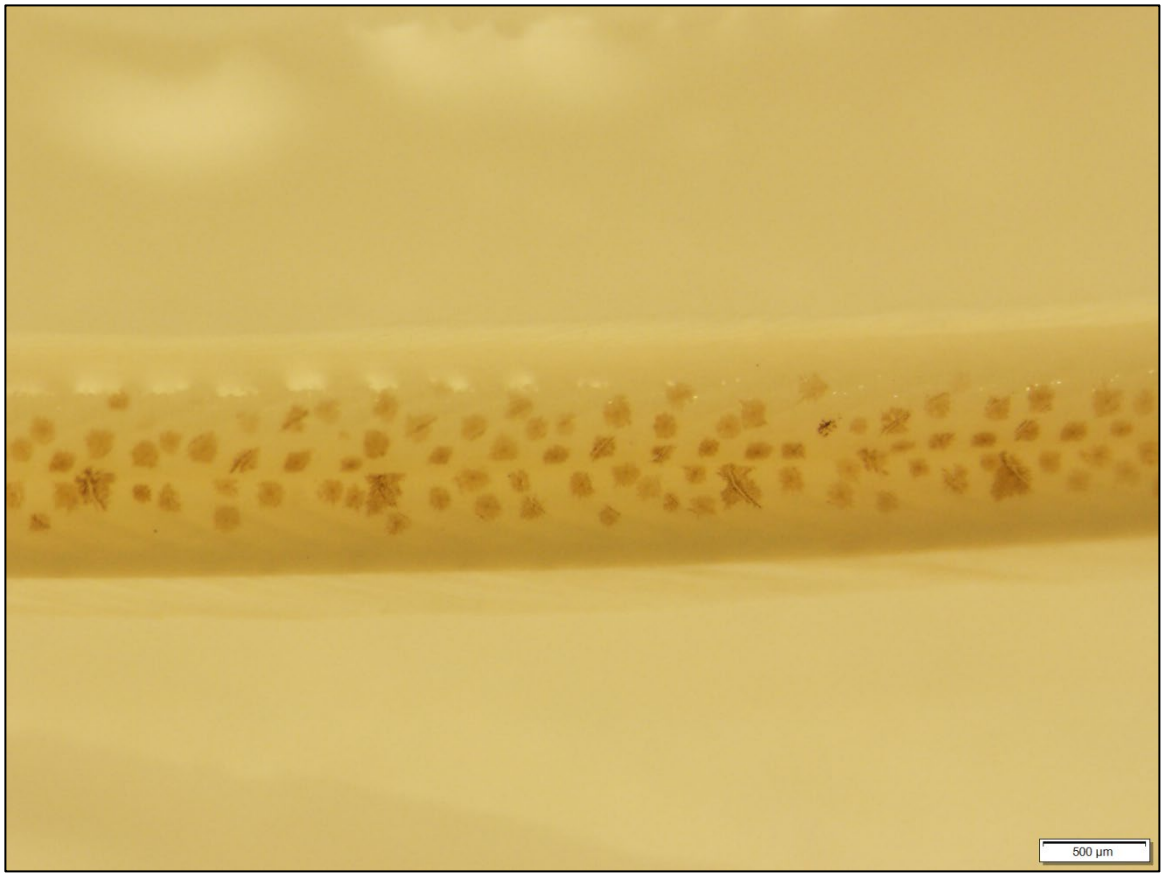

Figure 20 Photograph displaying lateral pigmentation of a glass eel with pronounced lateral melanophores (TL: 50.0mm, BD: 1.2mm).

Figure 21 Photograph displaying heads of metamorphic (top) and glass eels (middle and bottom) with pigmentation patterns indicative of each life stage.

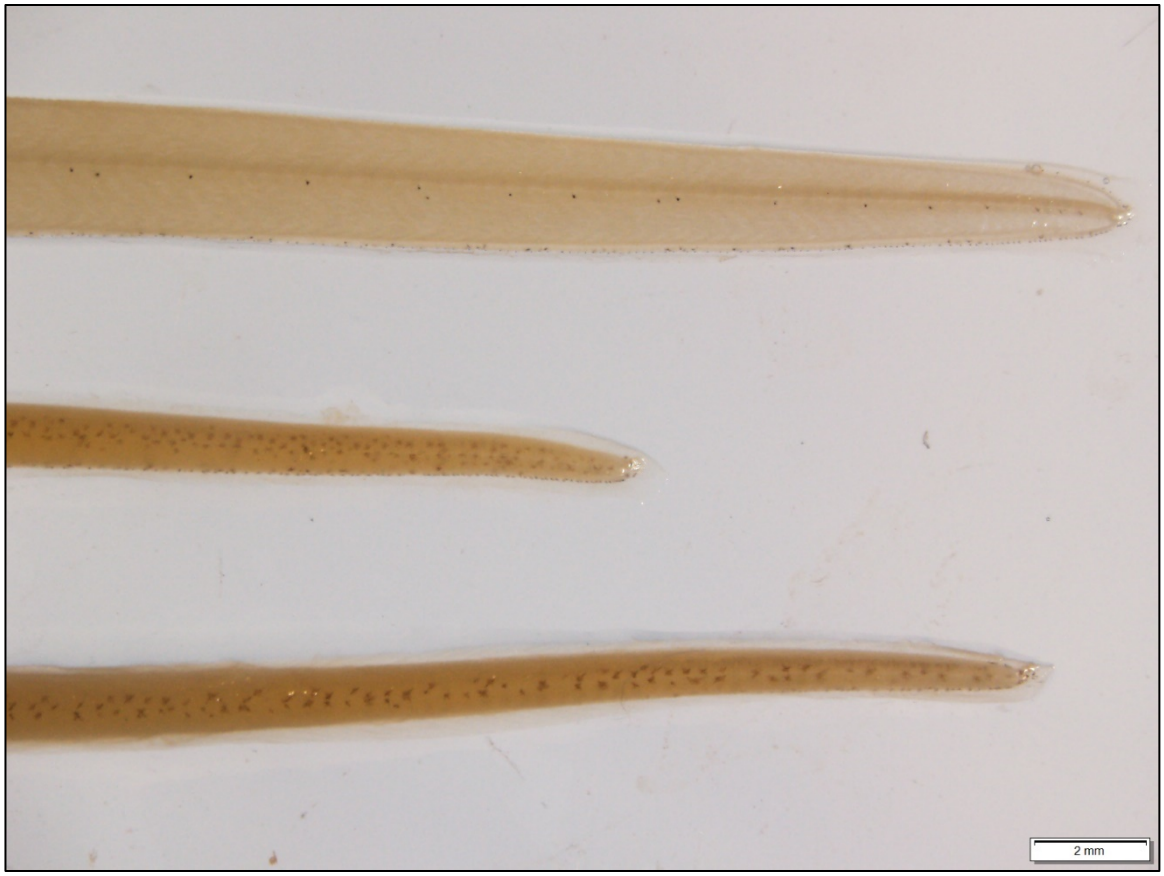

Figure 22 Photograph displaying metamorphic (top) and glass eel (middle and bottom) caudal fins showing changes in lateral pigmentation.

Figure 23 Photograph displaying the head of an elver eel with heavily scattered pigmentation along the dorsal region of the head (TL: 131.2mm , BD: 4.4mm).

Discussion

The results presented here are the first thorough documentation of Speckled Worm Eel in Texas that describe patterns in the temporal and spatial distribution, water quality and habitat associations and morphological characteristics between life history stages as ingression and recruitment occur.

Spatial and Temporal Patterns

Speckled Worm Eel share a similar life history strategy with other Anguilliform species where larvae drift with the current, yet their metamorphosis occurs as a continuum through space and time compared to several other Atlantic Anguillid species that ingress and settle in the coastal waters as glass eels (Miller, 2009b; Miller et al., 2015). The observance of glass eel and metamorphic eel during the winter and spring months demonstrates a recruitment window that is consistent with other observed periods of Speckled Worm Eel ingression (Fahay and Obenchain, 1978; Harnden et al., 1999; Able et al., 2011). Glass eels were observed from December 2018 to March 2019, while observations of metamorphic eel ranged from January 2018 to March 2019 (Figure 5). This suggests that Speckled Worm Eel may conduct multiple batch spawning events resulting in a bimodal ingression or recruitment where two pulses or peaks can occur. The glass eels captured in December would be the recently settled metamorphics from the first spawning event. Past studies have shown Speckled Worm Eel detection and ingression from November to April, and some evidence suggests multi-peaked movement event can occur (Warlen and Burke, 1990; Able et al., 2011).

The spatial occurrence of metamorphic and glass eel was highly variable while the elver life stage was highly ubiquitous within the sampling region (Table 5). Elvers were regularly detected through space and time, though in very low relative abundances.

Furthermore, Speckled Worm Eel detection occurred in 30% of the total net sets. The highest $CPUE_{SB}$ of Speckled Worm Eel were detected around major bays (Figure 7), though this result may be an artifact of the current sampling design. The efforts in this study covered a large spatial expanse on a biweekly basis. The first detection of glass eels in December 2018 was in the Colorado-Brazos sampling area. The next detection of both metamorphic and glass eel was in the Sabine Lake watershed in early January 2019, roughly 200km in distance, which means large expanses of space are not sampled between sampling events. However, it is not uncommon to have large variability between abundance and CPUE across extensive spatial expanses for recently ingressing or settling Anguillids (Sullivan et al., 2006; Sullivan et al., 2009b; Able et al., 2011).

The abundance of Speckled Worm Eel have been highly associated with strong onshore winds and along shelf winds (Harnden et al., 1999). The along shelf movement of water in the Northern GOM is primarily driven by wind, with two distinct patterns driving current to the east along shore in the summer and westward during winter (Cho et al., 1998). These patterns driven by prevailing storms, may have heavily influenced the outcome of the sampling and may be correlated to the highly variable densities observed within the sampling area and study period.

Habitat and Water Quality

Results from binomial logistic regression indicate water clarity plays an important role in the odds of detecting Speckled Worm Eel. The influence of moon illumination and water clarity on European Glass Eel (*Anguilla anguilla*) shows a more benthic movement pattern as opposed to utilization of the water column under darker and more turbid conditions (De Casamajor et al., 1999). Though illumination wasn't a significant factor in the context of the logistic regression during the course of this study, water clarity may be

an important determinant of survival and therefore in some instances may be enhanced when water visibility is low. Speckled Worm Eel are considered entirely nocturnal throughout their lifecycle (Taylor et al., 2015; Grace and Taylor, 2017) and are able to utilize chemical cues to avoid conspecifics buried in the sediment, especially when water clarity is low (Barreto et al., 2010). Having reduced light penetration from low water clarity may increase swimming activity. Water temperature displayed a negative relationship with eel detection. In some instances, water temperature is positively correlated with the outcome of Speckled Worm Eel (Able et al., 2011) and may actually increase range expansion in the context of a warming climate (Hare and Able, 2007; Schmidt and Wright, 2018).

The sampling design placed the majority of nets along the stream edge adjacent to vegetation. Eels were detected at 33 of the 68 sites in association with smooth cordgrass as the dominant shoreline vegetation species. The association between Speckled Worm Eel and coastal marsh have been documented previously in the GOM where the highest densities of eels were found along the coastal marsh edges in Barataria Bay, Louisiana while no eels were detected in open substrate (Rozas and Minello, 2006). The settling eel may actively select where structural complexity provides additional cover and potential protection from predation. Speckled Worm Eel were the most dominant species and estimated to be as dense as 1.66 individuals per m^2 in mangrove forests in Brazil (Barletta et al., 2000). These findings suggest that though they bury in sediment, most likely as predator avoidance as seen in other Anguillids (Barbin and Krueger, 1994), they may be using the structural complexity for another purpose, possibly foraging. Vaslet et al. (2011) showed that a juvenile Speckled Worm Eel maintained a proportion of their diet form mangroves as well as in sea grass beds, further supporting this theory.

Morphometrics and Length-Weight Relationships

Results from the morphometric ratios compared between life stages were consistent with Able et al. (2011). Able et al. (2011) has nicely summarized ranges of morphological characteristics across early life history stages of Speckled Worm Eel metamorphosis. For example, the ratio of *PL* to *TL* ranged from 45-37% for metamorphic, 42-39% for glass eel and 39% and up for elver. The average values presented here were all between 39% and 40% for each life stage (Table 10), which nicely fit within the ranges presented in Able et al. (2011). There is discrepancy in the ranges and values of body depth between life stages. Two factors may be at play: geographic variation in body shape and preservation method.

The potential for geographic variation in body morphometrics is important to consider. American Eel have been shown to metamorphose and ingress into southern regions of their range at much smaller sizes than their northern cohort (Pratt et al., 2014). Because the body proportions in this study are consistent with Able et al. (2011) with the exception of body depth, it may be reasonable to argue that differences arise from a spatial and more largely a genetic perspective where distinct breeding populations occur under differing life history strategies. This occurs with the Atlantic Blue Fin Tuna (*Thunnus thynnus*) which spawns at much larger sizes later in life within the Gulf of Mexico while the Mediterranean Sea spawning aggregation display a strategy of spawning earlier in life and at smaller sizes (Richardson et al., 2016).

The specimens measured in this study were preserved in 70% ethanol after formalin fixation and thus preservation may be reducing the size of the morphometric life stage. Powles et al. (2006) found that after a year preserved in 95% ethanol Speckled Worm Eel standard length decreased by 10.3%, preanal length decreased by 9.5 % and

body depth decreased by 17.5%. Though evidence shows generally that the initial reduction in morphology after preservation in alcohol solution isn't exacerbated through time and the changes in morphology may be due to habitat and geographic differences (Larochelle et al., 2016). The reduction in linear morphometrics is most likely the result of preservation method, though geographic variation in body morphology cannot be ruled out.

The length-weight relationships developed in this study for Speckled Worm Eel and its various life stages encourage a new perspective on what is considered growth and how to model such relationships. The metamorphic life stage displayed negative allometric growth ($b = 2.666$) which suggests the longer an individual, the slenderer it becomes, and the weight does not increase with the cube of its length. As normal growth occurs, this is to be expected. Yet metamorphic do not grow they shrink. It is well known that as metamorphosis occurs from leptocephali to glass eel, the larvae become more rounded and shrink as they pass through time. The measured metamorphic individuals exhibited negative allometric shrinkage.

Post metamorphosis, both glass eel ($b = 2.917$) and elvers ($b = 3.013$) displayed isometric growth, which is quite rare in fishes where a tendency towards slightly positive allometric growth is observed (Froese, 2006). However, when combining metamorphic and glass eel and elver combined the slope ($b = 3.127$) indicated positive allometric growth. These are the first known length-weight relationships developed for Speckled Worm Eel. Although there is not a standard point of comparison.

Some results presented here should be headed with caution. The length-weight relationships and morphometrics developed in this paper should be used for comparison

to other individuals from the Texas Coast and not to be compared to live specimens, due to the potential confoundment of spirit-based preservation.

The results of this study help to better describe the life history of a species that may be underrepresented in its distribution. A breadth of information has been collected regarding a species that is often set aside for taxa that are recreational or commercially important. The fyke nets used in this study may prove useful for continuous monitoring of Speckled Worm Eel and other elopomorphs as it has proved quite effective for detecting Ladyfish leptocephali in this study and useful in other studies at capturing species of Anguillids (Jellyman and Graynoth, 2005; Lake, 2013; Oliveira, 1999). Though fyke nets did not consistently capture high relative abundances of Speckled Worm Eel, they regularly detected all three life stages present within the bays and estuaries of the central and northern Coast of Texas. These findings underpin the importance of utilizing sampling techniques that are more inclusive of Speckled Worm Eel and other species that are traditionally underrepresented in their relative abundance and distribution within the GOM. The models and information in this study serve as a primer for continuing efforts to better understand this cryptic species in Texas.

LITERATURE CITED

Able, K.W., Allen, D.M., Bath-Martin, G., Hare, J.A., Hoss, D.E., Marancik, K.E., Powles, P.M., Richardson, D.E., Taylor, J.C., Walsh, H.J., Warlen, S.M., Wenner, C., 2011. Life history and habitat use of the speckled worm eel, Myrophis punctatus, along the east coast of the United States. Environmental Biology of Fishes 92, 237.

Antunes, C., Tesch, F.-W., 1997. A critical consideration of the metamorphosis zone when identifying daily rings in otoliths of European eel, Anguilla anguilla (L.). Ecology of Freshwater Fish 6, 102-107.

Arai, T., Otake, T., Tsukamoto, K., 2000. Timing of metamorphosis and larval segregation of the Atlantic eels Anguilla rostrata and A. anguilla, as revealed by otolith microstructure and microchemistry. Marine Biology 137, 39-45.

ASMFC, 2017. 2017 American Eel Stock Assessment Update. Atlantic States Marine Fisheries Commission pursuant to National Oceanic and Atmospheric Administration.

Barbin, G.P., Krueger, W.H., 1994. Behaviour and swimming performance of elvers of the American eel, Anguitta rostrata, in an experimental flume. Journal of Fish Biology 45, 111-121.

Barletta, M., Saint-Paul, U., Barletta-Bergan, A., Ekau, W., Schories, D., 2000. Spatial and temporal distribution of Myrophis punctatus (Ophichthidae) and associated fish fauna in a Northern Brazilian intertidal mangrove forest. Hydrobiologia 426, 65-74.

Barreto, R.E., Junqueira, M.F.C., Tjui-Yeuw, T., Volpato, G.L., 2010. Spatial choice is biased by chemical cues from conspecifics in the speckeled worm eel Myrophis punctatus. Neotropical Ichthyology 8, 899-902.

Béguer-Pon, M., Castonguay, M., Shan, S., Benchetrit, J., Dodson, J.J., 2015. Direct observations of American eels migrating across the continental shelf to the Sargasso Sea. Nature Communications 6, 8705.

Benchetrit, J., McCleave, J.D., 2016. Current and historical distribution of the American eel Anguilla rostrata in the countries and territories of the Wider Caribbean. ICES Journal of Marine Science 73, 122-134.

Biggs, D.C., 1992. Nutrients, plankton, and productivity in a warm-core ring in the western Gulf of Mexico. Journal of Geophysical Research: Oceans 97, 2143-2154.

Biggs, D.C., Zimmerman, R.A., Gasca, R., Suarez-Morales, E., Castellanos, I., Leben, R.R., 1997. Note on plankton and cold-core rings in the Gulf of Mexico. Fishery Bulletin 95, 369-375.

Bio-West, 2011a. Lower Sabine River Fishery Study, Downstream Fisheries Resources Report. Bio-West, Inc., Roud Rock, TX, p. 83.

BIO-West, I., 2011b. Lower Sabine River Fishery Study: downstream fisheries resources report.

Bonvechio, K.I., 2016. Comparison of glass eel stages of American eel and speckled worm eel in a northeast Florida estuary. Fisheries Management and Ecology 23, 350-355.

Bowser, C., 2018. The Hudson River Eel Project 2008-2018: Citizen Science Juvenile American Eel Surveys. Hudson River Estuary Program.

Campbell, P., Fuls, B., 2005. Trends in Relative Abundance and Size of Selected Finfishes and Shellfishes along the Texas Coast: November 1975-December 2003, Managment Data Series, p. 124.

Chen, J.-N., López, J., Lavoué, S., Miya, M., Chen, W.-J., 2013. Phylogeny of the Elopomorpha (Teleostei): Evidence from six nuclear and mitochondrial markers. Molecular phylogenetics and evolution 70.

Cho, K., Reid, R.O., Nowlin Jr., W.D., 1998. Objectively mapped stream function fields on the Texas-Louisiana shelf based on 32 months of moored current meter data. Journal of Geophysical Research: Oceans 103, 10377-10390.

Cohen, A.E., Garrett, G.P., Casarez, M.J., Hendrickson, D.A., Labay, B.J., Urban, T., Gentle, J., Wylie, D., Walling, D., 2018. Conserving Texas biodiversity: status, trends, and conservation planning for fishes of greatest conservation need.

Côté, C.L., Gagnaire, P.-A., Bourret, V., Verreault, G., Castonguay, M., Bernatchez, L., 2013. Population genetics of the American eel (Anguilla rostrata): FST = 0 and North Atlantic Oscillation effects on demographic fluctuations of a panmictic species. Molecular Ecology 22, 1763-1776.

Cresci, A., Paris, C.B., Durif, C.M.F., Shema, S., Bjelland, R.M., Skiftesvik, A.B., Browman, H.I., 2017. Glass eels (Anguilla anguilla) have a magnetic compass linked to the tidal cycle. Sci Adv 3, e1602007-e1602007.

Daverat, F., Limburg, K.E., Thibault, I., Shiao, J.C., Dodson, J.J., Caron, F., Tzeng, W.N., Iizuka, Y., Wickström, H., 2006. Phenotypic plasticity of habitat use by three

temperate eel species, Anguilla anguilla, A. japonica and A. rostrata. Marine Ecology Progress Series 308, 231-241.

De Casamajor, M., Bru, N., Prouzet, P., 1999. Influence de la luminosité nocturne et de la turbidité sur le comportement vertical de migration de la civelle d'anguille (Anguilla anguilla L.) dans l'estuaire de l'Adour. Bulletin Français de la Pêche et de la Pisciculture, 327-347.

Fahay, M.P., 1978. Biological and Fisheries Data on American eel, Anguilla rostrata (LeSueur). National Marine Fisheries Services, National Oceanic and Atmospheric Administration, U.S. Department of Commerce, Highlands, N.J., p. 96.

Fahay, M.P., Obenchain, C.L., 1978. Leptocephali of the Ophichthid Genera Ahlia, Myrophis, Ophichthus, Pisodonophis, Callechelys, Letharchus, and Apterichtus on the Atlantic Continental Shelf of the United States. Bulletin of Marine Science 28, 442-486.

Froese, R., 2006. Cube law, condition factor and weight–length relationships: history, meta-analysis and recommendations. Journal of Applied Ichthyology 22, 241-253.

Gagnaire, P.-A., Normandeau, E., Côté, C., Møller Hansen, M., Bernatchez, L., 2012. The genetic consequences of spatially varying selection in the panmictic American eel (Anguilla rostrata). Genetics 190, 725-736.

Grace, M., Taylor, S., 2017. Species-specifc development of retinal architecture in elopomorph fshes: Adaptations for harvesting light in the dark. Bulletin of Marine Science 93.

Greenwwod, P.H., Rosen, D.E., Weitzman, S.H., Myers, G.S., 1966. Phyletic studies of Teleostean Fishes, with a Provisional Classification of Living Forms. Bulletin of the American Museum of Natural History 131, 341-445.

GSMFC, 2016. SEAMAP ENVIRONMENTAL AND BIOLOGICAL
ATLAS OF THE GULF OF MEXICO. Gulf State Marine Fisheries Commission.

Hare, J.A., Able, K.W.J.F.O., 2007. Mechanistic links between climate and fisheries along the east coast of the United States: explaining population outbursts of Atlantic croaker (Micropogonias undulatus). 16, 31-45.

Harnden, C.W., Crabtree, R.E., Shenker, J.M., 1999. Onshore transport of elopomorph leptocephali and glass eels (Pisces: Osteichthyes) in the Florida Keys. Gulf of Mexico Science 17, 2.

Haro, A., Richkus, W., Whalen, K., Hoar, A., Busch, W.-D., Lary, S., Brush, T., Dixon, D., 2000. Population Decline of the American Eel: Implications for Research and Management.

Hendrickson, D.A., Cohen, A.E., 2015. Fishes of Texas Project Database (version 2.0). Texas Avanced Computing Center, University of Texas at Austin.

Hubbs, C., 2002. A preliminary checklist of the fishes of Caddo Lake in northeast Texas. The Texas journal of science 54, 111-124.

Hulet, W., Robins, C., 1989. The Evolutionary Significance of the Leptocephalus Larva: Part 9, Volume 2, pp. 669-678.

Jellyman, D., Lambert, P., 2003a. The how and when of catching glass eels. Water & Atmosphere 11, 22-23.

Jellyman, D.J., 1979. Upstream migration of glass-eels (Anguilla spp.) in the Waikato River. New Zealand Journal of Marine and Freshwater Research 13, 13-22.

Jellyman, D.J., Graynoth, E., 2005. The use of fyke nets as a quantitative capture technique for freshwater eels (Anguilla spp.) in rivers. Fisheries Management and Ecology 12, 237-247.

Jellyman, D.J., Lambert, P.W., 2003b. Factors affecting recruitment of glass eels into the Grey River, New Zealand. Journal of Fish Biology 63, 1067-1079.

Jessop, B., Cairns, D., Thibault, I., Tzeng, W.-N., 2008. Life history of American eel Anguilla rostrata: New insights from otolith microchemistry. Aquatic Biology 1, 205-216.

Jessop, B.M., Shiao, J.C., Iizuka, Y., Tzeng, W.N., 2002. Migratory behaviour and habitat use by American eels Anguilla rostrata as revealed by otolith microchemistry. Marine Ecology Progress Series 233, 217-229.

Johnson, M.W., Heck Jr, K.L., 2006. Effects of habitat fragmentation per se on decapods and fishes inhabiting seagrass meadows in the northern Gulf of Mexico. Marine Ecology Progress Series 306, 233-246.

Kleckner, R.C., McCleave, J.D., 1982. Entry of migrating American eel leptocephali into the Gulf Stream system. Helgoländer Meeresuntersuchungen 35, 329-339.

Kleckner, R.C., McCleave, J.D., 1985. Spatial and temporal distribution of American eel larvae in relation to North Atlantic Ocean current systems. Dana 4, 67-92.

Lake, M., 2013. Freshwater fish: passive nets - fyke nets. Department of Conservation, 19.

Lamson, H.M., Shiao, J.-C., Iizuka, Y., Tzeng, W.-N., Cairns, D.K., 2006. Movement patterns of American eels (Anguilla rostrata) between salt- and freshwater in a coastal watershed, based on otolith microchemistry. Marine Biology 149, 1567-1576.

Larochelle, C.R., Pickens, F.A., Burns, M.D., Sidlauskas, B.L.J.C., 2016. Long-term isopropanol storage does not alter fish morphometrics. 104, 411-420.

Lee, T.N., Clarke, M., Williams, E., Szmant, A.F., Berger, T., 1994. Evolution of the Tortugas Gyre and its influence on recruitment in the Florida Keys. Bulletin of Marine Science 54, 621-646.

Martin, M.H., 1995. The effects of temperature, river flow, and tidal cycles on the onset of glass eel and elver migration into fresh water in the American eel. Journal of Fish Biology 46, 891-902.

McCleave, J., 1987. Behavioral aspects of selective tidal stream transport in juvenile American eels (Anguilla rostrata), Am. Fish. Soc. Symposium, pp. 138-150.

McCleave, J.D., Kleckner, R.C., 1982. Selective tidal stream transport in the estuarine migration of glass eels of the American eel (Anguilla rostrata). ICES Journal of Marine Science 40, 262-271.

Miller, M., 2009a. Ecology of Anguilliform Leptocephali: Remarkable Transparent Fish Larvae of the Ocean Surface Layer. Aqua-bioscience Monographs 2.

Miller, M., 2009b. Ecology of Anguilliform Leptocephali: Remarkable Transparent Fish Larvae of the Ocean Surface Layer.

Miller, M., McCleave, J., 2007. Species Assemblages of Leptocephali in the Southwestern Sargasso Sea. Marine Ecology-progress Series - MAR ECOL-PROGR SER 344, 197-212.

Miller, M.J., 1995. Species assemblages of leptocephali in the Sargasso Sea and Florida Current. Marine Ecology Progress Series 121, 11-26.

Miller, M.J., Bonhommeau, S., Munk, P., Castonguay, M., Hanel, R., McCleave, J.D., 2015. A century of research on the larval distributions of the Atlantic eels: a re-examination of the data. Biological Reviews 90, 1035-1064.

Morrison, W.E., Secor, D.H., 2003. Demographic attributes of yellow-phase American eels (Anguilla rostrata) in the Hudson River estuary. Canadian Journal of Fisheries and Aquatic Sciences 60, 1487-1501.

Ogle, D.H., 2016. Introductory fisheries analyses with R. Chapman and Hall/CRC.

Oliveira, K., 1999. Life history characteristics and strategies of the American eel, Anguilla rostrata. Canadian Journal of Fisheries and Aquatic Sciences 56, 795-802.

Powles, P.M., Hare, J.A., Laban, E.H., Warlen, S.M., 2006. Does eel metamorphosis cause a breakdown in the tenets of otolith applications? A case study using the speckled worm eel (Myrophis punctatus, Ophichthidae). Canadian Journal of Fisheries and Aquatic Sciences 63, 1460-1468.

Pratt, T.C., Bradford, R.G., Cairns, D., Castonguay, M., Chaput, G., Clarke, K., Mathers, A., 2014. Recovery potential assessment for the American eel (Anguilla rostrata) in eastern Canada: functional description of habitat. Canadian Science Advisory Secretariat.

Ramsey, F., Schafer, D., 2012. The statistical sleuth: a course in methods of data analysis. Cengage Learning.

Richardson, D.E., Marancik, K.E., Guyon, J.R., Lutcavage, M.E., Galuardi, B., Lam, C.H., Walsh, H.J., Wildes, S., Yates, D.A., Hare, J.A.J.P.o.t.N.A.o.S., 2016. Discovery of a spawning ground reveals diverse migration strategies in Atlantic bluefin tuna (Thunnus thynnus). 113, 3299-3304.

Rozas, L.P., Minello, T.J., 2006. Nekton use ofVallisneria americana Michx.(Wild celery) beds and adjacent habitats in Coastal Louisiana. Estuaries and Coasts 29, 297-310.

Schmidt, R., Wright, J., 2018. Documentation of Myrophis punctatus (Speckled Worm Eel) from Marine Waters of New York. Northeastern Naturalist 25, N1-N3.

Schmitz Jr, W.J., Richardson, P.L., 1991. On the sources of the Florida Current. Deep Sea Research Part A. Oceanographic Research Papers 38, S379-S409.

Shanks, E., 2014. Part VI-B. Waterbody Management Plan Series: Lower Sabine River. Louisian Department of Wildlife and Fisheries.

Shepard, S., 2015a. American Eel Biological Species Report. United States Fish and Wildlife Service, 372.

Shepard, S., 2015b. Endangered and threatened wildlife and plants—12-month finding on a petition to list the American eel as threatened or endangered. Notice of 12-month

petition finding. Federal Register Federal Register. U.S. Government Printing Office, Washington, D.C. (8 October 2015). Docket Number FWS-HQ-ES-2015-0143.

Sola, C., Tongiorgi, P., 1996. The effect of salinity on the chemotaxis of glass eels, Anguilla anguilla, to organic earthy and green odorants. Environmental Biology of Fishes 47, 213-218.

Sorensen, P.W., 1986. Origins of the freshwater attractant (s) of migrating elvers of the American eel, Anguilla rostrata. Environmental Biology of Fishes 17, 185-200.

Sorensen, P.W., Bianchini, M.L., 1986. Environmental Correlates of the Freshwater Migration of Elvers of the American Eel in a Rhode Island Brook. Transactions of the American Fisheries Society 115, 258-268.

Springer, V.G., Woodburn, K.D., 1960. An ecological study of the fishes of the Tampa Bay area. Florida State Board of Conservation, Marine Laboratory.

Sturges, W., Hoffmann, N.G., Leben, R.R., 2010. A trigger mechanism for Loop Current ring separations. Journal of Physical Oceanography 40, 900-913.

Sturges, W., Leben, R., 2000. Frequency of ring separations from the Loop Current in the Gulf of Mexico: A revised estimate. Journal of Physical Oceanography 30, 1814-1819.

Sullivan, M., Able, K., Hare, J., Walsh, H., 2006. Anguilla rostrata glass eel ingress into two, U.S. east coast estuaries: Patterns, processes and implications for adult abundance. Journal of Fish Biology 69, 1081-1101.

Sullivan, M., Wuenschel, M., Able, K., 2009a. Inter and intra-estuary variability in ingress, condition and settlement of the American eel Anguilla rostrata: Implications for estimating and understanding recruitment. Journal of fish biology 74, 1949-1969.

Sullivan, M.C., Wuenschel, M.J., Able, K.W., 2009b. Inter and intra-estuary variability in ingress, condition and settlement of the American eel Anguilla rostrata: implications for estimating and understanding recruitment. Journal of Fish Biology 74, 1949-1969.

Taylor, S.M., Loew, E.R., Grace, M.S., 2015. Ontogenic retinal changes in three ecologically distinct elopomorph fishes (Elopomorpha: Teleostei) correlate with light environment and behavior. Visual neuroscience 32.

TPWD, 2012. Texas Conservation Action Plan (TCAP): Species of Greatest Conservation Need. Texas Parks and Widlife Department. http://tpwd.texas.gov/huntwild/wild/wildlife_diversity/nongame/tcap/sgcn.phtml.

Trancart, T., Lambert, P., Daverat, F., Rochard, E., 2014. From selective tidal transport to counter-current swimming during watershed colonisation: an impossible step for young-of-the-year catadromous fish? Knowl. Managt. Aquatic Ecosyst., 04.

USFWS, 2007. Endangered and threatened wildlife and plants - 12 month finding on a petition to list the American eel as threatened or endangered. Notice of 12-month petition finding. Federal Register 72:22, 4967-4997.

van Ginneken, V.J.T., Maes, G.E., 2005. The European eel (Anguilla anguilla, Linnaeus), its Lifecycle, Evolution and Reproduction: A Literature Review. Reviews in Fish Biology and Fisheries 15, 367-398.

Vaslet, A., France, C., Phillips, D., Feller, I.C., Baldwin, C.C., 2011. Stable-isotope analyses reveal the importance of seagrass beds as feeding areas for juveniles of the speckled worm eel Myrophis punctatus (Teleostei: Ophichthidae) in Florida. Journal of fish biology 79, 692-706.

Wang, C.H., Tzeng, W.N., 2000. The timing of metamorphosis and growth rates of American and European eel leptocephali: A mechanism of larval segregative migration. FISHERIES RESEARCH 46, 191-205.

Warlen, S.M., Burke, J.S., 1990. Immigration of Larvae of Fall/Winter Spawning Marine Fishes into a North Carolina Estuary. Estuaries 13, 453-461.

Wippelhauser, G.S., McCleave, J.D., 1987. Precision of behavior of migrating juvenile American eels (Anguilla rostrata) utilizing selective tidal stream transport. ICES Journal of Marine Science 44, 80-89.

Wippelhauser, G.S., McCleave, J.D., 2009. Rhythmic activity of migrating juvenile American eels Anguilla rostrata. Journal of the Marine Biological Association of the United Kingdom 68, 81-91.

APPENDIX A:

STATISTCAL OUTPUT

Linear regression and assumption checking output

```
morph <- read.csv("Morph_Speck_bar_exclude.csv", header = T)

# Natural log transformed Length Weight all

morph$lnW <-log(morph$Weight/10)

morph$lnL <-log(morph$Length)

attach(morph)

fit <- lm(lnW~lnL)

summary(fit)

##
## Call:
## lm(formula = lnW ~ lnL)
##
## Residuals:
##      Min       1Q   Median       3Q      Max
## -0.81178 -0.16500  0.02025  0.17937  0.80386
##
## Coefficients:
##             Estimate Std. Error t value Pr(>|t|)
## (Intercept) -10.75596    0.12820   -83.9   <2e-16 ***
## lnL           3.12704    0.03096   101.0   <2e-16 ***
## ---
## Signif. codes:  0 '***' 0.001 '**' 0.01 '*' 0.05 '.' 0.1 ' ' 1
##
## Residual standard error: 0.2525 on 735 degrees of freedom
## Multiple R-squared:  0.9328, Adjusted R-squared:  0.9327
## F-statistic: 1.02e+04 on 1 and 735 DF,  p-value: < 2.2e-16

confint(fit)
```

```
##                2.5 %     97.5 %
## (Intercept) -11.00763 -10.504284
## lnL           3.06625   3.187821

plot(fit, which = c(1,4,6),pch=as.character(Stage))
```

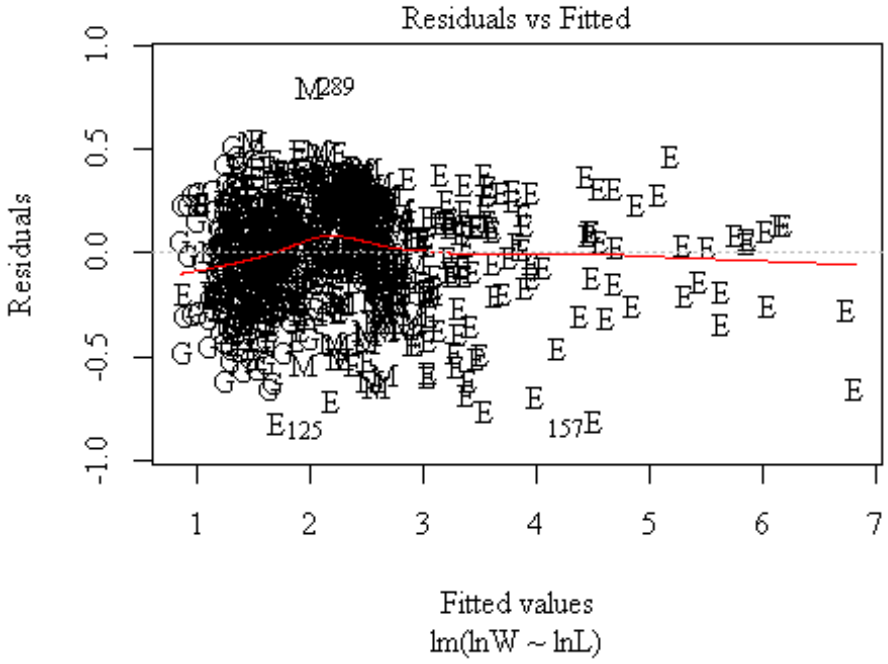

Figure 24 Residual plot of fitted versus residual values of Speckled Worm Eel from the linear regression of ln length vs ln weight.

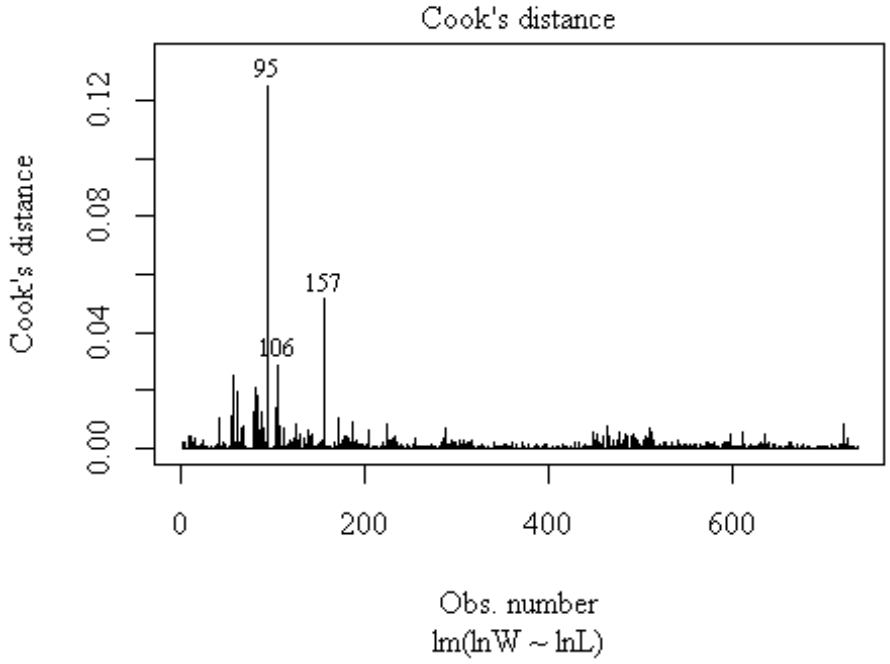

Figure 25 Plot of observation number versus Cooks distance for Speckled Worm Eel linear regression model ln length vs ln weight.

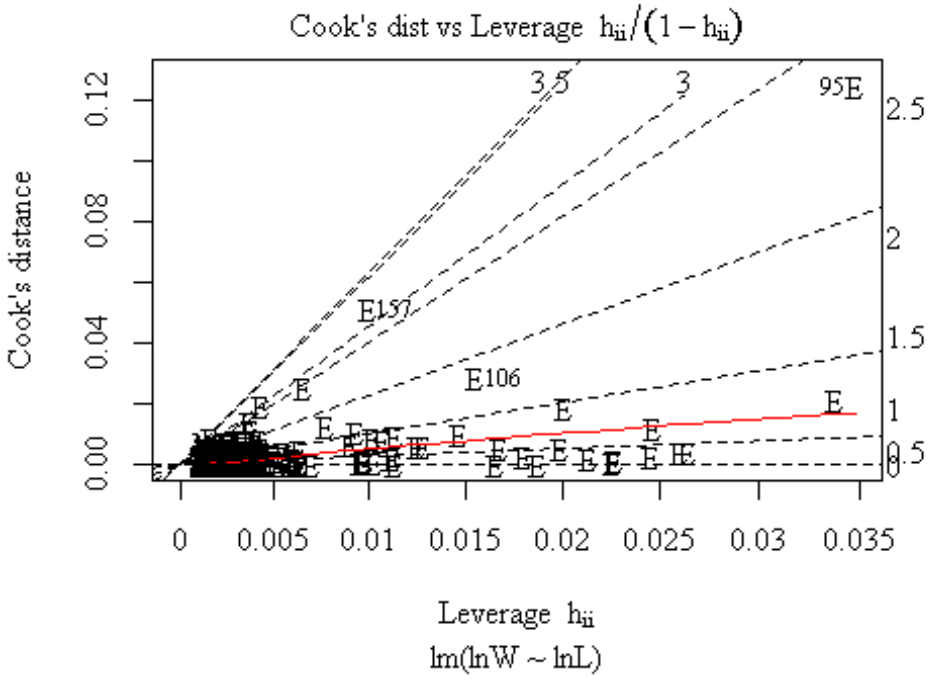

Figure 26 Plot of Leverage versus Cooks distance from the Speckled Worm Eel linear regression ln length vs ln weight.

```
plot(lnL,fit$residuals)
```

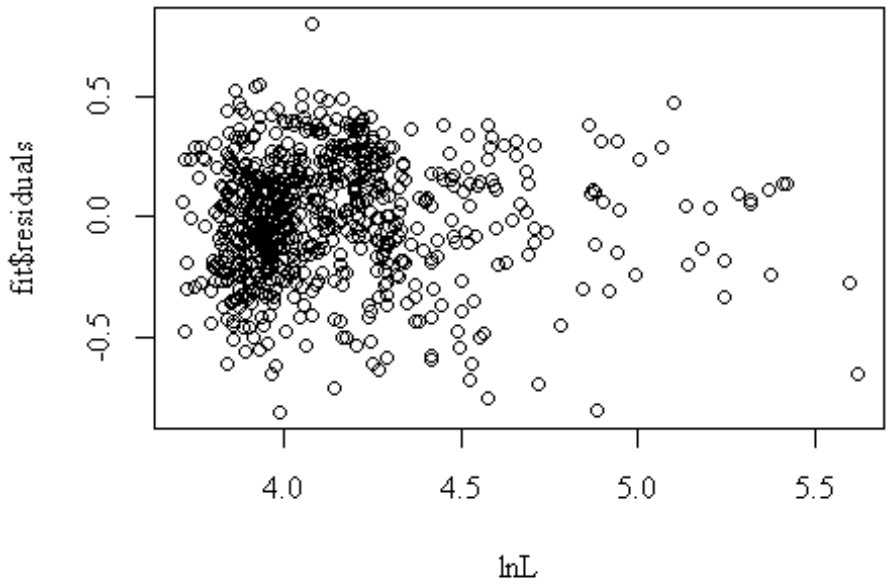

Figure 27 Plot of observed ln length versus fitted residuals from Speckled Worm Eel linear regression of ln length vs ln weight.

```
plot(Stage, fit$residuals, ylab="fitted residuals")
abline(h=0, col="gray75")
```

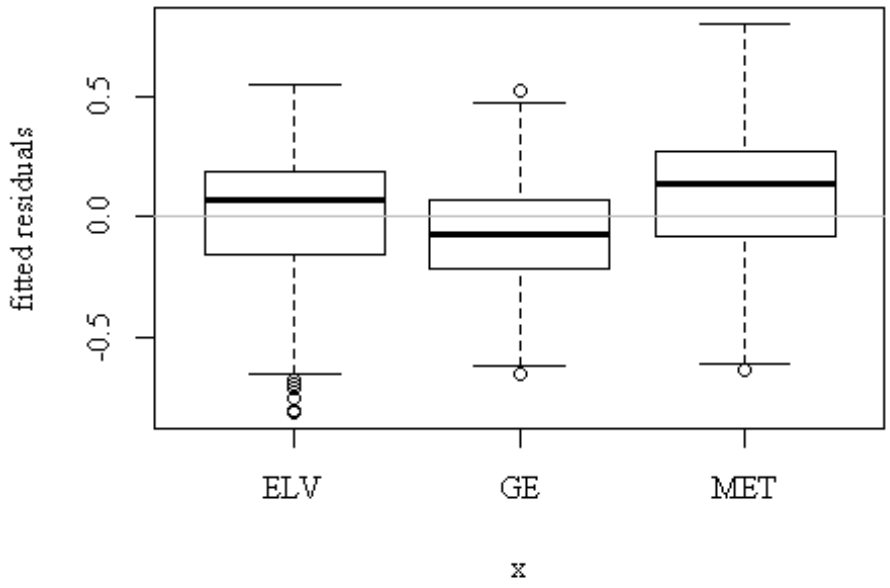

Figure 28 Boxplot of fitted residuals by each life stage, elver (ELV), glass eel (GE), and metamorphic (MET) from the linear regression of ln length vs ln weight.

```
qqPlot(fit, las = 1, id.n = 3, main="QQ Plot", pch=as.character(Stage))
```

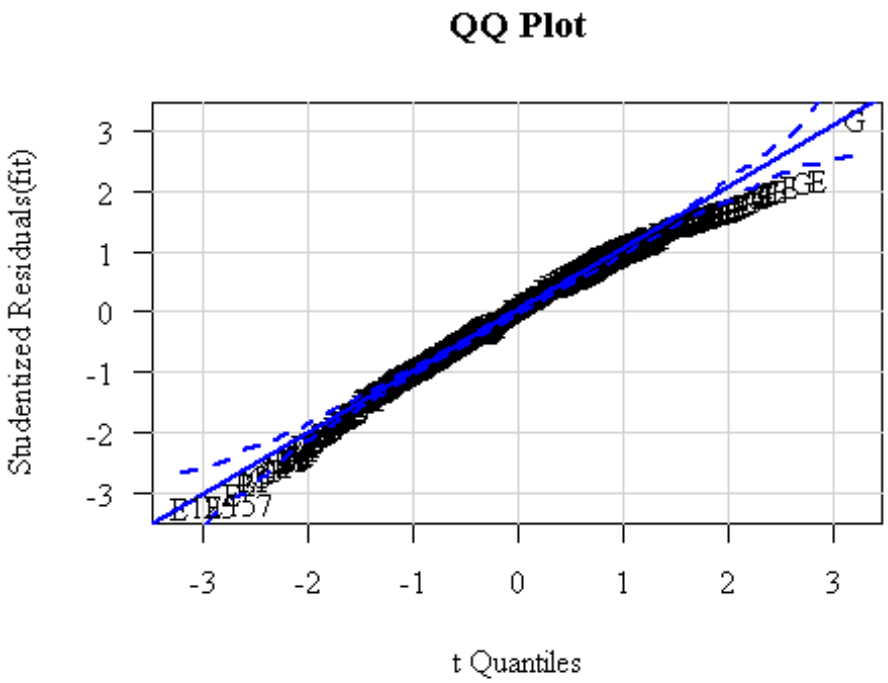

Figure 29 QQplot form the Speckled Worm Eel linear regression of ln length vs ln weight.

```
## [1] 125 157

morph <- read.csv("Morph_Speck_bar_exclude.csv", header = T)

# partioons metamoprhic out of data set =morph
met <- subset(morph, Stage=="MET")
met$lnW <- log(met$Weight/10)

met$lnL <- log(met$Length)
attach(met)

## The following objects are masked from morph:
##
##     Date, Depth, Entered.Date, Entered.Initials, General.Notes,
##     Head, Length, lnL, lnW, Month, Preanal, Preservation,
##     QC.d.Date, QC.d.Initials, Site, Specimen.number, Stage,
##     Unique.ID, Weight, Width
```

```
fit.met <-lm(lnW~lnL)

summary(fit.met)

##
## Call:
## lm(formula = lnW ~ lnL)
##
## Residuals:
##      Min       1Q   Median       3Q      Max
## -0.68467 -0.15322  0.06234  0.19927  0.66650
##
## Coefficients:
##             Estimate Std. Error t value Pr(>|t|)
## (Intercept)  -8.7381     0.6507  -13.43   <2e-16 ***
## lnL           2.6658     0.1553   17.16   <2e-16 ***
## ---
## Signif. codes:  0 '***' 0.001 '**' 0.01 '*' 0.05 '.' 0.1 ' ' 1
##
## Residual standard error: 0.2475 on 192 degrees of freedom
## Multiple R-squared:  0.6054, Adjusted R-squared:  0.6034
## F-statistic: 294.6 on 1 and 192 DF, p-value: < 2.2e-16

confint(fit.met)

##                 2.5 %    97.5 %
## (Intercept) -10.021547 -7.454631
## lnL           2.359511  2.972180

plot(fit.met, which = c(1,4,6),pch=as.character(Stage))
```

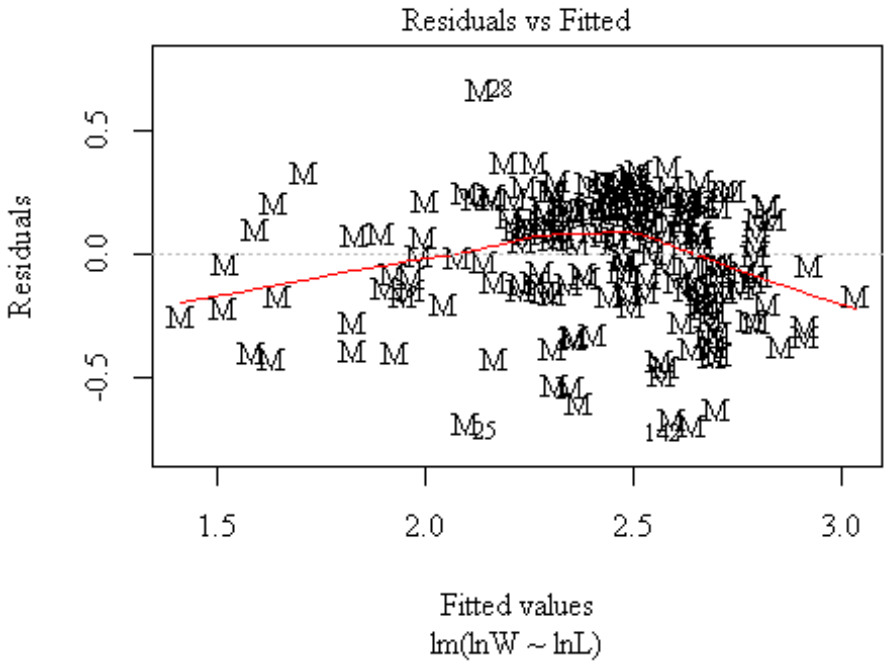

Figure 30 Residual plot of fitted versus residual values from the linear regression of ln length vs ln weight of Speckled Worm Eel metamorphic life stage.

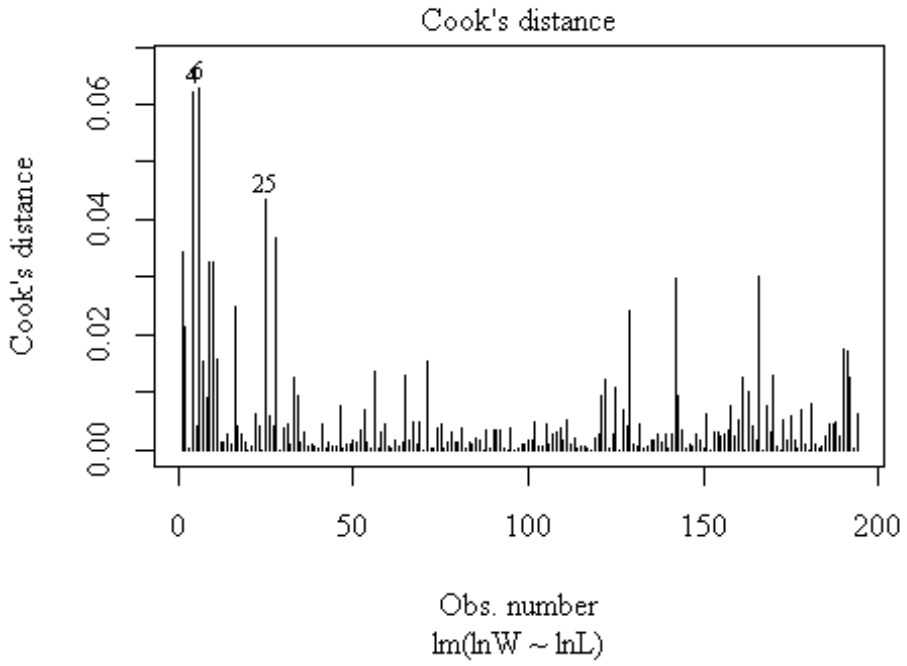

Figure 31 Plot of observation number versus Cooks distance from linear regression model ln length vs ln weight of Speckled Worm Eel metamorphic life stage.

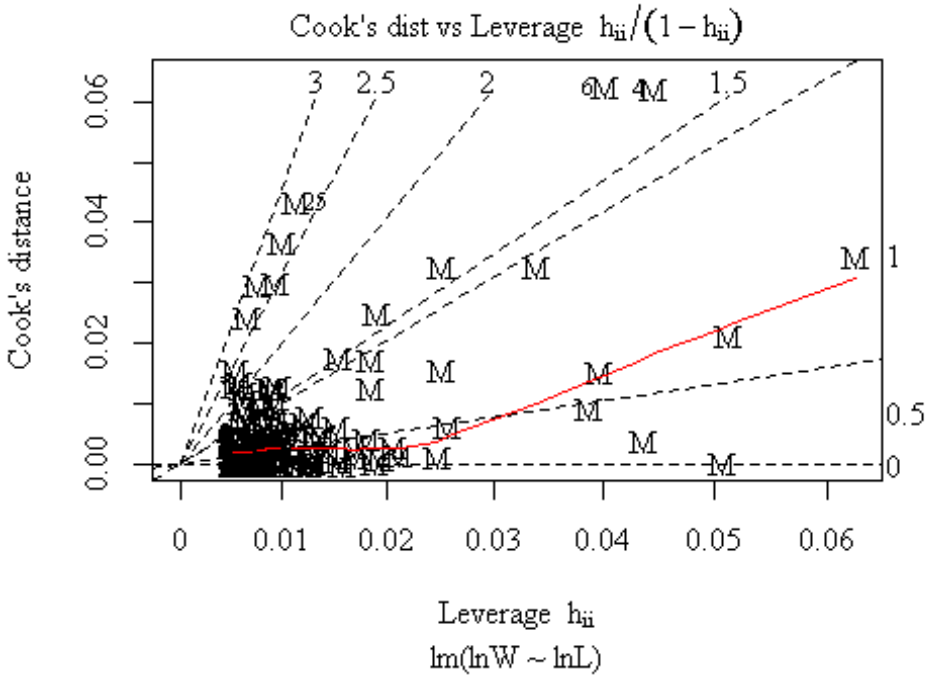

Figure 32 Plot of Leverage versus Cooks distance of the Speckled Worm Eel morphometric life stage from the linear regression ln length vs ln weight

```
plot(lnL,fit.met$residuals)
```

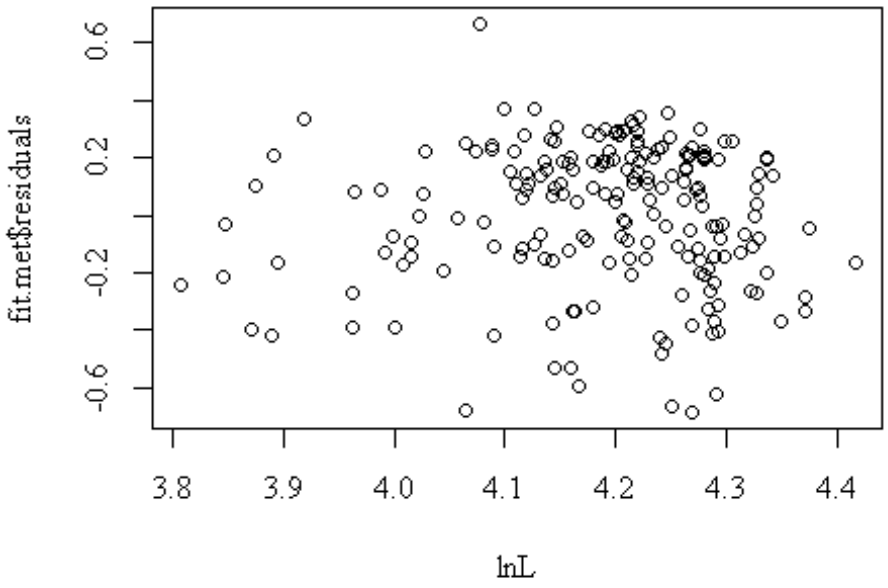

Figure 33 Plot of observed ln length versus fitted residuals from linear regression of ln length vs ln weight from Speckled Worm Eel metamorphic life stage.

```
plot(Stage, fit.met$residuals, ylab="fitted residuals")
abline(h=0, col="gray75")
```

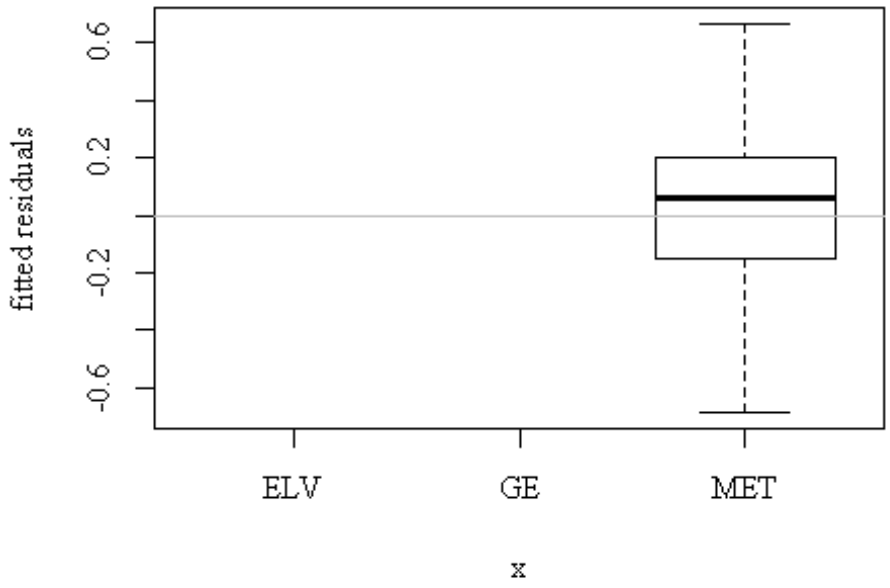

Figure 34 Boxplot of fitted residuals for metamorphic (MET) from the linear regression of ln length vs ln weight.

```
qqPlot(fit.met, las = 1, id.n = 3, main="QQ Plot", pch=as.character(Stage))
```

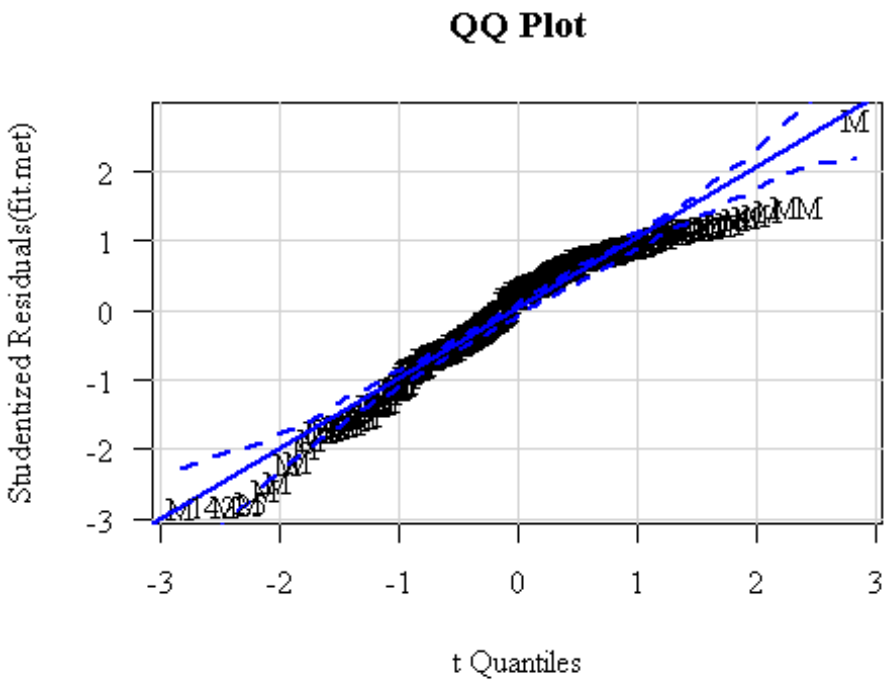

Figure 35 QQ plot form the Speckled Worm Eel linear metamorphic linear regression of ln length vs ln weight.

```
## [1]  25 142

### glass eel #####

ge <-subset(morph, Stage=="GE") # partitions glass eel out of data set


ge$lnW <-log(ge$Weight/10)

ge$lnL <- log(ge$Length)

attach(ge)

## The following objects are masked from met:
##
##     Date, Depth, Entered.Date, Entered.Initials, General.Notes,
```

```
##     Head, Length, lnL, lnW, Month, Preanal, Preservation,
##     QC.d.Date, QC.d.Initials, Site, Specimen.number, Stage,
##     Unique.ID, Weight, Width

## The following objects are masked from morph:
##
##     Date, Depth, Entered.Date, Entered.Initials, General.Notes,
##     Head, Length, lnL, lnW, Month, Preanal, Preservation,
##     QC.d.Date, QC.d.Initials, Site, Specimen.number, Stage,
##     Unique.ID, Weight, Width

fit.ge <-lm(lnW~lnL)

summary(fit.ge)

##
## Call:
## lm(formula = lnW ~ lnL)
##
## Residuals:
##      Min       1Q   Median       3Q      Max
## -0.56656 -0.13911  0.00772  0.14916  0.58561
##
## Coefficients:
##             Estimate Std. Error t value Pr(>|t|)
## (Intercept) -10.0070     0.6502  -15.39   <2e-16 ***
## lnL           2.9171     0.1660   17.57   <2e-16 ***
## ---
## Signif. codes:  0 '***' 0.001 '**' 0.01 '*' 0.05 '.' 0.1 ' ' 1
##
## Residual standard error: 0.2129 on 278 degrees of freedom
## Multiple R-squared:  0.5262, Adjusted R-squared:  0.5245
## F-statistic: 308.7 on 1 and 278 DF,  p-value: < 2.2e-16

confint(fit.ge)

##                 2.5 %    97.5 %
## (Intercept) -11.287023 -8.726984
## lnL           2.590227  3.243874

plot(fit.ge, which = c(1,4,6),pch=as.character(Stage))
```

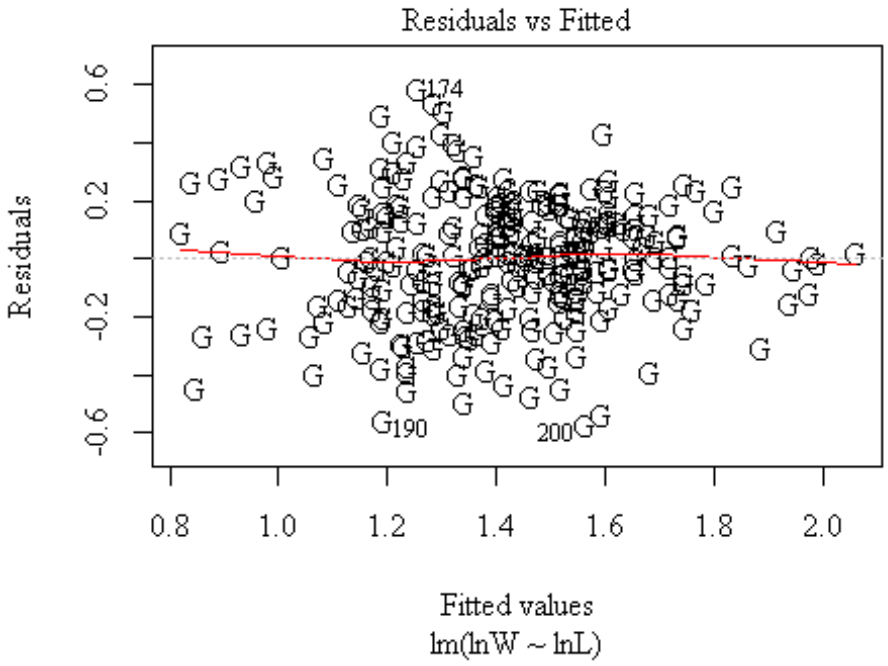

Figure 36 Residual plot of fitted versus residual values from the linear regression of ln length vs ln weight of Speckled Worm Eel glass eel life stage.

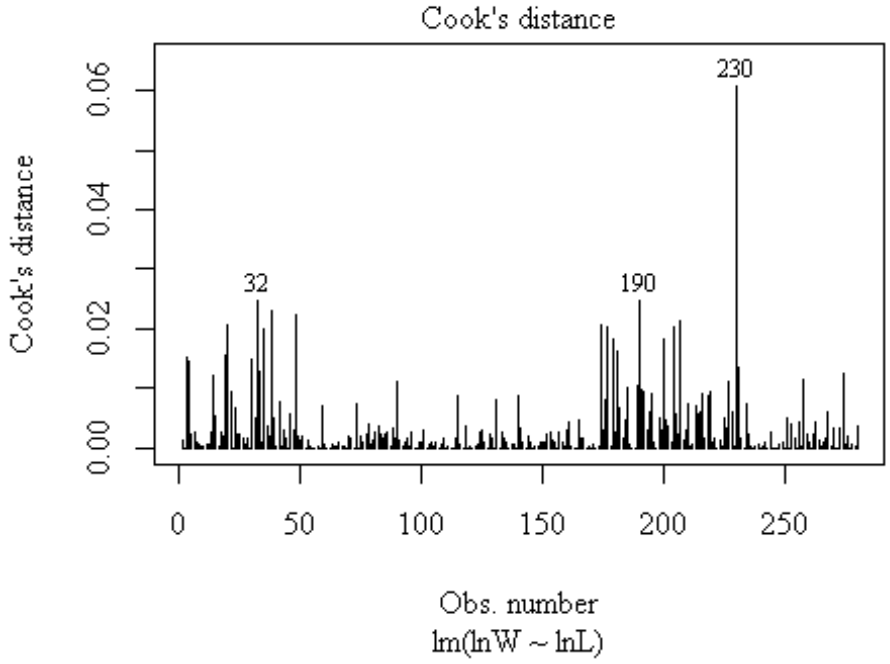

Figure 37 Plot of observation number versus Cooks distance from linear regression model ln length vs ln weight of Speckled Worm Eel glass eel life stage.

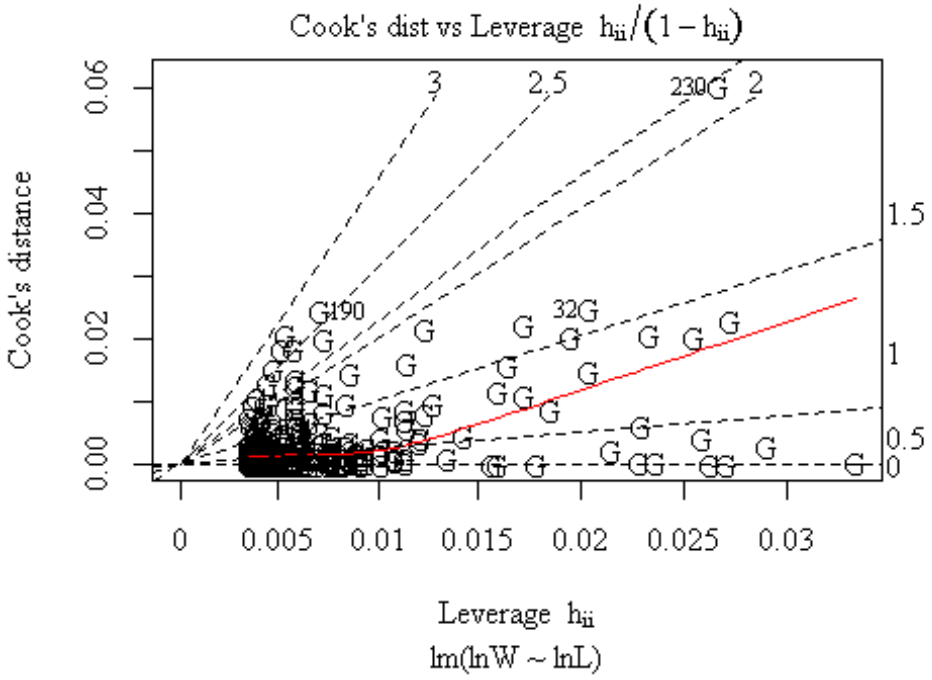

Figure 38Plot of Leverage versus Cooks distance of the Speckled Worm Eel glass eel life stage from the linear regression ln length vs ln weight.

```
plot(lnL,fit.ge$residuals)
```

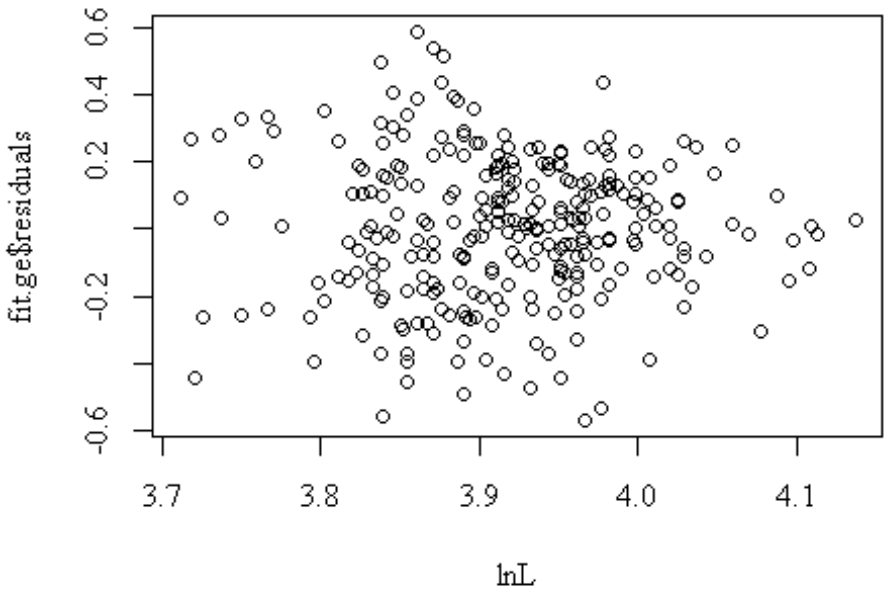

Figure 39 Plot of observed ln length versus fitted residuals from linear regression of ln length vs ln weight from Speckled Worm Eel glass eel life stage.

```
plot(Stage, fit.ge$residuals, ylab="fitted residuals")

abline(h=0, col="gray75")
```

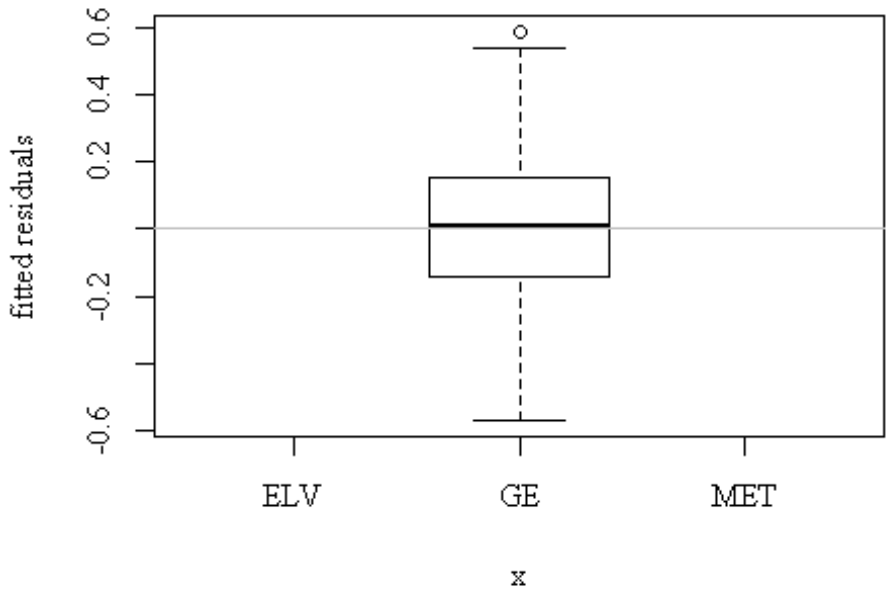

Figure 40 Boxplot of fitted residuals for glass eel (GE) from the linear regression of ln length vs ln weight.

```
qqPlot(fit.ge, las = 1, id.n = 3, main="QQ Plot", pch=as.character(Stage))
```

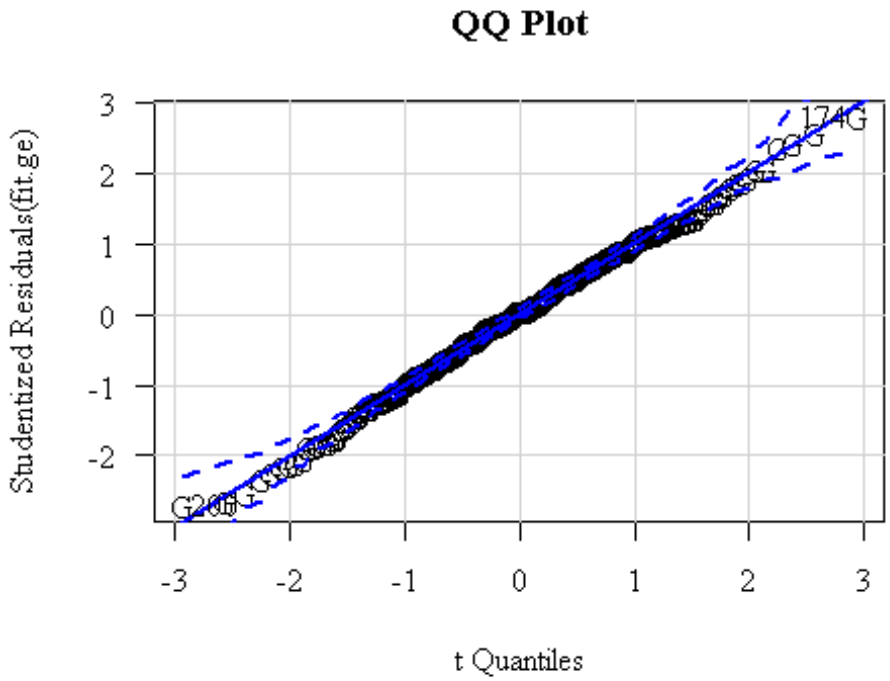

Figure 41 QQ plot form the Speckled Worm Eel glass eel life stage linear metamorphic linear regression of ln length vs ln weight.

```
## [1] 174 200

### Elver
elv <- subset(morph, Stage =="ELV")

elv$lnW <- log(elv$Weight/10)

elv$lnL <- log(elv$Length)

attach(elv)

## The following objects are masked from ge:
##
##     Date, Depth, Entered.Date, Entered.Initials, General.Notes,
##     Head, Length, lnL, lnW, Month, Preanal, Preservation,
##     QC.d.Date, QC.d.Initials, Site, Specimen.number, Stage,
##     Unique.ID, Weight, Width
```

```
## The following objects are masked from met:
##
##     Date, Depth, Entered.Date, Entered.Initials, General.Notes,
##     Head, Length, lnL, lnW, Month, Preanal, Preservation,
##     QC.d.Date, QC.d.Initials, Site, Specimen.number, Stage,
##     Unique.ID, Weight, Width

## The following objects are masked from morph:
##
##     Date, Depth, Entered.Date, Entered.Initials, General.Notes,
##     Head, Length, lnL, lnW, Month, Preanal, Preservation,
##     QC.d.Date, QC.d.Initials, Site, Specimen.number, Stage,
##     Unique.ID, Weight, Width
```

```
fit.elv.log <- lm(lnW~lnL)
```

```
summary(fit.elv.log)
```

```
##
## Call:
## lm(formula = lnW ~ lnL)
##
## Residuals:
##      Min       1Q   Median       3Q      Max
## -0.86333 -0.15340  0.04925  0.17394  0.55313
##
## Coefficients:
##             Estimate Std. Error t value Pr(>|t|)
## (Intercept) -10.25027    0.18176  -56.39   <2e-16 ***
## lnL           3.01313    0.04197   71.80   <2e-16 ***
## ---
## Signif. codes:  0 '***' 0.001 '**' 0.01 '*' 0.05 '.' 0.1 ' ' 1
##
## Residual standard error: 0.2652 on 261 degrees of freedom
## Multiple R-squared:  0.9518, Adjusted R-squared:  0.9516
## F-statistic:  5155 on 1 and 261 DF, p-value: < 2.2e-16
```

```
confint(fit.elv.log)
```

```
##                2.5 %    97.5 %
## (Intercept) -10.60817 -9.892363
## lnL           2.93050  3.095767
```

```
plot(fit.elv.log, which = c(1,4,6),pch=as.character(Stage))
```

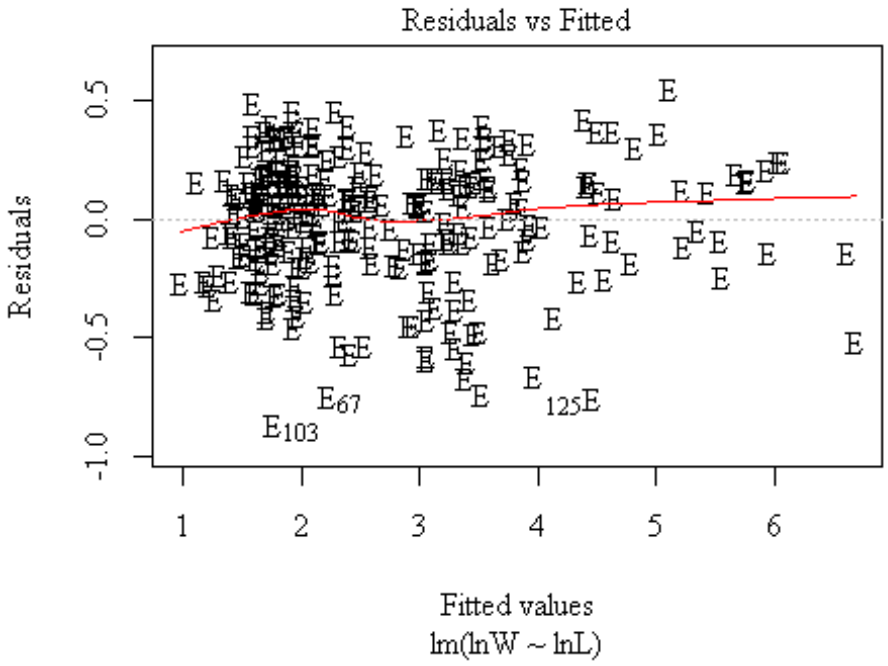

Figure 42 Residual plot of fitted versus residual values from the linear regression of ln length vs ln weight of Speckled Worm Eel elver life stage.

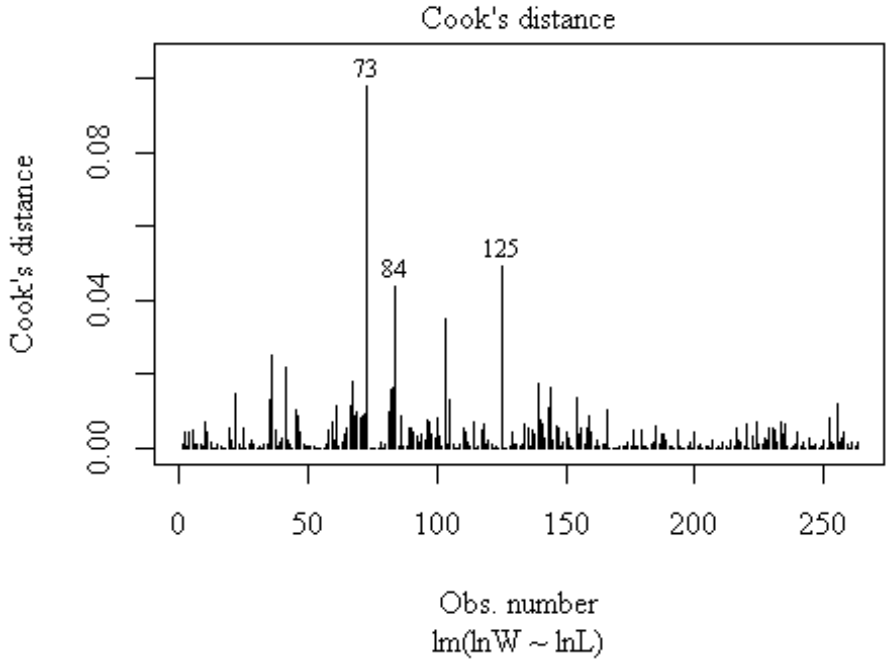

Figure 43 Plot of observation number versus Cooks distance from linear regression model ln length vs ln weight of Speckled Worm Eel elver life stage.

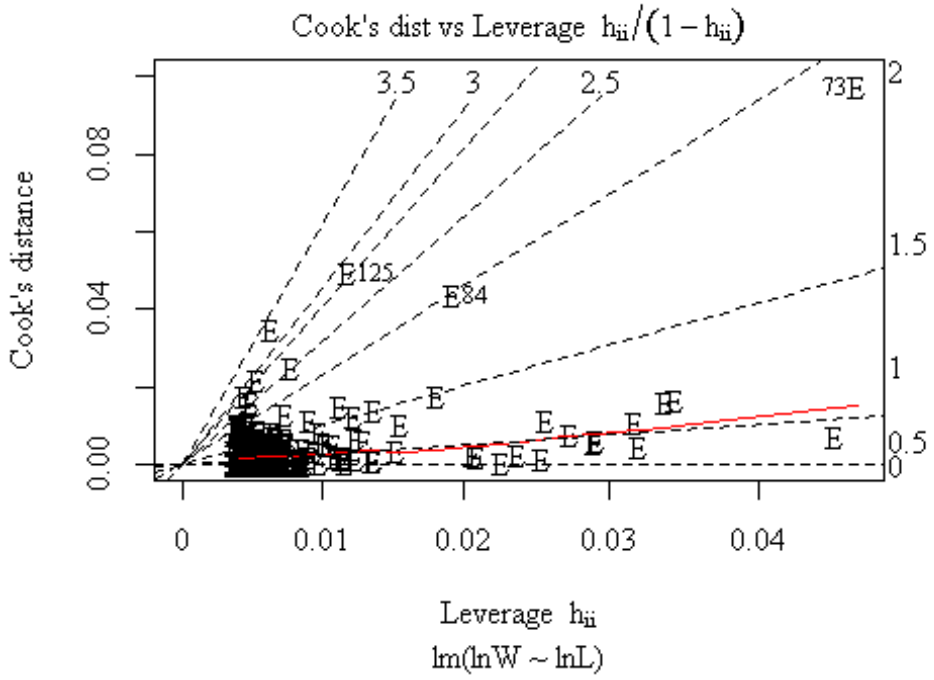

Figure 44 Plot of Leverage versus Cooks distance of the Speckled Worm Eel elver life stage from the linear regression ln length vs ln weight.

```
plot(lnL,fit.elv.log$residuals)
```

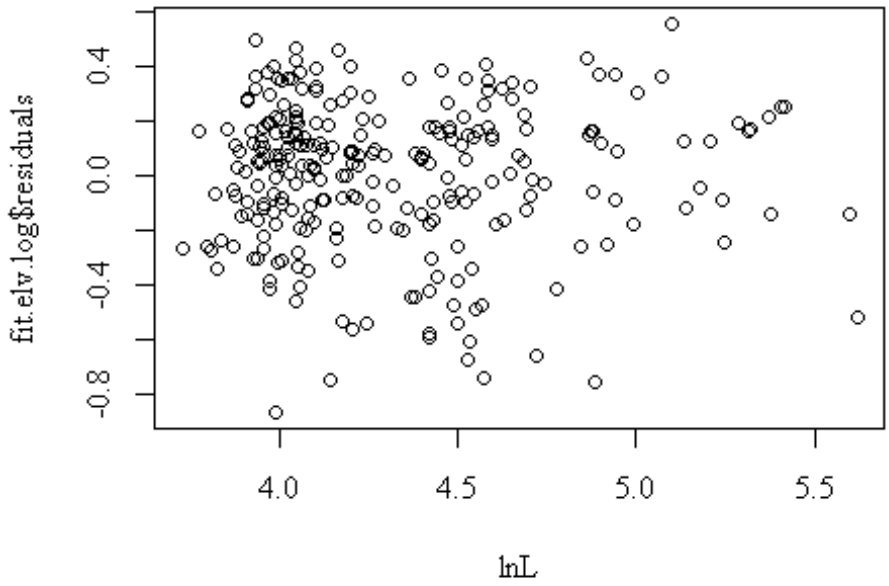

Figure45 Plot of observed ln length versus fitted residuals from linear regression of ln length vs ln weight from Speckled Worm Eel elver life stage.

```
plot(Stage, fit.elv.log$residuals, ylab="fitted residuals")
abline(h=0, col="gray75")
```

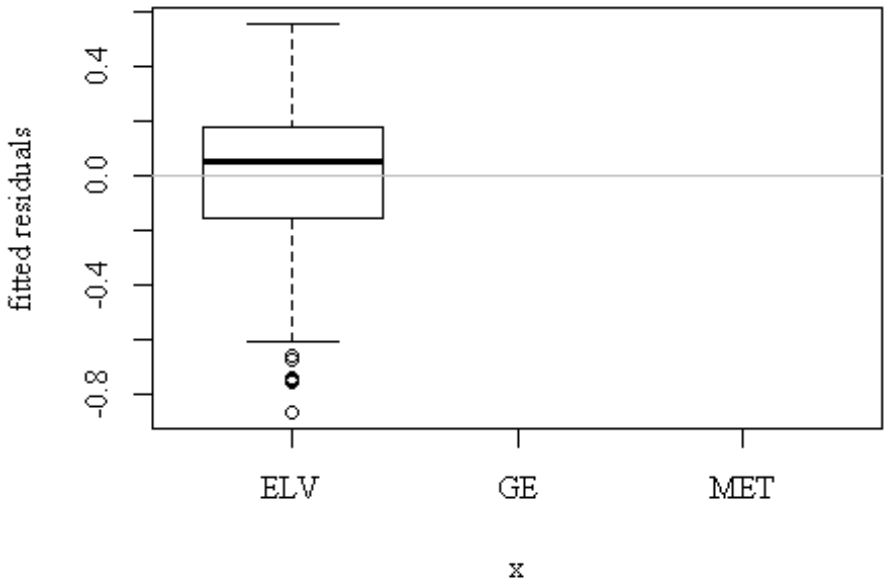

Figure 46 Boxplot of fitted residuals for elver life stage (ELV) from the linear regression of ln length vs ln weight.

```
qqPlot(fit.elv.log, las = 1, id.n = 3, main="QQ Plot", pch=as.character(Stage))
```

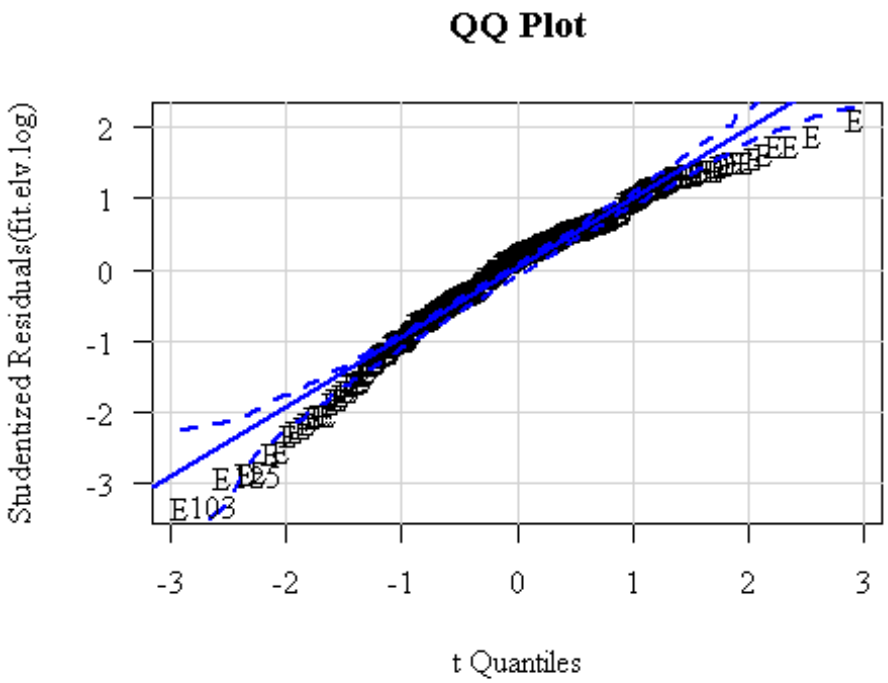

Figure 47 QQ plot form the Speckled Worm Eel elver life stage linear metamorphic linear regression of ln length vs ln weight.

```
## [1] 103 125

### Met and Glass eel #######

gl.el <-subset(morph, Stage=="MET" | Stage=="GE")

## removes ELV as factor

gl.el$lnW <-log(gl.el$Weight/10)

gl.el$lnL <-log(gl.el$Length)

attach(gl.el)

## The following objects are masked from elv:
##
##     Date, Depth, Entered.Date, Entered.Initials, General.Notes,
##     Head, Length, lnL, lnW, Month, Preanal, Preservation,
```

```
##     QC.d.Date, QC.d.Initials, Site, Specimen.number, Stage,
##     Unique.ID, Weight, Width

## The following objects are masked from ge:
##
##     Date, Depth, Entered.Date, Entered.Initials, General.Notes,
##     Head, Length, lnL, lnW, Month, Preanal, Preservation,
##     QC.d.Date, QC.d.Initials, Site, Specimen.number, Stage,
##     Unique.ID, Weight, Width

## The following objects are masked from met:
##
##     Date, Depth, Entered.Date, Entered.Initials, General.Notes,
##     Head, Length, lnL, lnW, Month, Preanal, Preservation,
##     QC.d.Date, QC.d.Initials, Site, Specimen.number, Stage,
##     Unique.ID, Weight, Width

## The following objects are masked from morph:
##
##     Date, Depth, Entered.Date, Entered.Initials, General.Notes,
##     Head, Length, lnL, lnW, Month, Preanal, Preservation,
##     QC.d.Date, QC.d.Initials, Site, Specimen.number, Stage,
##     Unique.ID, Weight, Width
```

```
fit.gl.el <-lm(lnW~lnL)
```

```
summary(fit.gl.el)
```

```
##
## Call:
## lm(formula = lnW ~ lnL)
##
## Residuals:
##      Min       1Q   Median       3Q      Max
## -0.69320 -0.16677  0.00092  0.17440  0.79809
##
## Coefficients:
##             Estimate Std. Error t value Pr(>|t|)
## (Intercept) -11.86442    0.27040  -43.88   <2e-16 ***
## lnL           3.40030    0.06709   50.69   <2e-16 ***
## ---
## Signif. codes:  0 '***' 0.001 '**' 0.01 '*' 0.05 '.' 0.1 ' ' 1
##
## Residual standard error: 0.2389 on 472 degrees of freedom
```

```
## Multiple R-squared:  0.8448, Adjusted R-squared:  0.8445
## F-statistic:  2569 on 1 and 472 DF,  p-value: < 2.2e-16

confint(fit.gl.el)

##                2.5 %    97.5 %
## (Intercept) -12.395747 -11.33309
## lnL           3.268472   3.53212

plot(fit.gl.el, which = c(1,4,6),pch=as.character(Stage))
```

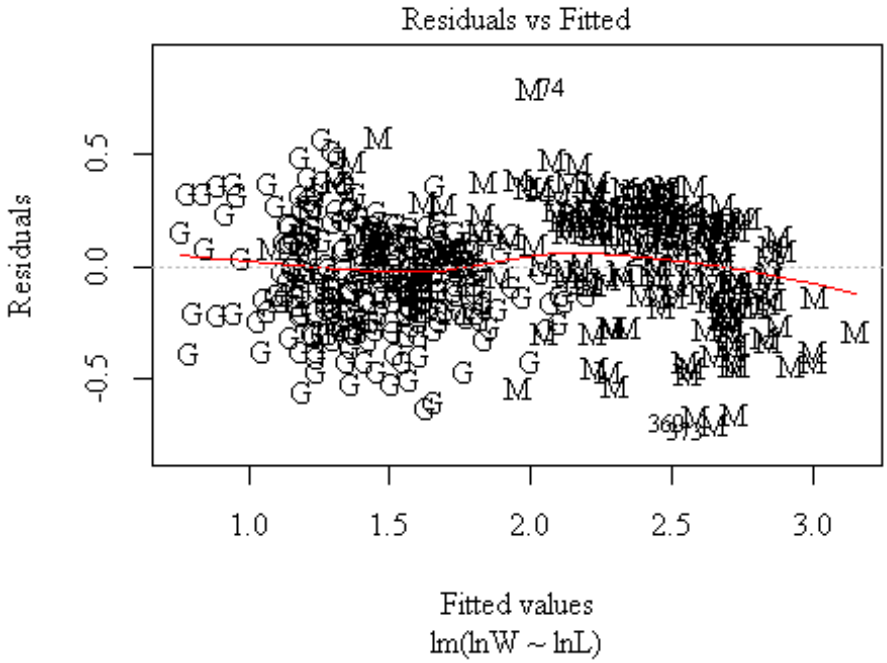

Figure 48 Residual plot of fitted versus residual values from the linear regression of ln length vs ln weight of Speckled Worm Eel metamorphic and glass eel life stages.

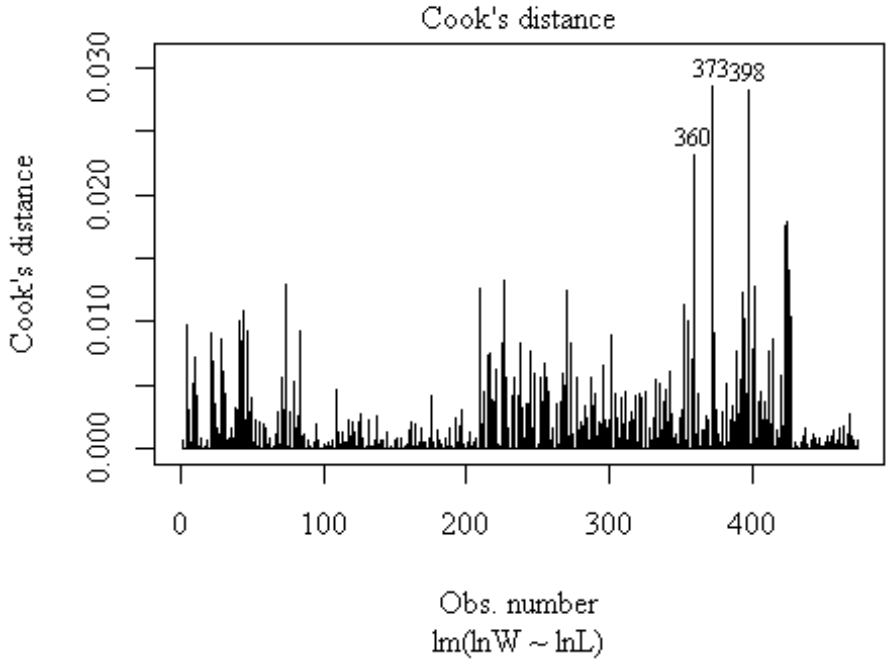

Figure 49 Plot of observation number versus Cooks distance from linear regression model ln length vs ln weight of Speckled Worm Eel metamorphic and glass eel life stages.

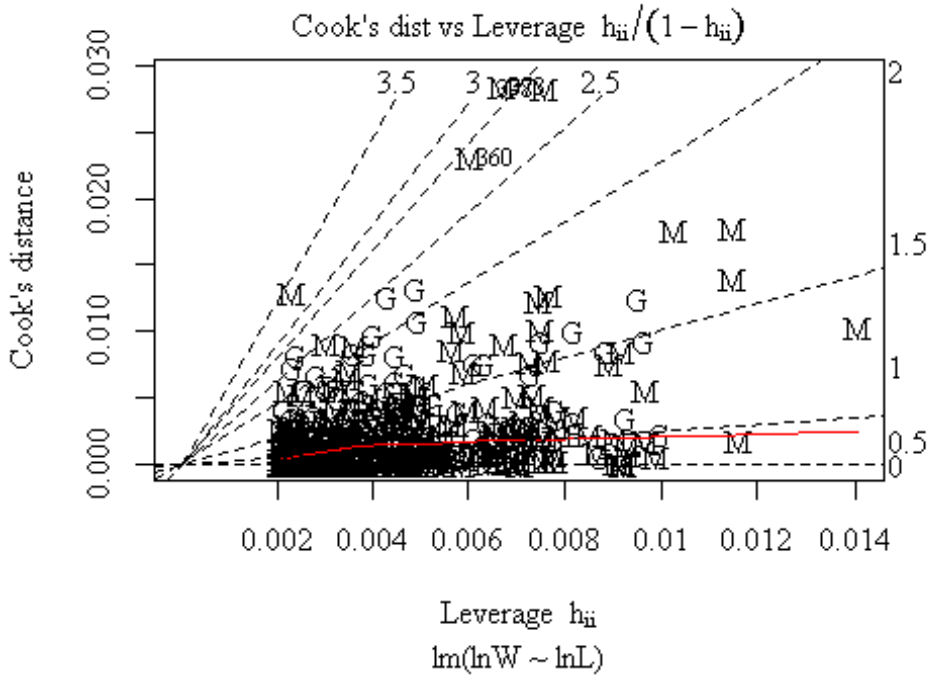

Figure 50 Plot of Leverage versus Cooks distance of the Speckled Worm Eel metamorphic and glass eel life stages from the linear regression ln length vs ln weight.

```
plot(lnL,fit.gl.el$residuals)
```

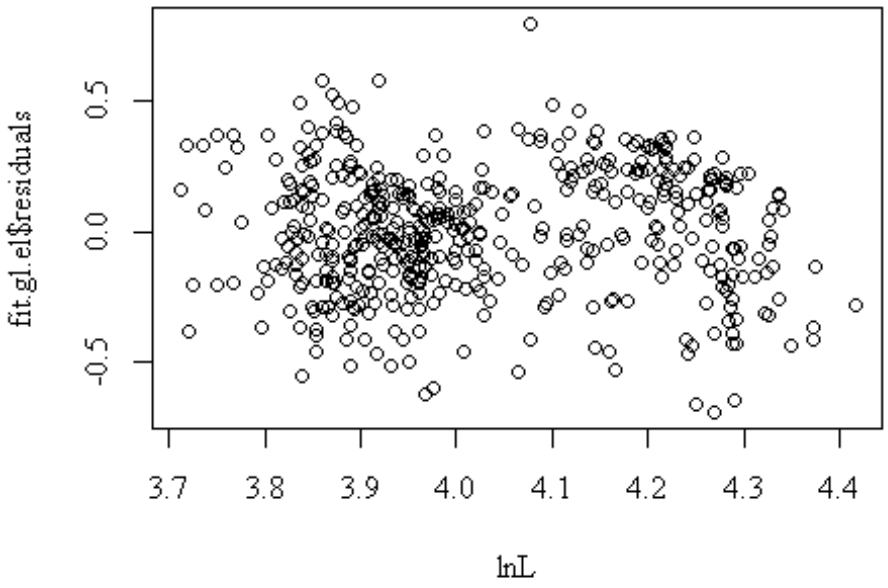

Figure 51 Plot of observed ln length versus fitted residuals from linear regression of ln length vs ln weight from Speckled Worm Eel metamorphic and glass eel life stages.

```
plot(Stage, fit.gl.el$residuals, ylab="fitted residuals")

abline(h=0, col="gray75")
```

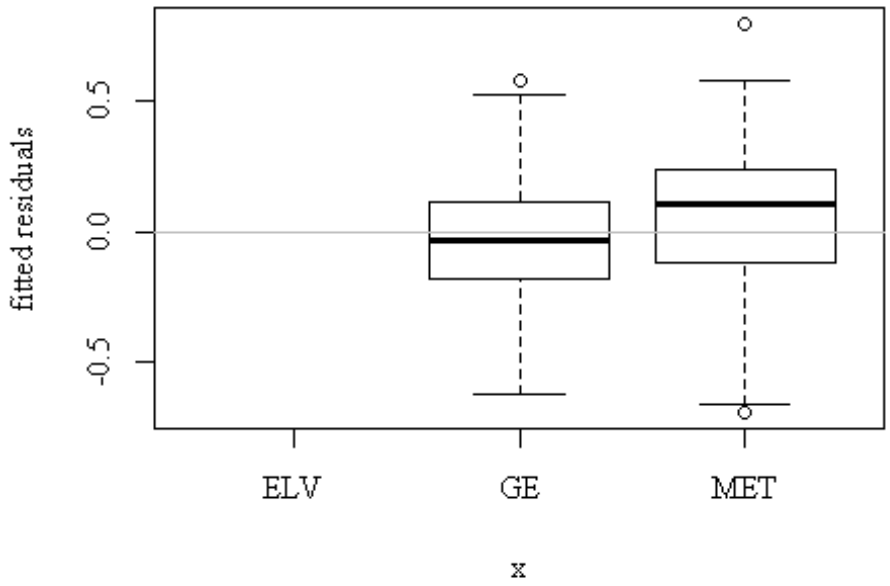

Figure 52 Boxplot of fitted residuals for metamorphic (MET) and glass eel (GE) life stage from the linear regression of ln length vs ln weight.

```
qqPlot(fit.gl.el, las = 1, id.n = 3, main="QQ Plot", pch=as.character(Stage))
```

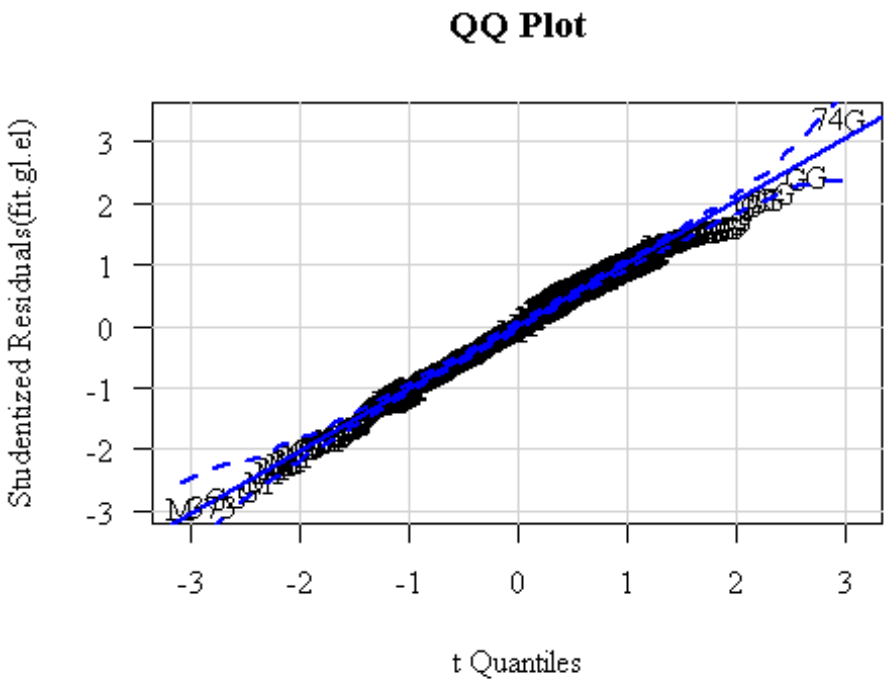

Figure 53 QQ plot form the Speckled Worm Eel metamorphic and glass eel life stages linear metamorphic linear regression of ln length vs ln weight.

```
## [1]  74 373
```

Nonparametric testing between life stages

```
### Non-Parametric test Appendix Material

morph<-read.csv("Morph_Speck_bar_exclude.csv", header= T)

morph$Head.L <- morph$Head/morph$Length

morph$Depth.L <-morph$Depth/morph$Length

morph$Width.L <-morph$Width/morph$Length

morph$Preanal.L <- morph$Preanal/morph$Length
```

```
morph$W.D.R <- morph$Width.L/morph$Depth.L

morph$lnL <- log(morph$Length)

morph$lnW <- log(morph$Weight)

attach(morph)

# Morphometrics comparisions between Life Stages

## Head Length

morph$Stage <- factor(morph$Stage,levels= c("MET","GE","ELV")) ## re orders the fa
ctor

morph$Head.L <- morph$Head/morph$Length

kruskal.test(morph$Head.L~morph$Stage)

##
##  Kruskal-Wallis rank sum test
##
## data:  morph$Head.L by morph$Stage
## Kruskal-Wallis chi-squared = 414.93, df = 2, p-value < 2.2e-16

pairwise.wilcox.test(morph$Head.L,morph$Stage, p.adjust.method = "none")

##
##  Pairwise comparisons using Wilcoxon rank sum test
##
## data:  morph$Head.L and morph$Stage
##
##     MET    GE
## GE  <2e-16 -
## ELV <2e-16 0.052
##
## P value adjustment method: none

######## Body Depth ###########

morph$Depth.L <-morph$Depth/morph$Length

kruskal.test(morph$Depth.L~morph$Stage)
```

```
##
##  Kruskal-Wallis rank sum test
##
## data:  morph$Depth.L by morph$Stage
## Kruskal-Wallis chi-squared = 470.39, df = 2, p-value < 2.2e-16

pairwise.wilcox.test(morph$Depth.L, morph$Stage, p.adjust.method = "none")

##
##  Pairwise comparisons using Wilcoxon rank sum test
##
## data:  morph$Depth.L and morph$Stage
##
##     MET    GE
## GE  <2e-16 -
## ELV <2e-16 <2e-16
##
## P value adjustment method: none

## Body Width

morph$Width.L <-morph$Width/morph$Length

kruskal.test(morph$Width.L~morph$Stage)

##
##  Kruskal-Wallis rank sum test
##
## data:  morph$Width.L by morph$Stage
## Kruskal-Wallis chi-squared = 107.21, df = 2, p-value < 2.2e-16

pairwise.wilcox.test(morph$Width.L,morph$Stage, p.adjust.method = "none")

##
##  Pairwise comparisons using Wilcoxon rank sum test
##
## data:  morph$Width.L and morph$Stage
##
##     MET     GE
## GE  1.6e-10 -
## ELV < 2e-16 7.4e-09
##
## P value adjustment method: none
```

```
## Pre-anal Length

morph$Preanal.L <- morph$Preanal/morph$Length

kruskal.test(morph$Preanal.L~morph$Stage)

##
##  Kruskal-Wallis rank sum test
##
## data:  morph$Preanal.L by morph$Stage
## Kruskal-Wallis chi-squared = 4.9548, df = 2, p-value = 0.08396

pairwise.wilcox.test(morph$Preanal.L,morph$Stage, p.adjust.method = "none")

##
##  Pairwise comparisons using Wilcoxon rank sum test
##
## data:  morph$Preanal.L and morph$Stage
##
##     MET   GE
## GE  0.806 -
## ELV 0.096 0.037
##
## P value adjustment method: none

## Body Width/ Body Depth Ratio ##

morph$W.D.R <- Width.L/Depth.L

w.d.r <- (morph$Width/morph$Depth)/morph$Length

kruskal.test(morph$W.D.R~morph$Stage)

##
##  Kruskal-Wallis rank sum test
##
## data:  morph$W.D.R by morph$Stage
## Kruskal-Wallis chi-squared = 444.4, df = 2, p-value < 2.2e-16

pairwise.wilcox.test(morph$W.D.R,morph$Stage, p.adjust.method = "none")

##
##  Pairwise comparisons using Wilcoxon rank sum test
##
```

```
## data:  morph$W.D.R and morph$Stage
##
##     MET     GE
## GE  < 2e-16 -
## ELV < 2e-16 3.9e-12
##
## P value adjustment method: none
```

Allometric vs Isometric growth t-test

```
# tests for allometric growth  on a species level

# log transform weight and turn mg into grams by dividing by 10
data$lnW <- log(data$Weight/10)

# log transforms length
data$lnL <- log(data$Length)

# creates a simple linear regression of natural log weight vs ln Length
fit <- lm (data$lnW ~data$lnL)

# FSA fucntion conducts one sample t-test using coefficients from the fit object and testin
g against slope of 3

hoCoef(fit,2,3)

##  term Ho Value Estimate Std. Error        T  df      p value
##     2        3 3.127035 0.03096249 4.102874 735 4.536917e-05

# calculates t-statistic
t. <- (3.12704 -3)/ (.03096)

# 2*P(T > |t|)

# calculated p-value
2*pt(t. , df=length(data$lnL)-1, lower.tail = F)

## [1] 4.526988e-05

# These steps are repeated for subsequent models below

# Metamorphic slope t.test

met <- subset(data, data$Stage== "MET")

met$lnW <- log(met$Weight/10)

met$lnL <- log(met$Length)

fit.met <- lm(met$lnW~met$lnL)
```

```r
hoCoef(fit.met,2,3)

##  term Ho Value Estimate Std. Error         T  df    p value
##     2        3 2.665845   0.155311 -2.151519 192 0.03268431

# calculates t statistic for MET
t <- abs(fit.met$coefficients[2]-3)/ (.1553)

2*pt(t,df=193, lower.tail = F)

##    met$lnL
## 0.03266562

# Glass Eel slope t.test
ge <- subset(data, data$Stage=="GE")


ge$lnW <-log(ge$Weight/10)

ge$lnL <- log(ge$Length)

fit.ge <- lm(ge$lnW~ge$lnL)

hoCoef(fit.ge,2,3)

##  term Ho Value Estimate Std. Error         T  df   p value
##     2        3 2.917051  0.1660237 -0.4996244 278 0.6177348

t.g <-abs(2.9171-3) / (.1660)

2*pt(t.g, df=length(ge$lnL)-1, lower.tail = F)

## [1] 0.6178929

# Elver slope t.test

elv <- subset(data, data$Stage=="ELV")

elv$lnW <- log(elv$Weight/10)

elv$lnL <- log(elv$Length)

fit.elv <- lm(elv$lnW~elv$lnL)
```

```
hoCoef(fit.elv,2,3)

##  term Ho Value Estimate Std. Error       T  df   p value
##     2        3 3.013134 0.04196535 0.312961 261 0.7545602

t.e <- abs(3.01313-3)/.04197

2*pt(t.e, df=length(elv$lnL)-1, lower.tail = F)

## [1] 0.7546492

# MEt + Elver slope t.test

m.g <- subset(data, data$Stage== ("MET") |data$Stage =="GE")

m.g$lnW <- log(m.g$Weight/10)

m.g$lnL <- log(m.g$Length)

fit.mg <- lm (m.g$lnW~m.g$lnL)

hoCoef(fit.mg,2,3)

##  term Ho Value Estimate Std. Error       T  df     p value
##     2        3 3.400296 0.06708573 5.96693 472 4.75011e-09

t.mg <-abs( (3.40030 - 3) / .06709)

2*pt(t.mg, df=length(m.g$Length)-1, lower.tail = F)

## [1] 4.752255e-09
```

Binomial logistic regression output and AIC model selection

```
## creates binary column 1= presence , 0= absence
dat$bin <- ifelse(dat$Count < 1,0,1)
```

```r
# defines binary column as own object
bin <- dat$bin

# makes variables more ledgable in output

secchi <-dat$Sechhi

RWD <-dat$RWD

Tide <- as.factor(dat$Net.Retrieve.Stage..1.low..2.rising..3.high..4.falling.)

Percent <-dat$Percent

Temp <- dat$Temp

DOmg <- dat$Domg

Sal <- dat$Sal

# fit with all variables included: secchi, retreive water depth, percent ill, Temp, DOmg, ti
de
fit1 <- glm(bin~secchi+RWD+Percent+Temp+DOmg+Tide+Sal,
          family =binomial(link = "logit"))

# regression output
summary(fit1)

##
## Call:
## glm(formula = bin ~ secchi + RWD + Percent + Temp + DOmg + Tide +
##     Sal, family = binomial(link = "logit"))
##
## Deviance Residuals:
##     Min       1Q   Median       3Q      Max
## -1.6509  -0.8368  -0.6534   1.1192   2.2159
##
## Coefficients:
##              Estimate Std. Error z value Pr(>|z|)
## (Intercept)  1.4753022  1.5487088   0.953  0.34079
## secchi      -3.8683369  1.3442944  -2.878  0.00401 **
## RWD         -0.8957694  0.8050325  -1.113  0.26583
## Percent     -0.0005689  0.0044305  -0.128  0.89783
```

```
## Temp        -0.0647618  0.0363861  -1.780  0.07510 .
## DOmg         0.0141699  0.1014825   0.140  0.88895
## Tide2        0.2369376  0.5223347   0.454  0.65011
## Tide3        0.1313684  0.7277006   0.181  0.85674
## Tide4       -0.0538904  0.5438369  -0.099  0.92106
## Sal          0.0621056  0.0228951   2.713  0.00668 **
## ---
## Signif. codes:  0 '***' 0.001 '**' 0.01 '*' 0.05 '.' 0.1 ' ' 1
##
## (Dispersion parameter for binomial family taken to be 1)
##
##     Null deviance: 276.45  on 225  degrees of freedom
## Residual deviance: 253.27  on 216  degrees of freedom
## AIC: 273.27
##
## Number of Fisher Scoring iterations: 4

# AIC step function to reduce variables
step(fit1)

## Start:  AIC=273.27
## bin ~ secchi + RWD + Percent + Temp + DOmg + Tide + Sal
##
##           Df Deviance    AIC
## - Tide     3   253.97 267.97
## - Percent  1   253.29 271.29
## - DOmg     1   253.29 271.29
## - RWD      1   254.52 272.52
## <none>         253.27 273.27
## - Temp     1   256.55 274.55
## - Sal      1   260.72 278.72
## - secchi   1   263.43 281.43
##
## Step:  AIC=267.97
## bin ~ secchi + RWD + Percent + Temp + DOmg + Sal
##
##           Df Deviance    AIC
## - DOmg     1   254.00 266.00
## - Percent  1   254.02 266.02
## - RWD      1   255.42 267.42
## <none>         253.97 267.97
## - Temp     1   256.81 268.81
## - Sal      1   261.55 273.55
```

```
## - secchi   1   264.29 276.29
##
## Step:  AIC=266
## bin ~ secchi + RWD + Percent + Temp + Sal
##
##           Df Deviance    AIC
## - Percent  1   254.04 264.04
## - RWD      1   255.63 265.63
## <none>         254.00 266.00
## - Temp     1   258.50 268.50
## - Sal      1   261.61 271.61
## - secchi   1   264.29 274.29
##
## Step:  AIC=264.04
## bin ~ secchi + RWD + Temp + Sal
##
##          Df Deviance    AIC
## - RWD     1   255.69 263.69
## <none>        254.04 264.04
## - Temp    1   258.54 266.54
## - Sal     1   261.64 269.64
## - secchi  1   264.52 272.52
##
## Step:  AIC=263.69
## bin ~ secchi + Temp + Sal
##
##          Df Deviance    AIC
## <none>        255.69 263.69
## - Temp    1   263.11 269.11
## - Sal     1   264.59 270.59
## - secchi  1   265.78 271.78

##
## Call:  glm(formula = bin ~ secchi + Temp + Sal, family = binomial(link = "logit"))
##
## Coefficients:
## (Intercept)       secchi         Temp          Sal
##     1.30064     -3.78780     -0.07242      0.06494
##
## Degrees of Freedom: 225 Total (i.e. Null);  222 Residual
## Null Deviance:       276.4
## Residual Deviance: 255.7     AIC: 263.7
```

```r
# Final model
fit3 <- glm(bin~ secchi+dat$Temp+dat$Sal, family= "binomial")

summary(fit3)

##
## Call:
## glm(formula = bin ~ secchi + dat$Temp + dat$Sal, family = "binomial")
##
## Deviance Residuals:
##     Min       1Q   Median       3Q      Max
## -1.5766  -0.8400  -0.6621    1.1341    2.1468
##
## Coefficients:
##             Estimate Std. Error z value Pr(>|z|)
## (Intercept)  1.30064    0.68350   1.903  0.05705 .
## secchi      -3.78780    1.32153  -2.866  0.00415 **
## dat$Temp    -0.07242    0.02708  -2.674  0.00749 **
## dat$Sal      0.06494    0.02189   2.967  0.00301 **
## ---
## Signif. codes:  0 '***' 0.001 '**' 0.01 '*' 0.05 '.' 0.1 ' ' 1
##
## (Dispersion parameter for binomial family taken to be 1)
##
##     Null deviance: 276.45  on 225  degrees of freedom
## Residual deviance: 255.69  on 222  degrees of freedom
## AIC: 263.69
##
## Number of Fisher Scoring iterations: 4

confint(fit3)

## Waiting for profiling to be done...

##                  2.5 %      97.5 %
## (Intercept) -0.02767939  2.66221192
## secchi      -6.54757941 -1.35995358
## dat$Temp    -0.12666783 -0.02012404
## dat$Sal      0.02234058  0.10865749

# calulates percent change in odds for secchi

1-exp(fit3$coefficients[2])
```

```
##    secchi
## 0.9773547

# calculates percent change in odds 95% CI for sechhi
1-exp(c(-6.54757941,-1.35995358))

## [1] 0.9985664 0.7433273

# calculates percent change in odds for temperature
1-exp(fit3$coefficients[3])

##   dat$Temp
## 0.06985723

# calculates percent change in odds 95% CI temperature
1-exp(c(-0.12666783,-0.02012404))

## [1] 0.1189737 0.0199229

# calculates percent chagne in odds for salinity
exp(fit3$coefficients[4])

##  dat$Sal
## 1.067091

# calculates percent change in odds 95% CI for salinity
1-exp(c(0.02234058,0.10865749))

## [1] -0.0225920 -0.1147805
```

APPENDIX B:

SITES COORDINATES

Table 13 Coordinates of sites sampled by EIH (Numbered codes) and TPWD (alphabetical codes).

Site ID	Latitude	Longitude	Waterbody Name	USGS 8 digit Subbasin Name
1	29.40783	-94.95193	Tributary to Moses Bayou	West Galveston Bay
2	29.65034	-95.0264	Little Cedar Bayou @ 8th st	West Galveston Bay
3	29.61816	-95.01836	Boggy Bayou	West Galveston Bay
4	29.5705	-95.03131	Tributary to clear lake	West Galveston Bay
5	29.58537	-95.1105	Tributary off Horspen	West Galveston Bay
6	29.59434	-95.14105	Horpsen @ spacenter	West Galveston Bay
7	29.35055	-94.97177	Culvert off Highland Bayou (2)	West Galveston Bay
8	29.45486	-95.06739	Dickinson Bayou @ Paul Hopkin Park	West Galveston Bay
9	29.54654	-95.10516	Cow Bayou @ Nasa pkwy	West Galveston Bay
10	28.52371	-96.51239	Blind Bayou @ Comal Road	West Matagorda Bay
11	28.5943	-96.6395	Little Chocolate Bayou @ Little Chocolate Bayou Park	West Matagorda Bay
12	28.62471	-96.62987	Lynn Bayou at Port Lavaca WWTP	West Matagorda Bay
13	28.68764	-96.48364	Keller Creek near Keller Bay @ 2143	East Matagorda Bay - W

Table 13 Coordinates of sites sampled by EIH (Numbered codes) and TPWD (alphabetical codes).

Site ID	Latitude	Longitude	Waterbody Name	USGS 8 digit Subbasin Name
14	28.73845	-96.39988	Tributary to Carancahua Bay	East Matagorda Bay - W
15	28.70126	-96.23455	Tributary to Palacios Bay	East Matagorda Bay - W
16	28.76637	-96.1484	Tres Palacios @ FM 3225	East Matagorda Bay - W
17	28.68317	-95.97595	Colorado River Downstream	Lower Colorado
18	28.71053	-95.9143	Little Boggy Creek @ S. Gulf Road	East Matagorda Bay - E
19	28.8109	-95.66693	Caney Creek @ FM 226	East Matagorda Bay - E
20	28.88416	-95.47675	San Bernard River @ FM 2918	San Bernard
21	28.98035	-95.28471	Oyster Creek @ Cone Island	Austin-Oyster
22	29.09417	-95.28365	Bastrop Bayou @ 227	Austin-Oyster
23	29.1282	-95.24247	Alligator Slough @ FM 227	Austin-Oyster
24	29.21217	-95.20902	Chocolate Bayou @ FM 2004	West Galveston Bay
25	29.693712	-93.852216	Bayou @ Jetty Road	Sabine Lake
26	29.70143	-93.85397	Beach @ Sabine Pass	Sabine Lake
27	29.71037	-93.8594	Texas Bayou @ Jetty Road (1)	Sabine Lake
28	29.7737	-93.94292	Keith Lake	Sabine Lake
29	29.65583	-94.69034	Double Bayou @ west bayshore boat ramp	East Galveston Bay
30	29.66423	-94.69244	Culvert @ Poncho St.	East Galveston Bay
31	29.48553	-94.93224	Factory Bayou	West Galveston Bay

Table 13 Coordinates of sites sampled by EIH (Numbered codes) and TPWD (alphabetical codes).

Site ID	Latitude	Longitude	Waterbody Name	USGS 8 digit Subbasin Name
32	29.34308	-94.97475	Highland Bayou (3)	West Galveston Bay
33	29.71257	-94.99318	Goose Creek at Goose Creek Park	Buffalo-San Jacinto
34	29.55886	-95.01926	Bridge @ Morristown	West Galveston Bay
35	28.45999	-96.41514	Boggy Bayou @ Port O'connor	West Matagorda Bay
36	28.47331	-96.55552	Powderhorn Lake @ Bridge	West Matagorda Bay
37	28.5598	-96.53803	Tributary off Old Town @ Indianola Beach	West Matagorda Bay
38	28.57846	-96.65005	Chocolate Bayou @ Hwy 238	West Matagorda Bay
39	28.63629	-96.45909	Vaes Bay @ Oliva 176	East Matagorda Bay - W
40	28.72114	-96.27312	Turtle Creek @ 35	East Matagorda Bay - W
41	28.71944	-96.25595	Turtle Bay @ Hwy 35	East Matagorda Bay - W
42	28.6605165	-95.9618533	ICW @ FM 2031	Lower Colorado
43	28.94636	-95.39108	Brazos River @ FM 217	Lower Brazos
44	29.0129	-95.32938	Oyster Creek @ Oyster Creek Park	Austin-Oyster
45	30.02951	-93.76238	Cow Bayou	Lower Sabine
46	30.02201	-93.76083	Tidal Creek off Cow Bayou (2)	Lower Sabine
47	29.9992	-93.86591	Old River @ 87	Sabine Lake
48	29.99092	-93.86979	Underpass off 87	Sabine Lake
49	30.03442	-93.77769	Tidal Creek off Cow Bayou (1)	Lower Sabine
50	30.03259	-93.77866	Tidal Creek off Cow Bayou (3)	Lower Sabine

Table 13 Coordinates of sites sampled by EIH (Numbered codes) and TPWD (alphabetical codes).

Site ID	Latitude	Longitude	Waterbody Name	USGS 8 digit Subbasin Name
51	29.96946	-93.9146	Molasses Bayou @ Port Neches Atlantic Rd	Lower Neches
52	29.93434	-93.88589	Trib near Procter ext	Sabine Lake
53	29.30897	-94.98602	Tributary off Highland Bayou	West Galveston Bay
54	29.33527	-94.97227	Tributary off Highland Bayou @ HWY 6	West Galveston Bay
55	29.42172	-94.96132	Moses Lake	West Galveston Bay
56	29.46261	-94.97354	Dickinson Bayou @ 146	West Galveston Bay
57	29.54368	-94.78329	Creek @ Smith Point Rd	East Galveston Bay
58	29.53618	-94.76449	Tributary off Smith Point Rd	East Galveston Bay
59	29.60231	-94.67567	Lone Oak Bayou @ Smith Point Rd	East Galveston Bay
60	29.68052	-94.93053	Ash Lake	Lower Trinity
61	28.738	-96.19599	Tributary off Palacios Bay	East Matagorda Bay - W
62	28.76388	-96.19344	Cash's Creek @ FM 2853	East Matagorda Bay - W
63	28.71779	-96.21054	Creek off Palacios @ 35	East Matagorda Bay - W
64	28.68855	-96.52068	Evaporation Lake	East Matagorda Bay - W
65	28.5186	-96.50497	Blind Bayou @ Comal Road (2)	West Matagorda Bay
66	28.52968	-96.51447	Blind Bayou @ Comal Road (3)	West Matagorda Bay
67	28.73624	-96.40894	Tributary off Vaes Bay	East Matagorda Bay - W
68	28.9892	-95.30499	Oyster Creek @ Culvert -Levee Road	Austin-Oyster

Table 13 Coordinates of sites sampled by EIH (Numbered codes) and TPWD (alphabetical codes).

Site ID	Latitude	Longitude	Waterbody Name	USGS 8 digit Subbasin Name
69	28.99377	-95.30656	Levee Ditch @ Low Water Crossing	Austin-Oyster
70	29.710842	-93.860951	Texas Bayou @ Jetty Road (2)	Sabine Lake
71	29.87792	-93.97953	Tributary off Taylor Bayou	Sabine Lake
72	30.00099	-93.86667	Tributary off Old River	Lower Neches
73	29.70192	-94.94357	Canal off of Cedar Bayou	North Galveston Bay
74	29.7149	-94.99196	Goose Creek (1)	Buffalo-San Jacinto
75	28.61961	-95.97284	ICW- Colorado	Lower Colorado
76	29.73693	-93.90118	Tidal Creek @ HWY 87	Sabine Lake
77	29.99028	-93.86796	Underpass near 87	Sabine Lake
78	29.61111	-94.67701	Lone Oak Bayou (2)	East Galveston Bay
79	29.82584	-94.25262	Tributary off Mayhaw Bayou @ 73	Sabine Lake
80	29.78741	-95.04262	Slap Out Gully	Buffalo-San Jacinto
81	29.78741	-95.04282	Goose Creek (4)	Buffalo-San Jacinto
82	29.72094	-94.9429	Cedar Bayou @ Roseland Park	North Galveston Bay
83	29.33158	-94.94631	Highland Bayou @ Hwy 6	West Galveston Bay
84	28.47863	-96.86266	Lower Guadalupe	Lower Guadalupe
85	28.49656	-96.84341	Hog Bayou @35	West Matagorda Bay
86	28.51179	-96.81661	Goff Bayou	East San Antonio Bay
87	28.77747	-96.6989	Garcita's Creek @ 616	West Matagorda Bay

Table 13 Coordinates of sites sampled by EIH (Numbered codes) and TPWD (alphabetical codes).

Site ID	Latitude	Longitude	Waterbody Name	USGS 8 digit Subbasin Name
88	28.83247	-96.59528	Creek under 616 near Lavaca-Navidad Junction	Lavaca
89	28.83187	-96.57837	Port Lavaca River @ 616	Lavaca
90	28.88962	-95.78584	Live Oak Bayou	East Matagorda Bay - E
91	29.28646	-95.13123	Halls Bayou @ FM 2004	West Galveston Bay
92	29.9901	-93.89979	Nig Bayou	Lower Neches
93	29.994797	-93.92631	Nig Bayou (2)	Lower Neches
94	30.01679	-93.94823	Lower Neches WMA	Lower Neches
95	30.01394	-93.9705	Channel of Neches	Lower Neches
96	29.771379	-93.95307	Side Channel Keith Lake	Sabine Lake
97	29.77157	-93.94838	Keith Lake above Weir	Sabine Lake
98	29.75336	-93.97027	Keith Lake Point	Sabine Lake
99	29.58517	-94.48905	Trib Near Love Tree Bayou	East Galveston Bay
100	29.58324	-94.49323	Trib Near Lone Tree Bayou (2)	East Galveston Bay
101	29.59977	-94.50584	Oyster @ Coulter Island	East Galveston Bay
102	29.610297	-94.51193	Oyster Upstream	East Galveston Bay
103	29.7904	-94.7411	Trib off Garden Bayou	Lower Trinity
104	29.80455	-94.74078	Old River/ Lost Lake Fork	Lower Trinity
105	29.76484	-94.70509	Trib Near Bulk Head Cove	Lower Trinity
106	29.75391	-94.69353	Anahuac Channel @ Boat Ramp	Lower Trinity

Table 13 Coordinates of sites sampled by EIH (Numbered codes) and TPWD (alphabetical codes).

Site ID	Latitude	Longitude	Waterbody Name	USGS 8 digit Subbasin Name
107	28.61435	-96.21178	Palacios Bayou @ Oyster Lake Rd	East Matagorda Bay - W
108	28.71071	-96.16323	Pilkington Bayou	East Matagorda Bay - W
109	28.7319	-96.43493	Carancahua Bay	East Matagorda Bay - W
110	029.88302	-094.05046	Taylor bayou @ 73	Sabine Lake
A	28.12299	-97.31043	Aransas River @ Aransas River Rd Ramp	Aransas
B	28.32236	-96.93536	Artesian Creek @ FM 774	Aransas Bay
C	28.21823	-96.98802	Cavasso Creek @ 35	Aransas Bay
D	27.93007	-97.18727	McCampbell Slough @ 35	Aransas Bay
E	28.1412	-97.22255	Mullens Bayou @ Mullens Bayou Rd	Aransas Bay
F	28.04429	-97.27035	Trib to Aransas Bay @ 188	Aransas
G	27.89697	-97.61603	Rincon Bayou @ Nueces Delta Preserve	North Corpus Christi Bay
H	27.65701	-97.40202	Oso Creek @ Staples St	South Corpus Christi Bay
I	28.204229	-97.295841	Chocolate Swale @ 136	Mission
J	27.88911	-97.60875	Nueces River @ Nueces Delta Preserve	Lower Nueces
K	28.18396	-97.21381	Mission River @ 2678	Mission
L	28.05029	-97.0423	Tule Creek @ 35	Aransas Bay
M	28.04565	-97.03870	Tule Creek Dnstrm of Tule Park Dr	Aransas Bay

Table 13 Coordinates of sites sampled by EIH (Numbered codes) and TPWD (alphabetical codes).

Site ID	Latitude	Longitude	Waterbody Name	USGS 8 digit Subbasin Name
N	28.03811	-97.86088	Nueces River @ 359	Lower Nueces

APPENDIX C:

DATA SHEETS

American Eel Study Field Datasheet (Front)

Environmental Institute of Houston – University of Houston-Clear Lake

Site ID: _____ ☐ Index ☐ Non-Index **Waterbody Name:** _____	**Date Set:** **Date Retrieve:**
Sub Basin:_____ **County**_____ **HUC 8:** _____ * For sub basin and HUC access Google Earth "American Eel" on EIH drive.	**Latitude:** **Longitude:**
Collected By:	
Shoreline Habitat: ☐ Emergent Aquatic Vegetation (e.g. saltmarsh cordgrass, needlerush, etc) ☐ Woody Vegetation ☐ Bare ground ☐ Oyster ☐ Rip/rap ☐ Artificial Substrate ☐ Other: _____	

	Net Set	Retrieve
Time (HH:MM)		
Temperature (°C)		
Conductivity (µS/cm)		
Spec. Conductivity (µS/cm)		
Salinity (psu)		
DO (% sat)		
DO (mg/L)		
pH		
Secchi (m)		
Thalweg (m)		
Stream Width (m)		

General Site Notes

HOBO Logger

Serial Number	Deploy Time (hh:mm)	Retrieve Time (hh:mm)

Tide Station: _____

Net Set: Stage _____ (1 = low, 2 = rising, 3 = high, 4 = falling) Level (MLLW, ft.) _____

Net Retrieve: Stage _____ (1 = low, 2 = rising, 3 = high, 4 = falling) Level (MLLW, ft.) _____

Moon Phase: _____ **Illumination %**_____

(For nearest tide station, access American eel file on google earth pro in EIH drive)

Fyke Nets (Instream habitat data taken 10m from mouth of net, recorded as percent, and summed for total)

Water Depth (m) Set	Water Depth (m) Retrieve	Sediment (Silt, Clay, Sand, other)	Dominant Veg	Instream Habitat (legend below notes section) (assess area in front of mouth of net to 10m downstream) M.P (%)	F.A (%)	W.D (%)	O.V (%)	U.C (%)	B/L (%)	A.S (%)	O.R (%)	Total (%)
Notes:												

M.P=Macrophyte, **F.A** = Filamentous Algae, **W.D** = Woody Debris, **O.V** =Overhanging Veg, **U.C**= Undercut Bank, **B/L**= Boulders/Ledges, **A. S** = Artificial Structure, O.R= oyster Reef

Catch in front of excluder (List species observed and abundance category: 1–Rare, 2–Common, 3–Abundant)

Species	Abund Cat	Species	Abund Cat	Species	Abund Cat

Standard wing width = 13.5 (ft)

Page _____ of _____

2018-2019 American Eel Study Field Datasheet (Back)
Fish Collection Bench Sheet

Site: _____ Date: _____

Additional Species

Gear F = Fyke, M = Mop	Rep	Species (Common Name)	(Target Species) Count	(Non-Target Species) Abundance Category 1–Rare, 2–Common, 3–Abundant	Notes

Page _____ of _____

Speckled Worm Eel Bench Sheet Completed By_____

Site	Date	Total Length (mm)	Body Depth (mm)	Body Width (mm)	Head Length (mm)	Pre-Anal Length (mm)	Weight (mg)	Stage (LEP,MET ,GE,ELV)	Notes

_____gf_____